ABSTRACT

Title of Dissertation:	*NEISSERIA GONORRHOEAE* MODULATES INFECTIVITY BASED ON PROPERTIES OF HUMAN CERVICAL EPITHELIA AND PHASE VARIABLE BACTERIAL SURFACE STRUCTURES
	Qian Yu Doctor of Philosophy, 2019
Dissertation Directed by:	Dr. Wenxia Song, Professor Department of Cell Biology and Molecular Genetics

Neisseria gonorrhoeae (GC) infection in the human female reproductive tract causes various clinical outcomes, from no symptom to severe complications. The major barrier to a better understanding of GC infection in women is the lack of experimental system closely mimicking *in vivo* infection. Here, I developed a human cervical tissue explant model, which maintains the heterogeneity of the cervical epithelium. Using this model, my thesis research examined the impact of the heterogeneity of the cervical epithelium and the phase variation of GC surface structures on GC infectivity. My research revealed that GC preferentially colonize the ectocervix and the transformation zone (TZ), but exclusively penetrate into the subepithelial tissues of the TZ and endocervix. Pili are essential for GC colonization in all regions of the cervix.

Expression of Opa isoforms that bind to the host receptors CEACAM (Opa_{CEA}) enhances GC colonization in the ecto/endocervix but inhibits GC penetration into the endocervix. However, GC infectivity in the TZ does not respond to Opa phase variation, due to the low expression level and intracellular location of CEACAMs in the TZ epithelial cells. Opa_{CEA} enhances GC colonization in the ecto/endocervix by inhibiting epithelial exfoliation and suppresses GC penetration into the endocervical subepithelium by inhibiting GC-induced disassembly of the apical junction. Opa-mediated modulation of GC infectivity depends on the immune receptor tyrosine-based inhibitory motif (ITIM) of CEACAM1 and its downstream phosphatase SHP. The effect of epithelial cell polarity on GC invasion was studied using a cell line model. My results show that GC invade more efficiently into non-polarized than polarized epithelial cells without changing the adhesion efficiency. Opa (phase variable) expression enhances both adhesion and invasion in both non-polarized and polarized cells. In non-polarized cells, Opa expression induces F-actin accumulation and microvilli elongation underneath GC microcolonies, suggesting an actin-mediated uptake of GC. In contrast, GC expressing no Opa reduce F-actin and demolish microvilli underneath microcolonies in both polarized epithelial cell line and endocervical epithelial cells potentially by increasing calcium flux, NMII activation and the redistribution of actin nucleation factor Arp2/3 from the apical surface. Taking together, my research demonstrates that both the heterogeneity of the cervical epithelium and the phase variation of bacterial surface structures regulate GC infectivity in the human cervix, either dominated by colonization or penetration, consequently influencing the clinical outcomes of the infection.

NEISSERIA GONORRHOEAE MODULATES INFECTIVITY BASED ON PROPERTIES OF HUMAN CERVICAL EPITHELIA AND PHASE VARIABLE BACTERIAL SURFACE STRUCTURES

By

Qian Yu

Dissertation submitted to the Faculty of the Graduate School of the
University of Maryland, College Park, in partial fulfillment
of the requirements for the degree of
Doctor of Philosophy,
2019

Advisory Committee:
Professor Wenxia Song, Ph.D. Chair
Professor Norma Andrews, Ph.D.
Professor Kevin McIver, Ph.D.
Professor Daniel. C. Stein, Ph.D.
Professor Xiaoping Zhu, Ph.D.

Dedication

I would like to dedicate this dissertation to my parents, Xiaoqiang Yu, and Qianqian Zhang, who always support me.

Acknowledgment

I would like to thank Dr. Wenxia Song, my mentor, for her invaluable guidance, insights, and expertise on my thesis project and life. I would also like to thank Dr. Daniel Stein for his expertise and insights on my thesis project, and my committee members, Dr. Norma Andrews, Dr. Kevin McIver, and Dr. Silvia Muro, and Dr. Xiaoping Zhu for all their input and help on my thesis project.

I would like to take this opportunity to thank all of my lab mates in both the Song lab and Stein lab, who made this journal so much easier. I would like to thank my lab mate, Liang-Chun Wang, for his friendship and all the support and help. I have to thank my former and current lab mates Katie, Michelle, Heather, Senthil, Salsawi, Sofia, Yanan, Anshuman, Jurri, Betty, Ebby, Melanie, and Grace, for being supportive, and being good friends. Last but not least, I would like to thank Amy Beaven from the imaging core to help me with all the fluorescence microscopy, and Timothy K Maugel for all the help and work on the TEM and SEM.

Table of Contents

List of Abbreviations

ARPC actin-related protein complex

AJ adherens junction

ASGP-R asialoglycoprotein receptor

ASM acidic sphingomyelinase

CEACAM carcinoembryonic antigen-related cell adhesion molecule

CR3 complement receptor 3

DAG diacylglycerol

DGI disseminated gonococcal infection

EGFR epidermal growth factor receptor

ERK extracellular signal-related kinase

FBS fetal bovine serum

FRT female reproductive tract

GCK gonococcal media base

GC *Neisseria gonorrhoeae*

HEC-1-B human endometrial adenocarcinoma cell line

HSPG heparan sulfate proteoglycans

IP3 inositol triphosphate

JAM junctional adhesion molecule

LOS lipooligosaccharide

MAPK mitogen-activated protein kinase

MLC myosin light chain

MLCK myosin light chain kinase

MOI multiplicity of infection

NMII non-muscle myosin II

NPRs nucleation promoting factors

N-WASP neuronal Wiskott–Aldrich syndrome protein

Opa opacity-associated proteins

PC-PLC phosphatidylcholine-specific phospholipase C

PI3K phosphoinositide 3-kinase

PID pelvic inflammatory disease

Pil pili

PIP_2 phosphoinositol 4, 5 bisphosphate

PIP_3 phosphoinositol 3, 4, 5 bisphosphate

PKC protein Kinase C

PLC phospholipase C

pMLC phosphorylated myosin light chain

pSHP1 phosphorylated protein tyrosine phosphatase 1B, PTP1B

pSHP2 phosphorylated protein tyrosine phosphatase 2B, PTP2B

ROCK Rho-associated coiled-coil kinase

RTK receptor tyrosine kinase

SH2 Src homology 2

SCJ squamocolumnar junction

SHP1 protein tyrosine phosphatase 1B, PTP1B

SHP2 protein tyrosine phosphatase 2B, PTP2B

T3SS type III secretion system

T84 human colorectal adenocarcinoma cell line

TEER transepithelial resistance

TJ tight junction

TZ transformation zone

ZO zonula occludens

List of Figures

Chapter 1: Introduction

1.1 Gonorrhea and Neisseria gonorrhoeae

Gonorrhea is the second most commonly reported sexually transmitted infection in the world, as well as in the U.S. Each year, there are an estimated 78 million new infections with gonorrhoeae worldwide [1]. In 2017, a total of 555,608 new cases reported in the US, which is 18.6% increase since 2016, and 75.2% increase since the historic low in 2009 [2]. The rates of reported gonorrhea cases are the highest among teenagers and young adults. Furthermore, the reported rates of gonorrhea are masked by the asymptomatic nature of gonococcal infection [3]. Particularly, 50 to 80% of gonococcal infection in the female reproductive tract (FRT) is asymptomatic [4].

Gonorrhea is caused by an exclusive human pathogen, gram-negative bacteria *Neisseria gonorrhoeae* (GC). The cases of GC infection that are resistant to currently available antibiotics are on the rise, which complicates gonorrhea treatment [2]. The decrease of susceptibility to ceftriaxone, cefixime, and azithromycin has been reported in recent years [5]. The only treatment of uncomplicated gonorrhea recommended by CDC is the combination of ceftriaxone and azithromycin or doxycycline [6]. The increased resistance of GC to available antimicrobials underscores the urgent need to develop a new treatment for gonorrhea.

GC primarily infect urethra in male, inducing inflammatory responses and causing acute urethritis with purulent discharge [4]. A smaller percentage of male infection develop asymptomatic gonococcal urethritis, compared to female infection. However, there has been an increase in asymptomatic male infection in recent years [7]. In females, GC primarily infect lower genital tract when transmitted from men, causing asymptomatic cervicitis [4]. 45% of such asymptomatic infection in lower reproductive tract lead to ascending infection in the upper genital tract, causing pelvic inflammatory disease (PID), which can lead to permanent fallopian tube scarring and blockage, and subsequently infertility and ectopic pregnancy [4]. It has been shown that gonorrhea can increase the risk of coinfection with other sexually transmitted infections such as Chlamydia, and HIV [8]. The risk may be even higher in the view of the high percentage of asymptomatic, subclinical female infection.

Asymptomatic female infection which does not get treatment and the increase in antibiotics resistance of GC makes gonorrhea an emerging public health crisis.

1.2 Neisseria gonorrhoeae infection in females

In females, GC primarily initiate infection in the female reproductive tract (FRT) from the mucosal surface of cervical epithelia [3, 9, 10]. GC are first deposited on vaginal epithelia. However, vaginitis caused by GC infection is rarely reported [3]. Vagina connects the outside of the body with the cervix, the gate of the female reproductive tract (FRT) that is often blocked by mucus plug. Ectocervix (Ecto) is the outmost part

of the cervix, connecting the cervix with vagina. The mucosal surface of both the vagina and the ectocervix is colonized by microbiota [11]. Ecto leads to the endocervix (endo) through transformation zone (TZ), which leads to the upper genital tract, composed of uterine, fallopian tube and ovary. Though previously believed to be sterile, several studies showed that the endocervix and upper genital tract also harbor microbial communities and is accessible by pathogens [12-14]. GC colonization in endo has been reported at a relatively low level compared to ectocervix. GC colonization in endo can lead to bacterial dissemination into the upper genital tract, also potentially causes inflammation, leading to serious complications, such as pelvic inflammatory disease (PID) and acute salpingitis [3, 4, 9]. Subepithelial GC was observed in the endocervix of patients' biopsies [15], suggesting the penetration of GC from the mucosal surface of the endo into subepithelial tissue. The penetrated GC potentially trigger immune responses causing symptomatic infection and have opportunities to further disseminate through bloodstream causing disseminated gonococcal infection (DGI) [16]. Moreover, it has been shown that the serum level of progesterone, one of the sex hormones controlling the menstrual cycle, is significantly higher in the asymptomatic patients than the symptomatic patients [17]. It indicates the impact of menstrual cycle on GC infection progression, which adds more complications to female gonorrhea. However, how the localized GC infection in the cervix leads to such variety of clinical outcome is unknown.

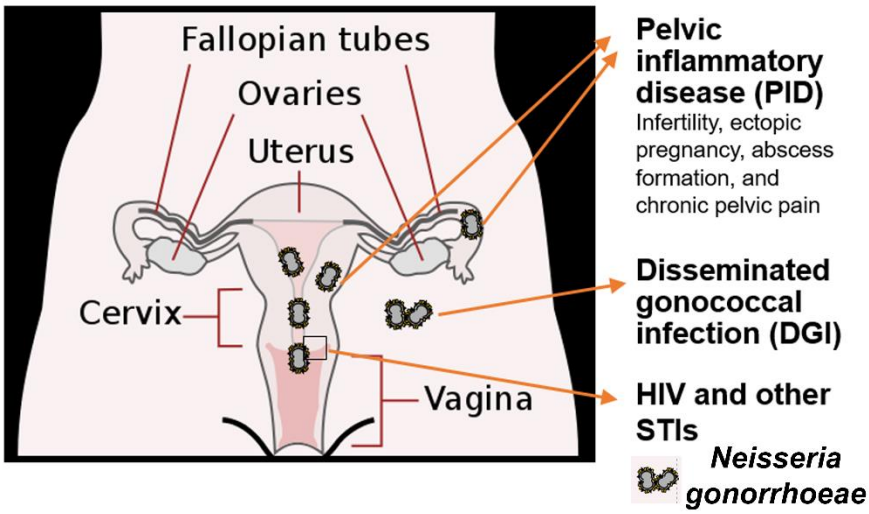

Figure 1. Unique features of female gonorrhea

A schematic diagram of *Neisseria gonorrhoeae* (GC) infection in the female reproductive tract (FRT). After first deposited in the vagina, GC initiate infection from the cervix, the gate of the FRT. GC have to overcome the barrier of the cervix and to ascend to the upper genital tract, which can cause pelvic inflammatory disease (PID). To disseminate into the bloodstream, GC need to penetrate across the epithelium of the FRT, causing disseminated gonococcal infection (DGI). Cervical gonorrhea can increase the risk of coinfection with HIV and other sexually transmitted infections (STI).

1.3 The cytoarchitecture of cervical epithelium

The cervix is the gate of the female reproductive tract, protecting the sterile upper genital tract from the unsterile vagina, which is exposed to the outer environment. The cervix is also the initiation site of GC infection. To establish infection, GC need to overcome the cervical epithelium, the first line of defense. The cervical epithelium exhibits distinct morphology at different anatomical regions. The ectocervix, connecting with the vagina, is covered by multiple layers of non-polarized stratified squamous epithelial cells. At the bottom of the ectocervical epithelium, a single layer of round basal cells attached to the basal membrane. The basal cells can divide and differentiate to form the next few layers of parabasal cells. Further differentiation of parabasal cells forms the intermediate layers of polygonal cells, which further differentiate into the large and flattened cells forming the superficial layers. The formation of intermediate and superficial layers is subjected to the change of female hormone.

Ascending to the upper genital tract, endocervix is covered by a single layer of polarized columnar epithelial cells. The endocervical epithelium does not form a flattened surface. In contrast, it is thrown into several longitude folds forming invaginations into the cervical stroma, also referred to as endocervical glands. The endocervical epithelial cells secrete mucus, forming a barrier against pathogen entrance. The components and amount of mucus secreted by the endocervical epithelial cells also change dramatically during the menstrual cycle [18], which further complicates the microenvironment of the endocervix.

The site where the endocervical epithelium meets with ectocervical epithelium is called the squamocolumnar junction (SCJ). Transformation zone (TZ) is the region located between newly formed SCJ and the original SCJ. The TZ is formed at the onset of puberty, when the endocervical epithelium proliferates under the influence of estrogen and extends into ectocervix, pushing the original SCJ into the ectocervix. The eversion of endocervical epithelium into the ectocervical region triggers squamous metaplasia. In the portion of endocervical epithelium invading into ectocervix, the reserve cells underneath the endocervical epithelium start to proliferate and gradually differentiate into ectocervical epithelial cells. The new SCJ is formed between the endocervical epithelium and the metaplastic TZ epithelium. At the ecto end of TZ, TZ epithelium eventually becomes indistinguishable from the ectocervical epithelium. Thus, the cytoarchitecture of TZ is a transformation from multiple layers (ecto) to a single layer (endo), and from non-polarized (ecto) to polarized (endo). The length of TZ varies with age, hormonal status and from person to person.

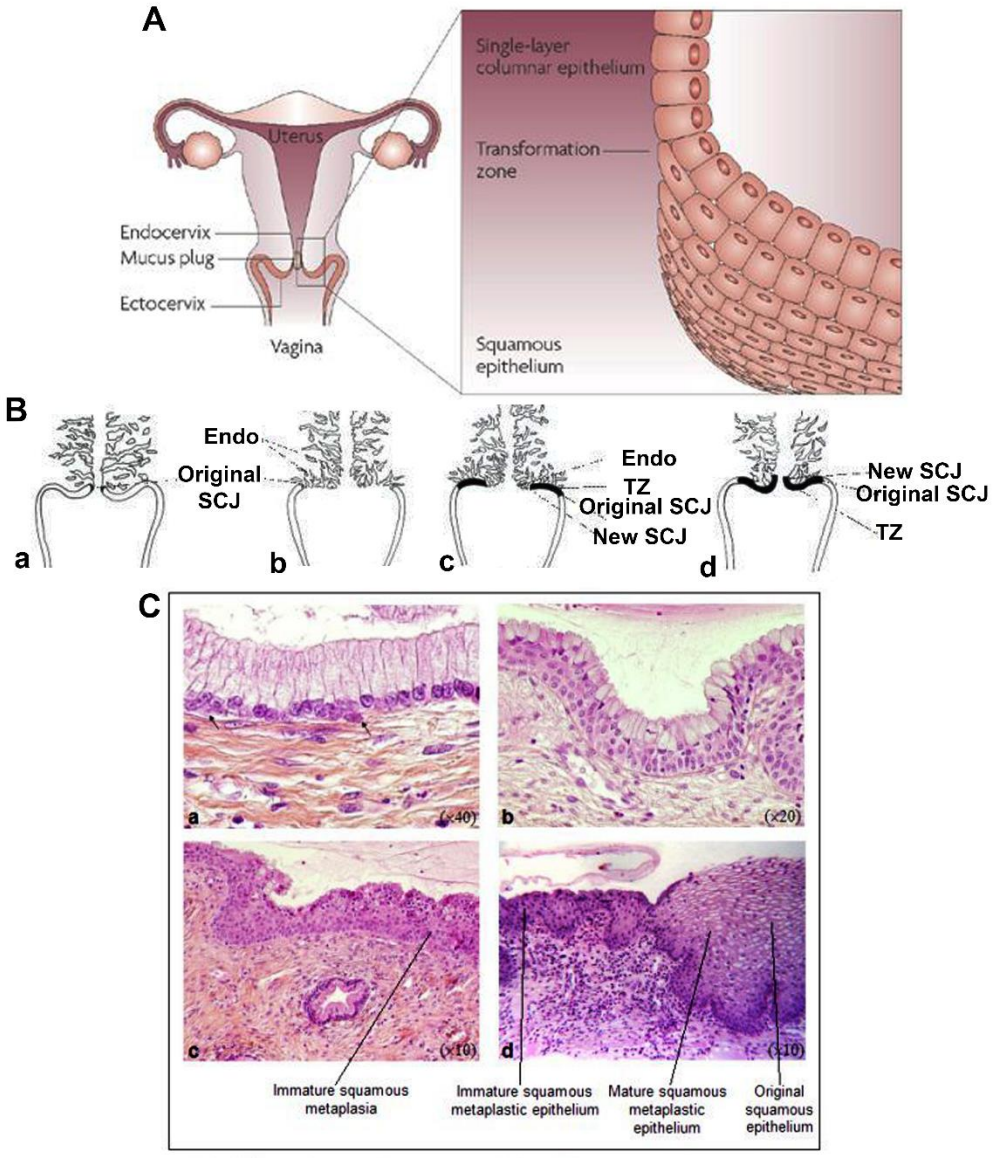
A
Uterus
Endocervix
Mucus plug
Ectocervix
Vagina
Single-layer columnar epithelium
Transformation zone
Squamous epithelium
B
Endo
Original SCJ
a
b
Endo
TZ
Original SCJ
New SCJ
c
New SCJ
Original SCJ
TZ
d
C
a
(×40)
b
(×20)
c
(×10)
d
(×10)
Immature squamous metaplasia
Immature squamous metaplastic epithelium
Mature squamous metaplastic epithelium
Original squamous epithelium

Figure 2. Distinct cytoarchitecture of the cervical epithelium at different anatomical regions (modified based on the Colposcopy and treatment of cervical intraepithelial neoplasia: a beginners' manual, and [19]).

A) A schematic diagram of the cytoarchitecture of cervical epithelium. The ectocervix is covered by the multiple-layered stratified squamous epithelial cells. The endocervix is lined with the single-layer columnar epithelial cells. The transformation zone (TZ) is the region located between ecto and endocervix. B) A schematic representation of the formation of TZ. TZ is located between the original squamocolumnar junction (SCJ) and the newly formed SCJ after puberty: (a) before puberty, (b) after puberty and at early reproductive age, (c) around 30 years old, and (d) perimenopausal. C) The TZ epithelium is formed through the squamous metaplasia. (a) polarized endocervical epithelium with reserve cells (arrows) underneath, (b) proliferation of reserve cells forming layers of reserve cells underneath the original endocervical epithelium, (c) further proliferation and differentiation of reserve cells forming immature metaplastic epithelium, and (d) mature squamous metaplastic epithelium indistinguishable from the original squamous epithelium.

Although data from clinical researches using patient biopsies and papsmear has shown the colonization in all three cervical regions, and penetration in TZ and endocervix [15, 20], little is known about the mechanism used by GC to infect different types of cervical epithelial cells *in vivo*. The questions that does the complicated cytoarchitecture of cervical epithelium have any impact on the various clinical outcomes of the localized cervical GC infection remains not answered.

1.4 Neisseria gonorrhoeae and its virulence factors

To survive in the various microenvironment of the cervix and facilitate infection, the surface molecules of GC undergo phase and antigenic variation. Pili are filamentous structure expressed on the surface of gram-negative bacteria. GC express the Type IV pili, which undergo both phase and antigenic variation [21]. Type IV pili are composed of PilE, a major pilus subunit protein, PilC, a minor pilus-associated protein, and PilT. The *pilE* gene can go through antigenic variation by recombination of *pilE* locus with one or more silent *pil* loci (*pilS*) [22]. Most strains harbor two *pilC* genes that are highly homogeneous, expressing two different proteins, PilC1 and PilC2 [23]. PilC protein has been identified as the adhesive component of pili. It is located at the tip of pili and mediates initial attachment of GC to host cells [24, 25]. PilT protein is involved in the GC twitching motility and pili retraction, thus mediating microcolony formation and the bringing GC close to host cell membrane [26-28]. Pili interact with complement receptor 3 (CR3) expressed on the mucosal surface of the FRT [29].

Opacity associated proteins (Opa) are a group of integral outer membrane proteins. A single bacterial cell can express up to 11 different Opa genes. Each of the 11 different Opa genes can be turned on or off independently due to the phase variation [30, 31]. The predicted secondary structure of Opa proteins has a β-barrel structure formed by 8 anti-parallel membrane spanning β-strands with four extracellular loops. Antigenic variations of Opa proteins are predominantly observed in the central two hypervariable (HV) loops [31]. Opa proteins can be grouped into two classes according to the receptors on human cells they bind to. The majority of the 11 Opa proteins interact with carcinoembryonic antigen-related cell adhesion molecules (CEACAMs), such as OpaH [21, 32]. OpaC, representing other class, interacts with heparan sulphate proteoglycan (HSPG) [33]. Studies showed that GC isolates from female patients at different stages of the menstrual cycle express different isoforms of Opa [34]. However, how the heterogeneous expression of Opa protein affects GC infection in the human cervix is not fully understood.

As Gram-negative bacteria, GC possess lipooligosaccharide (LOS) within its outer membrane, which undergoes antigenic variation. The structure of LOS is composed of three oligosaccharide chains tethered to a lipid A core [35]. The terminal oligosaccharide of LOS varies, depending on the expression of glycosyl transferases involved in LOS biosynthesis [36, 37]. It has been shown that LOS function as a ligand to the human asialoglycoprotein receptor (ASGP-R), contributing to the uptake of GC into primary human urethral epithelial cells [38]. Our lab has previously shown

that the terminal oligosaccharide structure of LOS alters the level of invasion into human endometrium cell line ME-180 [39].

Porin (PorB) is the most abundant protein in the outer membrane of GC [4]. PorB forms water-filled channel within gonococcal outer membrane, through which ion and small nutrients can transverse. However, PorB does not undergo phase and antigenic variation. It is present as one of the two isotypes, PI.A or PI.B [4]. It has been shown that porin can translocate into the plasma membrane of the eukaryotic cell [40] and further the mitochondrial membrane [41]. PorB has been shown to can manipulate phagosome maturation [42, 43] and triggers apoptosis [43, 44]. However, the anti-apoptotic effect of PorB was also observed in the human urethral epithelium, which was thought to be a strategy for GC to survive and proliferate within epithelial cells [45].

1.5 Neisseria gonorrhoeae engaged host receptors and downstream signaling

Each of the GC surface virulence factors interacts with specific receptors on host cells triggering downstream signaling to facilitate infection. It has been shown that CR3 plays important roles in GC infection as a receptor for pili, involving porin and LOS as well. CR3 is a member of the integrin family, known as integrin αMβ2, and is expressed by professional phagocytes. CR3 is the receptor for iC3b, a component of the complement system, and mediates phagocytosis of complement-opsonized microorganisms [46]. Dr. Apicella's groups first showed the expression of CR3 in primary human ectocervical and endocervical epithelial in culture and in the human

cervical tissue. GC adhered to primary cervical epithelial cells colocalized with CR3 antibody staining [29]. The cleavage products of C3, C3b-α, C3b-β, iC3bα$_1$i, iC3bα$_2$i, and C3dg, were found to be deposited onto GC in the infected primary cervical epithelial cells as well as in the cervical secretion specimen from patients. The deposition of C3b on GC surface occurs through the lipid A core of LOS [47]. Pili bind to the I-domain of CR3 in cooperating with porin and iC3b-opsonization, which is required for adhesion and subsequent invasion into primary cervical epithelial cells. [48, 49].

The majority of the 11 Opa proteins has been shown interacting with Carcinoembryonic antigen-related cell adhesion molecules (CEACAM) [50]. CEACAMs are first discovered as cell adhesion molecules in cancer cells, hence the name. CEACAM proteins mediate intercellular adhesion through homophilic and/or heterophilic interaction [51]. In humans, multiple isoforms have been identified. All CEACAM proteins belong to the immunoglobulin (Ig) superfamily and share similar overall structure at the N-terminus, one variable (V)-like domain followed by none or several constant C2-like Ig domains [51, 52]. At the C-terminus, different isoforms possess different structures, an intracellular domain or a glycosylphosphatidylinositol (GPI) anchor [52]. In human, CEACAM1, CEACAM3, CEACAM5, and CEACAM6 have been shown to bind to Neisserial Opa proteins [53], among which CEACAM1 and CEACAM3 possess a cytoplasmic domain. The long splicing form of CEACAM1 (CEACAM1L) has an immunoreceptor tyrosine-based inhibitory motif (ITIM) at the C-terminus of its cytoplasmic domain. In contrast, CEACAM3 has an immunoreceptor

tyrosine-based activation motif (ITAM) [52]. These features suggest the ability of CEACAM1 and CEACAM3 to transducing signals upon GC infection.

CEACAM1, CEACAM3, and CEACAM6 are expressed in granulocytes. Lee et al. showed that upon Opa-CEACAM1 binding, GC recruited CEACAM1 to the sites of attached GC on the surface of primary $CD4^{+}$T cells. Upon T cell receptor (TCR) ligation, CEACAM1 was phosphorylated on the tyrosine residues harbored in the ITIM. The phosphorylated ITIM recruited and activated the tyrosine phosphatase SHP-1 and SHP-2, which inhibited the phosphorylation of ZAP-70, a key adaptor protein in T cell signaling pathway, consequently inhibiting T cell activation [54]. Using human myelomonocytic cell line JOSK-M cells, Hauck et al. showed that inoculation with GC that express CEACAM-binding Opa triggered activation of acid sphingomyelinase (ASM) and downstream signaling involving Src-like tyrosine kinases Hck and Fgr and Jun-N-terminal kinases (JNK), eventually lead to activation of the Rho GTPase Rac1 and bacteria uptake [55]. CEACAM3 is expressed exclusively in neutrophils. Dr. Gray-Owen's group has done a series of studies showing that upon Opa-CEACAM3 interaction, tyrosine residues in the ITAM are phosphorylated by Src-family kinases, which is necessary for GC uptake by neutrophils [56]. The phosphorylated ITAM recruited and triggered the phosphorylation of the cytoplasmic tyrosine kinase Syk and activated downstream signaling pathways including phospholipase C (PLC), small GTPase and phosphatidylinositol 3-kinase (PI3K). This signaling activation led to the rearrangement of the actin cytoskeleton and GC uptake [57-59].

Epithelial cells express CEACAM1, CEACAM5, and CEACAM6. Using CEACAM1 transfected T293 cells, Voges et al. showed that the Opa-CEACAM1 dependent uptake of GC by epithelial cells requires PI3K activity and the cytoplasmic domain and the extracellular IgC2-like domain of CEACAM1 [60]. Using a CEACAM5 transgenic mouse model, ME-180 cells, and CEACAM1 or CEACAM6 transfected T293 cells, Muenzer et al. showed that Opa-CEACAM1 interaction inhibited epithelial exfoliation through upregulation of CD105, one of the transforming growth factor- β1 receptor family (TGFβ1R), and subsequent activation of integrin β1. The inhibition of epithelial exfoliation through this pathway required the cytoplasmic domain of CEACAM1 [61, 62].

The expression and distribution of various epithelial CEACAMs in human cervix has not been studied in detail. Islam et al. detected CEACAM1 on the apical surface of endocervical epithelial cells, but a low level of CEACAM1 and a moderate level of CEACAM5 in the intermediate and superficial layers of the ectocervical epithelium. They did not detect any expression of CEACAM6 along the cervical epithelium [63]. However, whether the differential expression of CEACAMs in different cervical regions affects host signaling response and GC infection process in corresponding regions, as well as clinical outcomes of GC infection, has not been well studied.

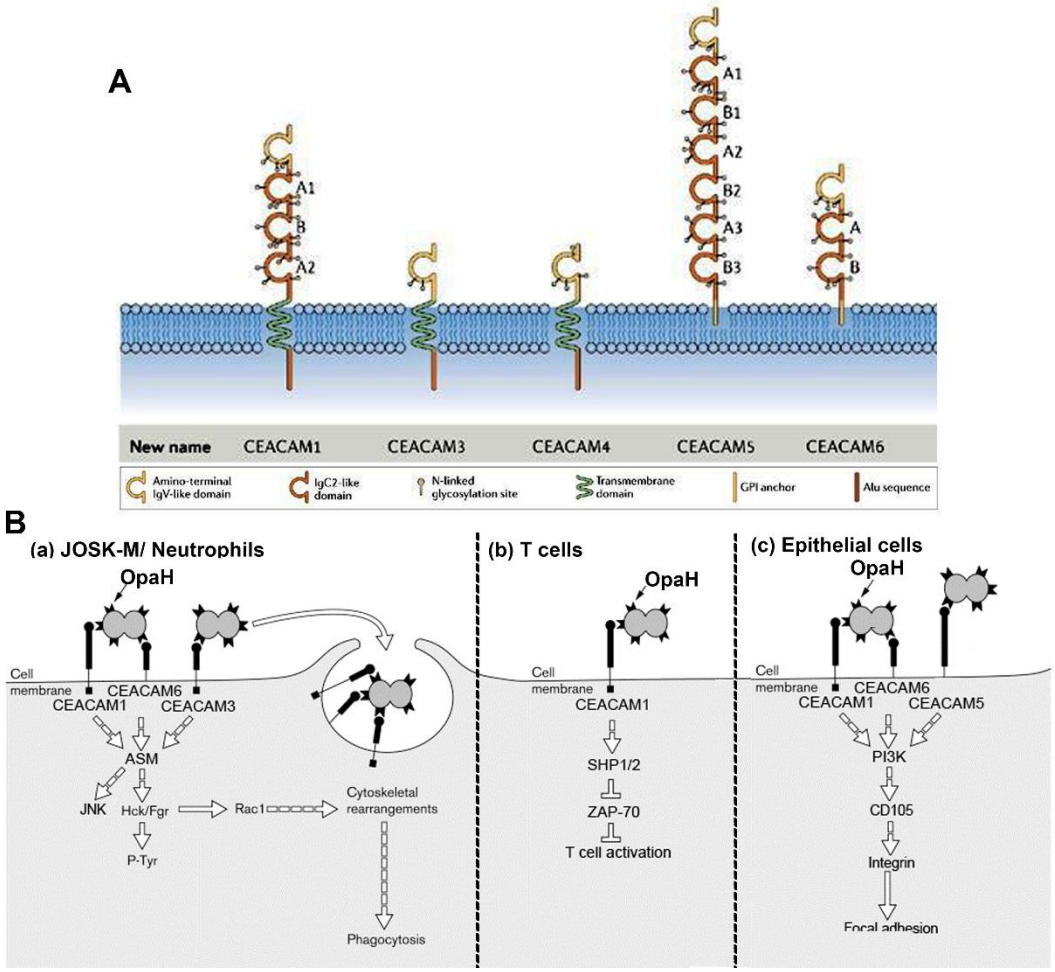
A
A1
B1
A2
B2
A3
B3
A
B
A1
B
A2
New name
CEACAM1
CEACAM3
CEACAM4
CEACAM5
CEACAM6
Amino-terminal IgV-like domain
IgC2-like domain
N-linked glycosylation site
Transmembrane domain
GPI anchor
Alu sequence
B
(a) JOSK-M/ Neutrophils
OpaH
Cell membrane
CEACAM1
CEACAM6
CEACAM3
ASM
JNK
Hck/Fgr
Rac1
Cytoskeletal rearrangements
P-Tyr
Phagocytosis
(b) T cells
OpaH
Cell membrane
CEACAM1
SHP1/2
ZAP-70
T cell activation
(c) Epithelial cells
OpaH
Cell membrane
CEACAM1
CEACAM6
CEACAM5
PI3K
CD105
Integrin
Focal adhesion

Figure 3. Structure and downstream signaling of carcinoembryonic antigen-related cell adhesion molecule (CEACAM) triggered by Opa (Modified based on [52, 64]).

A) A schematic diagram of the CEACAM structure. At the N-terminus, one variable (V)-like domain is followed by none (CEACAM3 and 4) or several constant C2-like Ig domains (CEACAM1, 5 and 6). At the C-terminus, CEACAM 1, 3 and 4 possess a cytoplasmic domain. CEACAM5 and 6 are GPI anchored proteins. B) In the phagocytic cells, such as JOSK-M and neutrophils (a), Opa interaction with CEACAM1, 6 or 3 leads to activation of Src family kinases Hck and Fgr through acidic sphingomyelinase (ASM) resulting in tyrosine phosphorylation (P-Tyr), and activation of the Rho GTPase Rac1. This pathway eventually leads to phagocytic bacterial uptake through cytoskeleton rearrangement. In T cells (b), Opa-CEACAM1 interaction activates SHP1/2 leading to the inhibition of T cell activation through inhibiting ZAP-70. In epithelial cells (c), Opa triggered downstream signaling involves CEACAM1, 5 and 6. This pathway leads to CD105 and integrin activation through PI3K, resulting in the enhanced focal adhesion of epithelial cells. Full arrows, direct activation of the downstream pathway. The dashed arrows, unknown downstream pathway.

Heparan sulphate proteoglycans (HSPG) is the other host receptors for Opa proteins. Proteoglycans (PG) are membrane-anchored core proteins, modified with glycosaminoglycans (GAGs) side chains. The side chains of HSPG are composed of heparan sulphates (HS). A specific isoform of Opa proteins (Opa_{HSPG}) interacts with HSPG on the mucosal surface of human epithelial cells [65]. Opa-HSPG interactions have been shown to mediate intimate adherence and invasion of GC into various epithelial cell lines. This process is facilitated by extracellular matrix, such as fibronectin (FN) in HEp-2 cell [66] and vitronectin (VN) in Chinese hamster ovary (CHO) cells [67] and Hela cells [66, 68]. Using Chang conjunctiva cells, Grassme et al. showed that the Opa-HSPG mediated GC uptake is dependent on the activity of phosphatidylcholine phospholipase C (PC-PLC), which generates diacylglycerol (DAG). DAG appears to activate acidic sphingomyelinase (ASM), which produces ceramide and promote GC uptake [69]. Syndecan is a major group of transmembrane HSPG. Freissler et al. showed expression of syndecan-1 and syndecan-4 in various epithelial cell lines, including the human endometrial cell line ME-180, human conjunctival epithelial cells (Chang), human endometrial cell line Hec-1-B and human cervical cell line Hela. They found that Opa-HSPG mediated GC uptake requires the cytoplasmic tail of both syndecans and the possible involvement of protein kinase C (PKC) and phosphatidylinositol-4,5-bisphosphate [$PI(4, 5)P_2$] in this process [70].

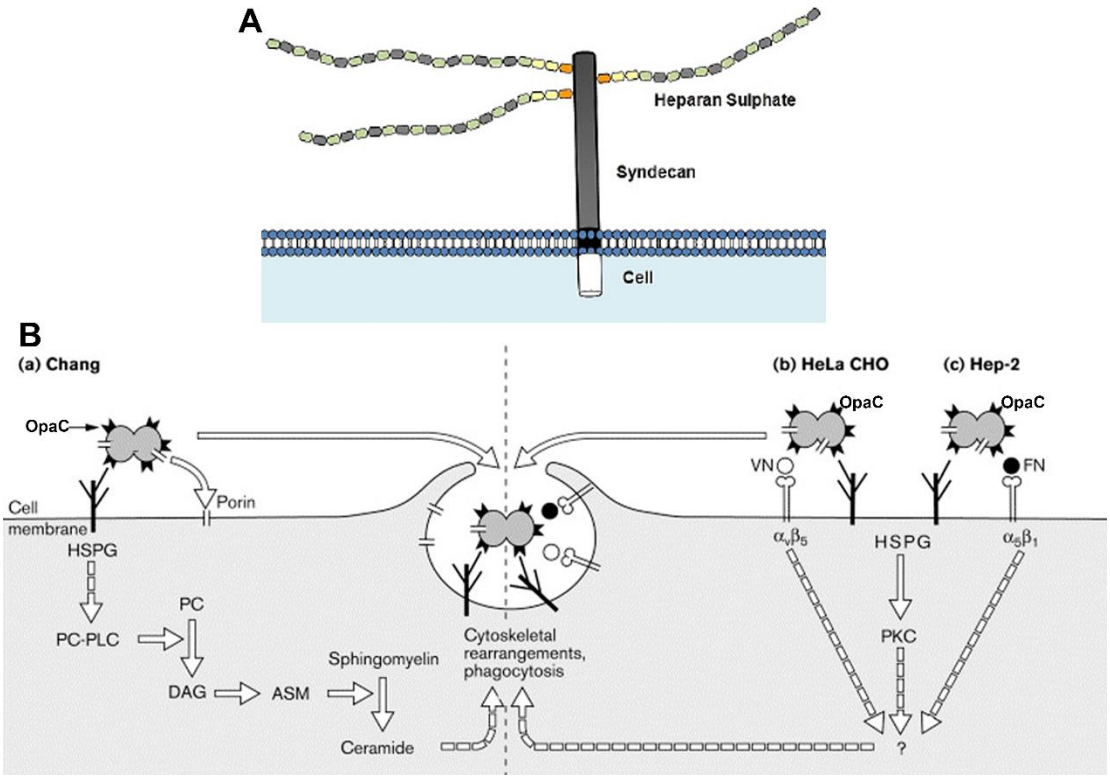
A
Heparan Sulphate
Syndecan
Cell
B
(a) Chang
(b) HeLa CHO
(c) Hep-2
OpaC
Porin
Cell membrane
HSPG
PC
PC-PLC
DAG
ASM
Sphingomyelin
Ceramide
Cytoskeletal rearrangements, phagocytosis
VN
FN
$\alpha_v\beta_5$
$\alpha_5\beta_1$
PKC
?

Figure 4. Structure and downstream signaling of heparan sulfate proteoglycans (HSPG) triggered by Opa (Modified base on [71] and doi:10.4172/2161-0703.1000157).

A) A schematic diagram of the HSPG structure using syndecan as an example. HSPG is composed of a membrane-anchored core protein and several heparan sulphates (HS) side chains. B) GC Opa-induced HSPG signaling has been studied in Chang conjunctival epithelial cells (a), where Opa-HSPG interaction triggers activation of phosphatidylcholine phospholipase C (PC-PLC), leading to acidic sphingomyelinase (ASM) activation through diacylglycerol (DAG) and eventually uptake of GC. In Hela and CHO cells (b), Opa-HSPG interaction, facilitated by the vitronectin (VN) bridged integrin αvβ5 signaling leads to protein kinase C (PKC) activation. In Hep-2 larynx carcinoma cells (c), OpaC-HSPG interaction, facilitated by the fibronectin (FN) bridged integrin α5β1 signaling leads to PKC activation. Both pathways (b, c) are involved in the efficient uptake of GC in corresponding cell lines. Full arrows, direct activation of the downstream pathway. The dashed arrows, unknown downstream pathway.

The human asialoglycoprotein receptor (ASGP-R) is a membrane glycoprotein belonging to C-type lectin. ASGP-R recognizes terminal asialylated galactose or N-acetylgalactosamine residues and mediates clathrin-dependent endocytosis [72]. Using hepatoma cell line HepG2, Porat at al. showed that GC producing LOS with lacto-*N*-neotetraose-terminal bind specifically to ASGP-R, and the binding enhanced the expression of ASGP-R [73]. GC-induced increase in the surface level of ASGP-R was also observed in primary human urethral epithelial cells (PHUECs) [74]. Furthermore, the interaction of ASGP-R with the lacto-*N*-neotetraose-terminal of gonococcal LOS has been shown to play a role in GC invasion into PHUECs in culture, by recruiting clathrin to the adherence site of GC microcolonies. Inhibition of clathrin-mediated endocytosis inhibited GC invasion into PHUECs [38].

The members of the ErbB family, epithelial growth factor receptor (EGFR, or ErbB1) and ErbB2, are commonly expressed in epithelial cells and have been shown to play a role in bacterial infection including GC. Our lab has previously shown that GC inoculation induced cellular redistribution of EGFR and ErbB2 from the basolateral surface to the apical surface under GC adherent sites of polarized epithelial cells and the activation of EGFR and ErbB2. However, GC do not directly engage EGFR and ErbB2, instead transactivate them by inducing the transcription of EGFR ligands. GC-induced transactivation of EGFR and ErbB2 contributes to GC invasion into human endometrial epithelial cell line HEC-1-B and ME180 [75] and GC transmigration across the polarized human colonic epithelial cell line T84 and HEC-1-B cell by disruption of the apical junction [76]. GC has been shown to activate several

downstream signaling cascades of EGFR, including mitogen-activated protein kinase/extracellular signal-related kinase (MAPK/ERK) [77, 78], phospholipase C γ (PLCγ) and calcium flux, and PI3K [79]. Dr. So's group found that GC recruited EGFR together with f-actin, ezrin, I-CAM and CD44 in A431 cells, in a PilE/PilC dependent manner [80]. Inoculation of GC activated PI3 kinase and Akt, which is involved in the *pilT*-dependent invasion of GC into A431 cells [81]. However, whether GC trigger above pathways through EGFR activation remains unknown.

While GC have been shown to bind to various host surface receptors through their surface molecules and trigger signaling in various experimental systems, whether these occur *in vivo*, such as during GC infection of the three cervical epithelium with heterogeneous cytoarchitecture, is unknown. The expression level and distribution of host receptors may vary in different cervical regions. It is reasonable to hypothesize that GC interaction with cervical epithelial cells and host cell signaling responses vary with the expression of host receptors and the intrinsic signaling machinery in the different types of cervical epithelial cells they encounter.

1.6 Neisseria gonorrhoeae interaction with human epithelial cells

Epithelial cells, which lines the outer surface of organs protecting hosts from the outer environment, are the front line defense against bacterial infection. When GC is first deposited onto the lumen of the genital, Pili, the long filamentous structure extending from the surface of GC, establish the initial interaction with the mucosal surface of epithelia [24]. The retraction of pili overcomes the electrostatic force at the luminal

surface of epithelia and brings the bacteria closer to the luminal surface of epithelia [82]. It has been shown that, only at this close distance, Opa proteins can interact with their receptors on the epithelial cells, CEACAM and HSPG, which establish an intimate adherence or colonization [21]. LOS also contributes to the intimate adherence by interacting with ASGP-R [73].

Following colonization, GC can invade into epithelial cells intracellularly. Intracellular GC has been observed in the gram stained cervical papsmear samples [83]. Fichorova et al. showed that immortalized endocervical, ectocervical, and vaginal epithelial cells derived from the primary cell can uptake GC [84]. GC invasion into epithelial cells in the fallopian tube organ culture has also been observed [85]. The Opa-CEACAM interaction has also been shown to contribute to GC invasion in the CEACAM-transfected Hela cell line [86]. Opa-HSPG mediated invasion has been shown in various epithelial cell lines such as ME-180 and CHO-K1 [67, 87]. Our lab has previously shown that the lacto-*N*-neotetrose in LOS is required for GC invasion [39]. Furthermore, GC can manipulate the distribution and activity of the epidermal growth factor receptor (EGFR) in the polarized HEC-1-B cells to facilitate invasion [75].

The fate of GC inside the epithelial cells remains unclear. It has been shown that a subpopulation of GC can survive intracellularly by resisting the proteolytic activity of host lysosomes with the help of Porin [42]. The type 2 IgA1 protease secreted by GC

can also promote intracellular survival of GC [88]. Using primary human cervical epithelial (pex) cells, Edwards et al showed GC intracellular survival is affected by the level of the female sex hormones estrogen and progesterone in culture [89].

The intracellular survival of GC may eventually lead to GC transcytosis or penetration into subepithelial tissues. McGee et al. first observed penetration of GC into subepithelial tissue in fallopian tube organ culture by transmitted electron microscopy (TEM) [85, 90]. GC transmigration across epithelial cells has also been observed in various cell line culture. Ilver et al. described the transcellular passage of GC in three cell line cultures, HEC-1-B (endometrial adenocarcinoma), ME-180 (cervical carcinoma) and Chang conjunctiva, which involves pili phase variation [91]. Data from our lab showed that GC can disrupt the apical junction in polarized T84 and HEC-1-B cell by activating EGFR, which facilitates transmigration [76]. Wang et al. showed the transcytosis of GC expressing CEACAM-binding Opa through the polarized epithelial T84 cell requires the cytoskeleton and motor proteins [92]. Opa-CEACAM interaction has been shown to mediates GC transcytosis across T84 cell culture [93]. However, data from our lab and Dr. Stein's lab show that Opa expression reduces the level of GC transmigration in polarized human epithelial cell line models as well as human endocervical tissue culture [94, 95]. Stein et al. suggest that Opa expression reduces the level of transmigration across T84 cell culture by inducing CEACAM redistribution [94]. Our lab showed that GC can transmigrate across polarized T84 epithelial cells and polarized endocervical epithelial cells in tissue explants by activating the actin motor non-muscle myosin II (NMII), and the

expression of CEACAM-binding Opa reduces the level of transmigration [95]. The results of studies on the role of GC surface molecules on infection vary with GC strains and infection models that were used. Despite the inconsistency, taken together, these data showed that GC can use phase variation of its surface molecules to manipulate epithelial cell responses and facilitate transmigration.

GC in the paracellular space between epithelial cells have also been observed in three different cell line culture by TEM [91], suggesting another route of transmigration across the epithelium. Ward et al. observed a population of GC in between epithelial cells in fallopian tube organ culture [96, 97]. However, whether GC penetrate into subepithelial tissues preferentially through an intracellular route or a paracellular route is unknown. The mechanism underlying GC penetration remains to be elucidated.

GC has been shown to induce exfoliation of epithelial cells to facilitate penetration and infection in fallopian tube organ culture [98], cell line culture[62], mouse model [61], and endocervical tissue explant model [95]. However, understanding of the underlying mechanism remains limited. Dr. Hauck's group first showed that Opa-CEACAM interaction inhibited epithelial exfoliation by increase the expression of CD105 and downstream activation of integrin β1 in both human cell line and transgenic mouse model that expresses CEACAM [61, 62]. The results from our lab showed that expression of CEACAM-binding Opa reduces epithelial exfoliation by inhibition of GC-induced calcium flux, NMII activation, and epithelial cell-cell

junction disruption in cell line and endocervical tissue explant models [95]. Exfoliation naturally occurs during epithelial turnover, which is controlled by a balance between eliminating damaged cells and replenishing new cells while maintaining the integrity of the epithelium [99]. Epithelial exfoliation is also a part of the defense mechanism against infection: eliminating epithelial cells colonized or damaged by pathogens. However, epithelial exfoliation induced by pathogens may leave unsealed gaps in the epithelium, especially the single-layered columnar epithelium, which may provide a portal for pathogens to reach subepithelial tissues. A similar process has been observed in the case of uropathogenic *Escherichia coli* (UPEC) infection in the bladder [100, 101]. However, epithelial exfoliation does not seem to be sufficient to eliminate UPEC infection. In contrast, it may expose the underlying epithelium to UPEC. The mechanism of epithelium turnover and pathogen-mediated manipulation of this process for infections have been studied extensively in intestine epithelium. However, the turnover of the cervical epithelium and its regulation is unknown.

Despite the numerous studies on GC-epithelial interaction discussed above, the mechanism by which GC infect the heterogeneous cervical epithelium remains elusive, partly because most previous research was done in experimental systems that did not mimic human cervical epithelium. Consequently, whether GC modulate the above infection processes, colonization, invasion, penetration, and epithelial exfoliation, in different types of cervical epithelial cells in the same way as shown using currently available infection models is unknown.

1.7 Epithelial cell-cell junction and its regulation

The integrity of epithelium is essential for the protection of the host from the pathogen. Epithelial cells are organized into the epithelium by the formation of junctional complexes with neighboring cells [102]. Epithelial junction formation keeps the neighboring cells in strict contact to form single- or multiple-layered three dimensional architecture. There are two major types of epithelial junction complexes, adherens junction (AJ) and tight junction (TJ).

In epithelial cells, one of the major components of adherens junction is a single pass transmembrane protein, E-cadherin, and various adaptor proteins regulate and connect E-cadherin to the actin cytoskeleton [103]. The extracellular domain of E-cadherin consists of five repetitive subdomains called cadherin repeats (EC). Each EC contains the calcium-binding sequence. E-cadherin mediates cell-cell contact by intercellular homophilic interaction of EC domains in a calcium-dependent manner. Thus, adherens junction is characterized by a 10-20 nm distance between the plasma membrane of two neighboring cells. The cytoplasmic domain of E-cadherin binds a number of proteins, collectively called catenins. β-catenin is associated with E-cadherin and also α-catenin through p120 catenin ($p120^{ctn}$). α-catenin has been shown to link the E-cadherin-catenin complex to the actin cytoskeleton through unknown components. The binding of E-cadherin with catenins regulates the stability of the adherens junction [104]. The binding of E-cadherin with β-catenin is enhanced by the phosphorylation of three serine residues (S684, S686, S692) in the cytoplasmic domain of E-cadherin, which is mediated by casein kinase II (CKII) and glycogen synthase kinase 3β (GSK-3β) [105-

107]. In contrast, the phosphorylation of tyrosine residues (Y489, Y654) in β-catenin reduces the affinity to E-cadherin, and the phosphorylation at Y142 reduces the affinity to α-catenin. These phosphorylation has been shown involving abelson (Abl) kinase at Y489 [108], $pp60^{c\text{-}src}$ at Y654 [109], and Fer kinase at Y142 [110]. The tyrosine phosphorylation of β-catenin is balanced by tyrosine phosphatase, such as SHP1 (PTP1B, protein tyrosine phosphatase 1B) [107, 111]. Without binding to β-catenin, the cytoplasmic domain of E-cadherin becomes unstructured, which leads to its internalization and degradation [112-114].

Similar to the adherens junction, the tight junction is composed of transmembrane proteins, occludins, claudins and junctional adhesion molecules (JAMs), and adaptor proteins connecting transmembrane proteins to the cytoskeleton. Occludin and claudin are tetraspan proteins with two extracellular loops, mediating intercellular homophilic interactions with neighboring cells. JAMs are single-pass transmembrane proteins, which have two extracellular immunoglobulin-like domains [115]. The tight junction is characterized by an intercellular space ranging from 0.2 to 0.5 μm. Zonula occludens (ZOs) are the best-studied adaptor proteins in tight junction. ZO proteins are peripheral membrane-associated components of the tight junction, which belongs to the membrane-associated guanylate kinase (MAGuK) homolog family. The C-terminus of occludin and claudin bind to the PDZ-1 domain of ZO proteins, which is required for directing occludin and claudin to the tight junction [116]. JAMs also interact with ZO proteins. The permeability of the tight junction is regulated by a wide range of growth factors, cytokines, and hormones. Protein kinase C (PKC) mediated

phosphorylation of occludin and tyrosine phosphorylation of ZO-1 have been suggested to decrease the epithelial permeability [116]. Actomyosin rings associated with the tight junction and it's regulation by myosin light chain (MLC) also play important roles in tight junction regulation [117]. Two functions have been proposed for the tight junction, fence function, and gate function. The fence function is the ability of the tight junction to prevent the lateral movement of membrane molecules between the apical and basolateral domains. Gate function is the ability of the tight junction to control the paracellular permeability of the epithelium [104].

In the epithelium consisting of single-layered polarized columnar epithelial cells, such as the intestinal epithelium, the apical junction (AJ) is formed to maintain the integrity and polarity of the epithelium, forming apical and basolateral domain [102]. The apical and basolateral membrane have distinct membrane and protein components which are generated and maintained by the polarized membrane trafficking machinery. The polarized trafficking machinery includes secretory and endocytic pathways that sort and delivers different proteins and lipids to the apical or basolateral membranes [118]. The apical junction is composed of both the tight junction and the adherens junction and is located close to the lumen surface of polarized epithelial cells, with the tight junction at the apical end of the lateral membrane domain. Assembly of the adherens junction leads to the formation of the tight junction to stabilize epithelium. However, the depletion of E-cadherin by RNA interference in Madin-Darby Canine Kidney (MDCK) Epithelial Cells did not lead to the disruption of the tight junction,

indicating that the adherens junction formation plays a role in apical junction assembly, but not required for maintenance [119].

Rho family small GTPases, such as Rho, Rac, and Cdc42 and Rap1, play important roles in cell-cell junction formation, maintenance, and dynamics. During the adhesion junction establishment and maintenance, the initial homophilic trans-interaction of E-cadherin between neighboring cells eventually activates Rac through recruitment of the tyrosine kinase c-Scr. The recruitment of c-Src leads to phosphorylation of Crk adaptor protein and C3G, one of the Rap1-GEF (Guanine nucleotide exchange factors), and subsequent activation of Rap1. Rap1 activation mediates PI3K activation, and eventually Rac activation through Vav2 [120, 121]. Such Rac activation together with Cdc42 stabilizes adherens junction by inhibiting E-cadherin endocytosis through reorganization of the actin cytoskeleton [120, 122]. Once stable adhesion junction is established, Cdc42 comes into play in the regulation of adhesion junction stability by controlling adhesion junction components turnover. Cdc42 also activates N-WASP, and together they interact with Arp2/3 complex to promote polymerization of the branched actin filament. This process has been shown to be required to maintain adherens junction integrity.

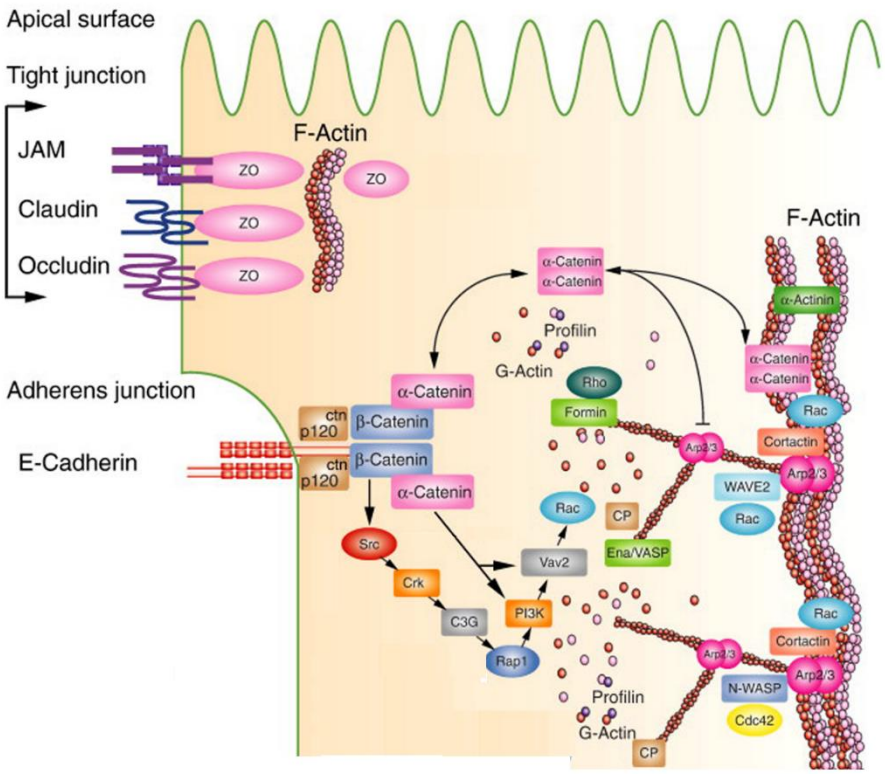

Figure 5. Organization and regulation of the tight junction (TJ) and the adherens junction (AJ) (Modified based on [121])

The tight junction is located at the apical end of the lateral membrane. Tight junctions are composed of transmembrane proteins, JAM, claudin and occludin, and an adaptor protein, ZO. ZO proteins connect tight junction to the actin cytoskeleton. E-cadherin is the major transmembrane proteins of the adherens junction in epithelial cells. E-cadherin is connected to p120 catenin, which interacts with β-catenin and α-catenin. β-catenin and α-catenin connect the adherens junction to the actin cytoskeleton and regulates the assembly and disassembly of the adherens junction through small GTPases and formin and Arp2/3 mediated actin polymerization.

The distinct cytoarchitecture of endo and ectocervical epithelia is maintained by differential epithelial cell-cell junction complexes and organization. The multiple layers of stratified squamous epithelial cells covering the ectocervix are held together mostly by adherens junction [123]. Visualized by SEM, the luminal layer of ectocervix is flattened and appears to be detached from the layers underneath [123, 124]. Shown by TEM and immunofluorescence, the most luminal layers (three to four layers) are cornified and lose cell-cell contact, thus permeable to mucosal IgG. The adherens junction staining is absent from the luminal layers and only detected three to four layers from the luminal surface, present through the intermediate, suprabasal and basal layers. Staining of tight junction proteins, claudin-1, JAM 3, and ZO-1 also was also detected most abundantly in the intermediate, suprabasal and basal layers of the ectocervical epithelium [123, 125].

The single-layered polarized epithelium covering the endocervix possesses the classical apical junction. SEM visualized abundant microvilli at the apical surface of endocervical epithelial cells [126]. TEM visualized the tight and adherens junctions located close to the apical surface between neighboring cells with the tight junction on the top, showing a classical columnar epithelial morphology. Because of the formation of the tight junction, the endocervical epithelium is not permeable to luminal IgG. Immunofluorescence microscopy showed staining of claudin-1, occludin, ZO-1, and E-cadherin between epithelial cells, but not at the basal membrane attached to the extracellular matrix (ECM) [123].

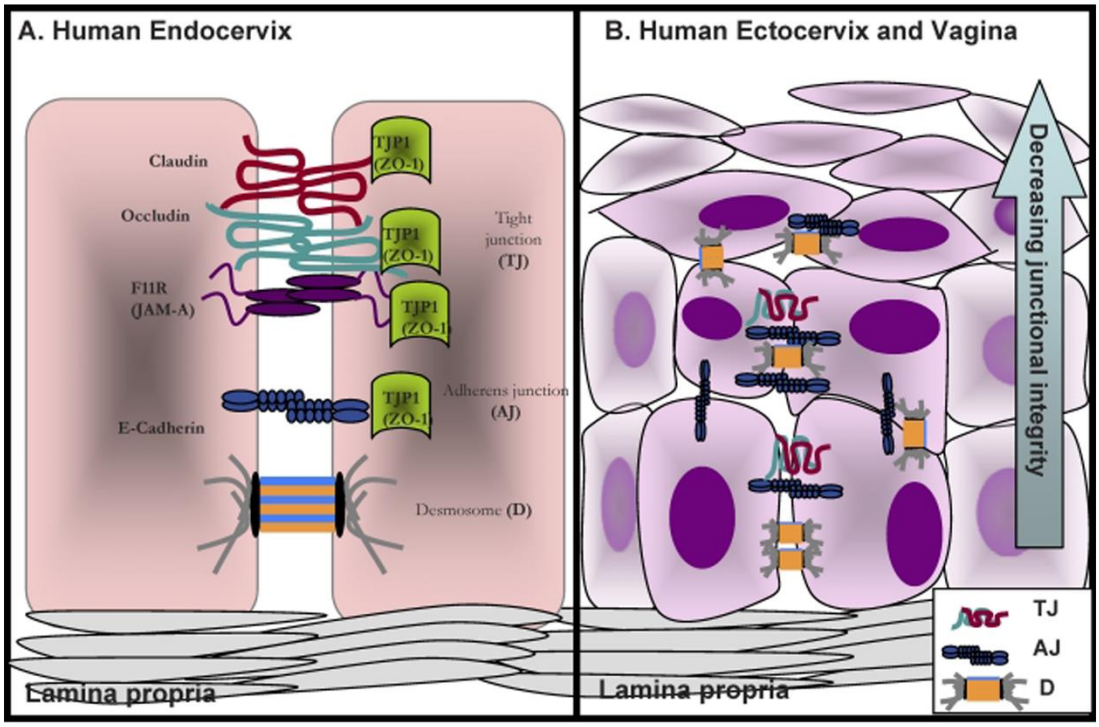

Figure 6. Organization of cell-cell junction complexes in the human cervical epithelium [123]

A schematic diagram of the cell-cell junction organization in the endocervix and ectocervix. A) The paracellular space of the endocervical epithelium is sealed by classic apical junctions composed of the tight junction (claudin, occludin, JAM, and ZO-1) and the adherens junction (E-cadherin). Neighboring cells are also connected by desmosomes. B) The parabasal and basal layers of epithelial cells in the ectocervix form the adherens junction, but the most luminal layers of the ectocervical epithelium gradually lose cell-cell contact and the expression of adherens junction proteins.

It has been shown that cell-cell junction is a frequent target of gut pathogens to breach the epithelial barrier and to establish infection. Enteropathogenic *E. coli* (EPEC) has been shown to deliver effector proteins, EspM, EspF, and Map, into intestinal epithelial cells causing disruption of the tight junction and consequently the epithelial integrity [127]. EspF has been shown interacting with N-WASP and the endocytic regulators sorting nexin 9 (SNX9), modifying the tight junction through the actin cytoskeleton and the endocytic pathway [128]. Map has been shown to activate Cdc42, modifying cell-cell junction through actin remodeling [127]. EspM has been shown to disrupt the tight junction by activating RhoA [129] and subsequent NMII. Similarly, *Salmonella Typhimurium* (*S. Typhimurium*) and *Helicobacter pylori (H. pylori)* also deliver effector proteins into intestinal epithelial cells, such as SopB and SopE for *S. Typhimurium* and CagA for *H. pylori* which target myosin light chain (MLC) to disrupt the tight junction and the adherens junction [99].

However, the effect of GC infection on cell-cell junction has not been studied in details. Our lab has shown that GC can disrupt the apical junction to facilitate GC transmigration in both polarized HEC-1-B and T84 cell lines. GC induce the junction disruption by activating EGFR [76] and NMII [95]. However, it remains unknown whether GC disrupt epithelial cell-cell junctions of the human cervical epithelial cells *in vivo* using similar mechanisms. The distinct properties of cell-cell junctions in the ecto and endocervical epithelia potentially alter the strategy that GC use to infect corresponding cervical regions. Moreover, the organization of cell-cell junction in the

TZ epithelium has not been examined, despite the fact that penetration [15] and high level of colonization of GC at the TZ has been shown [20] [124].

1.8 The role of the actin cytoskeleton in Neisseria gonorrhoeae infection

The actin cytoskeleton regulates the remodeling of the plasma membrane in response to pathogen infection at pathogen-host cell interface. It also regulates the dynamics of cell-cell junction assembly and disassembly, which can also be exploited by pathogens to facilitate infection.

The actin cytoskeleton has been shown to play an important role in GC infection in epithelial cells, but the detailed mechanism is still lacking. Edwards et al. showed that GC inoculation induced extensive membrane ruffling and cytoskeleton rearrangement in the primary endocervical and ectocervical epithelial cells [130]. Griffiss et al. showed that GC use both Opa and Pili to induce microvilli elongation at the surface of HEC-1-B cells [131]. Our lab has previously shown that the lacto-*N*-neotetraose in LOS induced elongation of microvilli warping around GC and form the intimate interaction between GC outer membrane and the plasma membrane of ME180 cells, which leads to the uptake of GC [39]. Grassme et al. showed that Opa promoted bacterial entry in an actin polymerization-dependent manner, as treatment of cytochalasin D that disrupts the actin cytoskeleton inhibited GC invasion [132]. Dr. So's group showed that pili also played a role in inducing dramatic membrane microvilli and cortical plaque [133, 134]. There is no effector protein secreted by GC discovered so far. GC entry into epithelial cells is shown to be mediated by the

bacterial surface molecule and its interaction with host receptors, which fits the zipper mechanism. But the membrane ruffling and microvilli formation observed by multiple groups argue against it [59]. As the membrane ruffling and microvilli formation are mediated by the actin cytoskeleton, GC targeted actin regulators have not been identified. The role and underlying mechanism of actin reorganization for GC infection remain unclear.

The plasma membrane remodeling induced by pathogens has been studied the most in the process of bacteria entry into non-phagocytic cells, by stimulating endogenous uptake processes, such as phagocytosis and macropinocytosis. Such processes all involve plasma membrane protrusion driven by Arp2/3 complex-mediated actin polymerization [135]. Arp2/3 complex is one of the actin nucleators and is composed of seven subunits, including Arp2, Arp3, and five additional subunits, ARPC1-ARPC5 (actin related protein complex 1-5). Arp2/3 complex is recruited and positioned at the sides of existing actin filament by actin nucleation-promoting factors (NPF), such as N-WASP and cortactin. This allows the Arp2/3 complex to initiate actin polymerization to generate branched actin networks, which drives membrane protrusion [136]. The Arp2/3 complex-mediated bacteria uptake is divided into two types of mechanisms, zipper and trigger mechanism [135]. The zipper mechanism is best studied in *Listeria monocytogenes* uptake, which is induced by the interaction of bacteria surface molecules with host receptors. In this case, induced plasma membrane protrusion formed by actin cytoskeleton reorganization is limited and closely surrounding the bacteria. The trigger mechanism is best studied in *Salmonella enterica*

serovar *Typhimurium (Salmonella)* and *Shigella flexneri*. It is stimulated by the injection of bacterial effector proteins into host cells through type III secretion system (T3SS). Injected effector proteins trigger actin reorganization, forming actin-rich membrane ruffles, which leads to the uptake of bacteria by macropinocytosis.

The actin cytoskeleton is linked to the apical junction and the adherens junction in polarized and non-polarized epithelial cells. The perijunctional actin filaments form the cortical belt at the apical junction, which is required for formation of the apical junction and the maintenance of the polarized epithelial barrier. Disruption of the actin cytoskeleton by cytochalasin D or latrunculin A increases the permeability of polarized epithelial monolayers [137]. E-cadherin, the major component of the adherens junction, has been shown to be coimmunoprecipitated with Arp2/3 complex and cortactin [121]. The adaptor protein of the adherens junction, α-catenin, links E-cadherin to the actin cytoskeleton as monomers, while homodimers of α-catenin have been shown to interact with Arp2/3 complex and regulate actin polymerization [104, 107, 138]. Arp2/3, N-WASP, and cortactin have been found to be localized at the tight junction as well [121]. Taken together, the dynamics of the actin cytoskeleton at the apical junction can regulate the dynamics of apical junction assembly and disassembly, consequently modulating epithelial cell polarity and barrier function.

The actin motor protein myosin is a major component in the perijunctional actin ring. Myosin converts the energy from ATP hydrolysis to mechanical force, mediating

static tension and contractility of actin filament [139]. Non muscle myosin II (NMII) is the major type of myosin expressed in the epithelial cells and is enriched at the apical junction. The structure of NMII is similar to the myosin expressed in muscle cells, consisting of two heavy chains, which are responsible for the ATP hydrolysis, actin filament binding and oligomerization, and two essential light chains and two regulatory light chains (MLC), which are responsible for NMII activation by phosphorylation. Multiple kinases have been reported to phosphorylate MLC, including myosin light chain kinase (MLCK) and Rho-dependent coiled-coil kinase (ROCK). MLCK is activated by calcium-bound calmodulin. ROCK is activated by the small GTP-binding protein RhoA. The phosphorylation of MLC mediated by both ROCK and MLCK has been linked to apical junction disassembly and increased epithelial permeability. *H. pylori* and EPEC have been shown to disrupt the apical junction by inducing MLCK mediated NMII activation [99, 139, 140]. Our lab has shown that GC induce activation of NMII by MLCK, leading to apical junction disruption and GC transmigration across polarized epithelial cells [95].

Whether myosin-mediated contraction plays any role in the cell-cell junction of non-polarized or stratified epithelial cells, like the ectocervical epithelial cells, is unknown. Furthermore, how non-polarized epithelial cells change morphology by reorganization of the actin cytoskeleton in response to pathogens are also not well studied. Polarized epithelial cells are known to form densely packed microvilli at the apical surface, which are support by dense bundled F-actin, and these microvillar actin bundles are inserted into the actin terminal web underneath [141]. In non-polarized epithelial cells,

data from our lab and Dr. Stein's lab show that the non-polarized ME180 cells form irregular microvilli-like plasma membrane protrusion at the luminal surface, which indicates the different organization of actin cytoskeleton at luminal surface in non-polarized epithelial cells. Infection of polarized epithelium with EPEC induces microvilli disruption [142]. In contrast, GC inoculation, as described above, induces microvilli elongation in non-polarized epithelial cells. The difference in the actin cytoskeleton organization suggests different responses to GC infection in non-polarized ectocervical and polarized endocervical epithelial cells.

1.9 The advantages and disadvantages of various current GC infection models

One of the major research barriers of GC pathogenesis is the limitation of experimental models to closely mimic human infection. The majority of research on GC infection relies on immortalized mammalian cell lines. Cell lines are readily available, easy to maintain and manipulate in laboratories. However, being cancerous cell itself and completely out of the context of tissue architecture may alter the morphology, protein components and receptor distribution and expression compared to the *in vivo* scenario in human tissues. For example, the endocervix is covered with polarized epithelial cells. However, the cell line derived from cervical epithelial cancer ME-180 completely lose the ability to polarize and form the apical junction in culture. The origin of some cell lines used is not the natural infection sites of GC. For example, the colon epithelial cell line T84 has been used to study GC infection in polarized epithelial cells, because of the ability of T84 cells to polarize in culture. Consequently, different cell lines used for studies generate different and sometimes

conflicting results. It is unclear whether results obtained from cell line models can be applicable for explaining infection *in vivo*.

Primary cervical epithelial cell culture has been developed and has generated interesting and potentially physiological relevant data [29, 130]. However, primary cells isolated from the human cervix, again are removed from their tissue architecture and are not capable of polarizing to the level as epithelial cells in the endocervix. Fallopian tube organ culture has been enabling us to better understand GC infection in this particular location, which associates with PID [85, 143]. However, the fallopian tube epithelium is distinct from the cervical epithelium. The fallopian tube organ culture maintains the polarity and columnar nature of epithelial cells and dispersion between non-ciliated and ciliated epithelial cells, unlike the cervix, where epithelial cells progressively change from non-polarized stratified to polarized columnar epithelial cells**.** Furthermore, the current experimental systems are highly controlled and consistent, which does not reflect the complicated microenvironment *in vivo, potentially* driving the phase and antigenic variation of the virulence determinants of GC. Thus results obtained from these systems may be overly simplified.

Since GC is a human exclusive pathogen, the humanized mouse model has been established by hormone treatment [5, 144] and by expressing the human CEACAM transgene [61, 145]. Vaginal inoculation of GC in these mouse models results in GC colonization for up to 10-40 days [5], thus does not cause the infection observed in

women. Besides CEACAM, mice do not express several other human specific receptors, such as CR3, which have been shown to play important roles in GC infection. While the mouse model has significantly advanced our understanding of GC pathogenesis in females, we still do not know whether data gathered from mouse models are applicable to human female infection.

Therefore, an experimental system that closely mimics the heterogeneity of the cervical epithelium in its native tissue organization and environment is essential to understand the initiation of GC infection from the human cervix and the mechanisms leading to the wide range of clinical outcomes.

Rational

This research aims to understand the mechanism by which GC establish infection at the heterogeneous mucosal surface of the human cervix, the gate of the female reproductive tract (FRT).

The unique features of GC infection in females make gonorrhea a severe threat to women's health. GC initiate infection at the mucosal surface of the cervix, the gate of FRT. The properties of the epithelium at different cervical regions vary significantly from non-polarized multiple-layered to polarized single-layered epithelial cells. Majority of GC infection in the lower part of the FRT (50-80%) is asymptomatic, thus untreated, which allows GC to further ascend to the upper genital tract, causing severe complications. The penetration of GC through the cervical epithelium into sub-epithelium tissues, which has been shown previously, can lead to symptomatic and disseminated gonococcal infection (DGI). However, whether the heterogeneous cervical epithelia affect GC infection and how asymptomatic, localized GC infection in the cervix lead to a wide range of clinical outcomes is unknown. Thus, I focus my Ph.D. research on GC infection in human cervix. Because there is no experiment system that can mimic the heterogeneous epithelia of the human cervix, previous studies using cell line and mouse models give rise to conflicting results. To overcome this barrier, I developed a human cervical tissue explant model that preserves the *in vivo* properties of the human cervical epithelium and mimics *in vivo* GC infection processes when inoculated with the bacteria. This tissue explant model enabled me to

examine the impact of distinct properties of cervical epithelial cells at different anatomical regions on GC infectivity and infection mechanisms and the role of pili and Opa phase variation in GC infection of the cervix.

Central hypothesis

GC modulate infectivity, colonization or penetration, based on the GC surface structures and properties of epithelial cells, with which they interact, by inducing differential signaling and cytoskeleton responses through different host receptors. GC colonization may only lead to localized asymptomatic infection, while GC penetration into the subepithelial tissue can lead to symptomatic and disseminated infection.

Aim 1

To determine the impact of the heterogeneous epithelia of the cervix on GC infectivity.

Aim 2

To determine the roles of the Opa phase variation and Opa interaction with the host receptor CEACAM in GC infection in different cervical regions.

Aim 3

To determine the effect of epithelial cell polarity on GC infectivity.

Chapter 2: Infectivity of *Neisseria gonorrhoeae* in the human cervix varies with the properties of cervical epithelial cells and bacterial phase variable surface structures

2.1 Abstract

The epithelium is the front line defense against pathogens in the outer environment. The heterogeneity of cervical epithelium further complicates the environment GC need to overcome to establish infection. To mimic the heterogeneous cervical epithelium, the human cervical tissue explant model was first established. GC colonize and penetrate the most in the transformation zone (TZ) of the cervix. In the ectocervix, GC colonize at a high level without any penetration. In the endocervix, the level of colonization is low, but penetration is observed. Pili is required for colonization in all three cervical regions. Expression of CEACAM-binding Opa, OpaH, enhances colonization in the ecto- and endocervix, where CEACAM is abundantly expressed at the luminal surface but inhibits penetration solely in the endocervix. In contrast, expression of different Opa proteins does not affect GC infectivity in the TZ, which expresses little CEACAM. This OpaH-CEACAM interaction-mediated differential infectivity involves ITIM domain of CEACAM1 and the subsequent activation of SHP. Such CEACAM1-SHP signaling pathway leads to the inhibition of cell-cell junction disruption, epithelial exfoliation, and eventually the penetration across the cervical epithelium into subepithelium tissue. Therefore, GC modulate its infectivity between colonization and penetration based on both the properties of cervical epithelial cells and phase variation of bacterial surface structure.

2.2 Introduction

Gonorrhea, caused by Gram-negative bacterium *Neisseria gonorrhoeae* (GC), is the second most common sexually transmitted infection (STI) in the United States. The unique features of female infection make gonorrhea a severe threat to women's health. 50-80% of female infection is asymptomatic [2], leading to susceptibility to severe complications such as pelvic inflammatory disease (PID), fallopian tubes scarring and blockage, with subsequent ectopic pregnancy and infertility. An upsurge of multidrug-resistant strains of GC further complicates gonorrhea treatment [5]. However, the mechanism by which GC and other STI pathogens interact with the human female reproductive tract (FRT) and cause a wide range of clinical outcomes remains elusive. A primary obstacle for a better understanding of STIs is a lack of infection models that mimic human infection.

In women, GC initiate infection primarily from the cervix, the gate of the female reproductive tract (FRT) [10]. The cervical epithelium is the first line of defense GC need to overcome to establish infection, which exhibits distinct properties at different anatomical regions. The ectocervix is the outmost part of the human cervix, line with multiple-layered stratified epithelial cells, and exposed to the outer environment. The endocervix, connecting to the upper genital tract, is the upper portions of the human cervix, covered by a single-layered polarized columnar epithelial cells. The squamocolumnar junction (SCJ), or transformation zone (TZ), is a specialized region between the ecto and endocervix. The morphology of the epithelium covering the TZ transforms from multiple-layered to single-layered, and from noon-polarized stratified

to polarized columnar epithelial cells. The ecto and endocervical epithelium display distinct organization of cell-cell junction complexes, which maintains the integrity and regulates the dynamics of cervical epithelia [123]. Clinical studies suggest that GC colonization at the ectocervical epithelium leads to asymptomatic infection [3]. In contrast, clinical studies using patient biopsies only found subepithelial GC in the TZ and endocervix [15]. However, how the heterogeneity of the mucosal surface of the cervix impacts GC infection and subsequent clinical outcomes has not been examined.

GC have evolved multiple mechanisms to cope with the heterogeneous mucosal surface in humans, including phase and antigenic variation of their surface molecules. GC can vary the structure of the lipooligosaccharide (LOS) [36, 146], turn the expression of pili on and off [23], and express any of 11 opacity-associated (Opa) protein isoforms at any time [30]. It has been shown that pili mediate the initial interaction of GC with the mucosal surface of epithelial cells [147] and that the interaction of Opa proteins with their host receptors mediate an intimate interaction. Most Opa isoforms bind to carcinoembryonic antigen-related cell adhesion molecules (CEACAMs) (Opa_{CEA}) [148] while others bind to heparan sulfate proteoglycans (HSPG) (Opa_{HSPG}) [33]. It has been shown that Opa_{CEA}-CEACAM interaction inhibited epithelial exfoliation, thus increased GC colonization in CEACAM transgenic mouse model [61]. Among the CEACAM isoforms expressed in epithelial cells, CEACAM1L is the only one harbors an immune-receptor tyrosine-based inhibitory motif (ITIM) motif in its cytoplasmic domain; while its splicing isoform CEACAM1S does not. The differential expression of CEACAM isoforms in different

anatomic regions of the FRT has been shown in patient biopsies [63]. However, the role of each of GC surface structures and their interactions with human receptors in GC pathogenesis has not been systematically examined in the human cervical epithelia.

Here, I established the human cervical tissue explant model to examine the impact of the heterogeneous human cervical epithelia and the phase variation of pili and Opa on GC infection. The human cervical tissue explants preserve the distinct cytoarchitecture of the three cervical regions *in vivo* and mimic GC infectivity observed in patient biopsies. Using this model, I found that the outcome of GC infection depends on the type of cervical epithelial cells GC interact with and the Opa isoforms GC express. Expression of Opa_{CEA} drives GC colonization on the mucosal surface of the ecto and endocervix, which express CEACAM. Furthermore, Opa_{CEA} expression suppresses GC penetration across the endocervical epithelium through inhibition of GC-induced cell-cell junction disassembly and epithelial shedding. The low expression level of CEACAM in the TZ epithelial cells abolishes the regulatory role of Opa_{CEA} expression. The above results provide a potential mechanism for the various clinical outcomes derived from localized cervical GC infection in women.

2.3 Materials and Methods

Neisseria Strains

N. gonorrhoeae strain MS11 that expressed both pili and Opa (MS11Pil+Opa+) was obtained from Dr. Herman Schneider, Walter Reed Army Institute for Research. Derivatives of this strain, MS11ΔOpa, MS11 OpaH (Opa_{CEA}, CEACAM-binding), and MS11OpaC (Opa_{HSPG}, HSPG-binding) have previously been described [149]. MS11Opa+ and MS11ΔOpa strains express similar LOS [149]. MS11 Pil+Opa+ and Pil-Opa+ colonies were identified based on their morphology using a dissecting light microscope. GC were grown on plates with GC media (Difco, BD Bioscience, Franklin Lakes, NJ) and 1% Kellogg's supplement [150] for 16-18 h before inoculation. The concentration of GC in suspension was determined using a spectrophotometer and inoculated with epithelial cells at MOI ~10.

Human cervical tissue explants

The tissue explants were cultured as previously described [151]. Briefly, cervical tissues were obtained from patients undergoing voluntary hysterectomies and received within 24 h post-surgery. Age of patients ranges from 28 to 40. Supporting muscle tissue was removed by using a carbon steel surgical blade. Remaining cervical tissue samples were cut into ~2.5 cm (L) X 0.6 cm (W) X 0.3 cm (H) pieces, incubated in 6-well tissue culture plate in cervical tissue culture media conataining CMRL-1066 (GIBCO), with 5% heat-inactivated fetal bovine serum, 2 mM L-glutamine, bovine insulin (1 μg/ml, Akron Biotech) and penicillin/streptomycin for 24 h and then in

antibiotic-free media for another 24 h, before inoculation with GC as previously described [152].

Immunofluorescence analysis of human cervical tissue explants

Individual pieces of cervical tissue explants were inoculated with GC at MOI ~10. The number of epithelial cells at the mucosal surface is determined by the area of the mucosal surface of the individual piece and the average luminal area of individual cervical epithelial cells. When indicated, tissue pieces were inoculated with GC with or without the SHP inhibitor NSC-87877 (20 μM, EMD Millipore). GC were collected by using a sterile applicator to swab GC from the plate and re-suspend GC in pre-warmed antibiotic-free cervical tissue culture media. An aliquot of the GC suspension was added directly onto each tissue piece to make an MOI = 10 bacteria to 1 epithelial cell. The cervical tissue explants were incubate at 37 °C with 5% CO2 with gentle shaking for 24 h. The infected cervical tissue explants were rinsed with antibiotic-free cervical tissue culture medium at 6 and 12 h to remove un-adhered bacteria and replace with fresh media without bacteria. Tissue explants were then fixed 24 h post inoculation, embedded in 20% gelatin, cryopreserved, sectioned by cryostat across the luminal and basal surfaces of the epithelium, stained for F-actin (Cytoskeleton), E-cadherin (BD Bioscience), CEACAMs (cross-react with CEACAM1, 3, and 6, Santa Cruz Biotechnology, Dallas, TX), SHP1 (Santa Cruz Biotechnology), SHP2 (Santa Cruz Biotechnology), phospho-SHP2 Tyr542 (Thermo Fisher Scientific) and GC by specific antibodies, and nuclei by Hoechst (Life Technologies), and analyzed using confocal fluorescence microscope (Zeiss LSM 710, Carl Zeiss Microscopy LLC) as

previously described [152]. Images of the luminal surface were randomly acquired from the ectocervix to the endocervix as single images or Z-series of 0.57 μm/image, and 3D composites obtained using Zeiss Zen software.

The level of GC colonization was quantified by two methods using confocal images: (1) percentage of the number of GC-associated luminal epithelial cells versus the total number of luminal epithelial cells through visual inspection, and (2) fluorescence intensity (FI) of GC staining per μm^2 at the luminal surface using the NIH ImageJ software. The level of GC penetration was determined by two methods: (1) percentage of the number of epithelial cells associated with GC staining at and underneath the basal membrane versus of the total number of epithelial cells through visual inspection, and (2) percentage of the FI of GC staining at sub-epithelial tissue versus the total FI of GC staining at both the subepithelium and the luminal surface in each randomly acquired image.

The level of epithelial exfoliation in the endocervix was determined by the percentage of the number of epithelial cells localized on top of the epithelial monolayer versus the total number of epithelial cells through visual inspection. Level of epithelial exfoliation in the ectocervix and the transformation zone (TZ) was determined by two methods: (1) the percentage of the thickness (μm) of the epithelium in ectocervical and TZ tissue explants with or without inoculation of GC, and (2) the percentage of

number of epithelial layers in ectocervical and TZ tissue explants with or without inoculation of GC.

The recruitment of CEACAM staining to GC microcolony was evaluated by the percentage of the number of GC microcolonies colocalizing with CEACAM staining underneath versus the total number of GC microcolonies through visual inspection.

The redistribution of E-cadherin staining from the cell-cell junction to the cytoplasm was evaluated by the fluorescence intensity ratios (FIR) of E-cadherin staining at cell-cell junction versus that in the cytoplasm in individual epithelial cells using confocal images and the NIH ImageJ software.

Each of the above results was generated from cervical tissue explants of 3-5 human subjects and >7 randomly acquired images from each cervical region and each tissue explant.

Epithelial cells and CEACAM1 transfection

HEC-1-B, a human endometrial adenocarcinoma cell line (ATCC), was maintained in Eagles MEM alpha medium supplemented with 10% heat-inactivated FBS. Cells were seeded at 3.5 $x10^5$ per 60 mm diameter cell culture dish, (Thermo Fisher Scientific) and cultured for 2 days before transfection. Cells were transiently transfected with 5

μg of a plasmid containing CEACAM1L or CEACAM1S cDNA using lipofectamine 3000 reagents (Thermo Fisher Scientific). Transfected cells were seeded at $6x10^4$ per transwell (6.5 mm diameter, 3 μm pore size, Corning) and cultured for 2 days before inoculation with GC at MOI ~10.

T84, a human colorectal carcinoma cell line (ATCC), was maintained in DMEM:Ham F12 (1:1) supplemented with 7% heat-inactivated FBS. Cells were seeded at $6x10^4$ per transwell (6.5 mm diameter, 3 μm pore size, Corning) and cultured for ~10 days until the transepithelial electrical resistance (TEER) reached ~2000Ω before GC inoculation. TEER was measured using a Millicell ERS volt-ohm meter (EMD Millipore).

Immunofluorescence analysis of epithelial cells

Transfected HEC-1-B cells were inoculated with GC at MOI of ~10 for 6 h. Cells were rinsed, fixed with 4% paraformaldehyde, permeabilized with 0.1% Triton X-100, and stained with anti-β-catenin (EMD Millipore), anti-CEACAMs (Santa Cruz Biotechnology), anti-GC antibodies, and Hoechst for nuclei. Images were randomly acquired using CFM. The level of GC adherence to cells with or without CEACAM transfection was compared by the fluorescence intensity ratio (FIR) of GC staining in CEACAM-positive cells versus CEACAM-negative cells in the same image using the same ROI. Epithelial exfoliation was quantified using xz images by the percentage of HEC-1-B cells moving above the monolayer versus the total number of epithelial

cells. The redistribution of β-catenin staining from the cell-cell junction to the cytoplasm was quantified as described for the E-cadherin in tissue explants. The results were obtained from 3-5 independent experiments and >5 randomly acquired images of each condition and each experiment.

GC transmigration assay

The assay was performed as previously described [76]. Briefly, polarized T84 epithelial cells that were pretreated with or without the SHP inhibitor NSC-87877 (20 μM, EMD Millipore) for 1 h were inoculated apically with GC at MOI ~10 for 6 h. The basolateral media were collected and cultured by plating, and the resulting colonies were counted as transmigrated bacteria.

Statistical analysis

Statistical significance was assessed by using the Student's t-test by Prism software (GraphPad Software, San Diego, CA). P-values were determined using unpaired t test with Welch's correction in comparison with no infection controls.

Ethics statement

Human cervical issue explants were obtained from the National Disease Research Interchange (NDRI, Philadelphia, PA). Human cervical tissues used were anonymized.

The use of human tissues for this research has been approved by the Institution Review Board of the University of Maryland.

2.4 Results

2.4.1 GC exhibit distinct infectivity patterns on different mucosal surfaces of the human cervix

We sought to preserve the heterogeneity of cervical epithelium by using human cervical tissue explants. Cervical tissue explants were cultured mucosal side up. Thin sections of cryo-preserved cervical tissue were sectioned, stained and analyzed using three-dimensional confocal fluorescence microscopy (3D-CFM). Images showing both the mucosal and subepithelial sides of the ectocervix, TZ and endocervix were analyzed. I identified epithelial cells on the tissue section by staining cytokeratin (Fig. 7 A), the marker of epithelial cells. The cell-cell junction was visualized by staining adherence junction protein E-cadherin (Fig. 7 B). I first used a 10X object lens to scan the mucosal surface of the cervical section from ecto to endocervix continuously. The three cervical regions were identified by the distinct features of the epithelial cells: 1) ectocervix, multiple-layered non-polarized epithelial cell, 2) TZ, multiple-layered cubical epithelial cells, 3) endocervix, single-layered polarized epithelial cells. I found that the human cervical tissue explant model can preserve the overall morphology of cervical epithelium (Fig. 7 B).

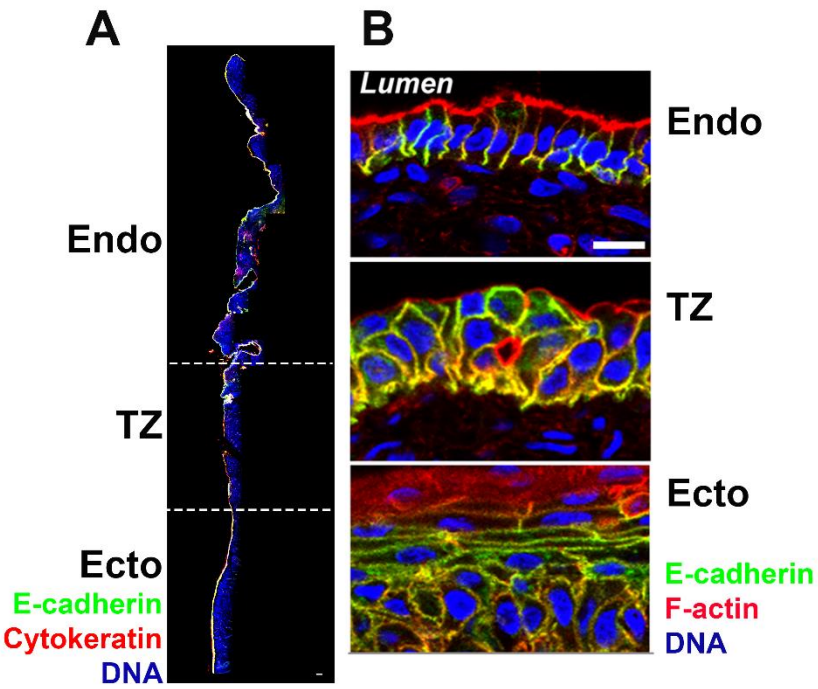

Figure 7. Human cervical tissue explants maintain the *in vivo* characteristics in culture.

Human cervical tissue explants were cultured for three days and cryopreserved. Tissue sections across the luminal and basal surface of epithelia were collected, stained for DNA, E-cadherin, cytokeratin and/or F-actin, and analyzed using CFM. (A) Representative images of the mucosal epithelial regions of cervical tissue explants obtained by combining >30 images acquired using the 10X objective. Dashed lines indicate the boundary between the endocervix and the TZ and between the TZ and the ectocervix. Scale bar, 100 μm. (B) Representative images of the epithelium of three cervical regions. Scale bar, 20 μm.

To determine whether the heterogeneity of cervical epithelium affects GC infectivity in the same way or differently, I inoculated cervical tissue explants from the same patient sample with or without MS11 Pil+Opa+, a GC strain expressing phase variable opa genes, for 24 h. Each tissue explant contains all three cervical regions and inoculated with GC at MOI~10. Unassociated bacteria were rinsed at 6 and 12 h post inoculation. Cervical tissue explants were cryopreserved and sectioned across the luminal surface to subepithelial tissue. Tissue sections were stained for GC, F-actin, and nuclei and analyzed by CFM. I used two methods to quantify the level of GC colonization using CFM images (Fig. 8 B, C): 1) the percentage of number of luminal epithelial cells associated with GC staining (Fig. 8 B), and 2) the fluorescence intensity (FI) of GC staining per μm^2 of the luminal surface of the cervix (Fig. 8 C). The two methods showed consistent results. MS11Pil+Opa+ colonize the mucosal surface of all three cervical regions. However, the level of colonization in the ectocervix and TZ is significantly higher than the endocervix (Fig. 8 B, C). Similarly, I used two methods to quantify the level of penetration: 1) percentage of the number of epithelial cells associated with GC staining below basal membrane (Fig. 8 D), and 2) percentage of FI of GC staining at and below basal membrane versus total FI of GC staining (Fig. 8 E). Penetrating GC were only detected in the TZ and endocervix, and the level of penetration into the subepithelial tissue in the TZ is significantly higher than into the endocervix. These results are consistent with clinical observation, indicating GC infection in human cervical tissue explant model mimics GC infection *in vivo*. It further suggests that GC modifies its infectivity based on the different properties of the cervical epithelial cells they encounter.

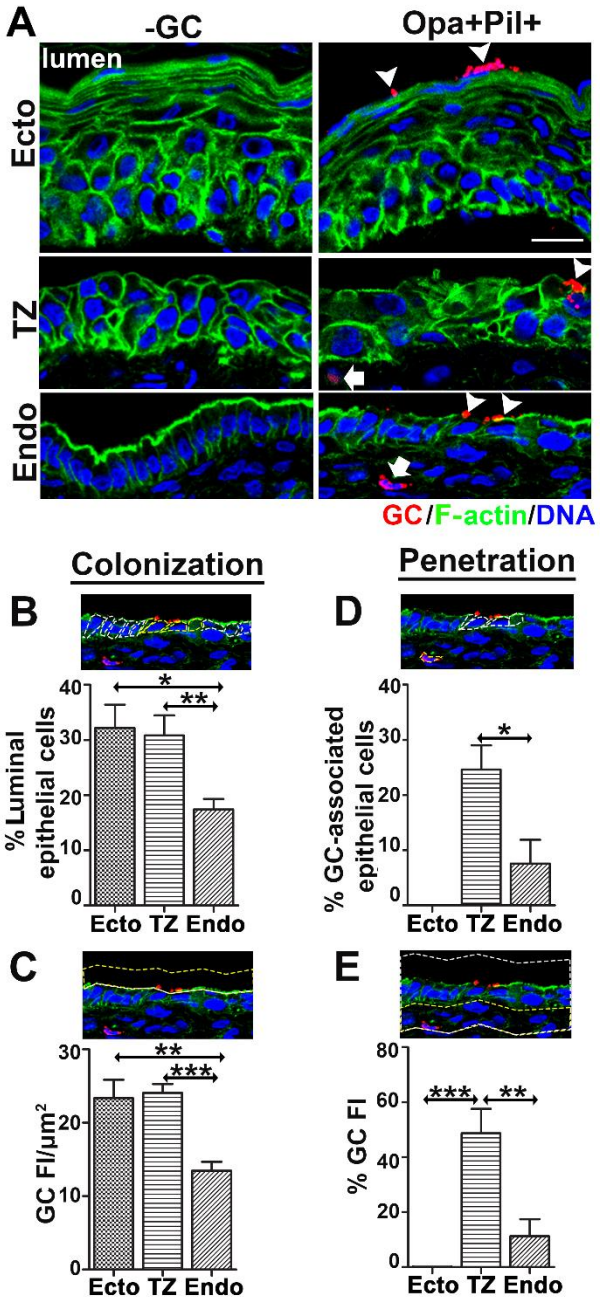
A
-GC
Opa+Pil+
lumen
Ecto
TZ
Endo
GC/F-actin/DNA
Colonization
Penetration
B
% Luminal epithelial cells
Ecto TZ Endo
C
GC FI/µm²
Ecto TZ Endo
D
% GC-associated epithelial cells
Ecto TZ Endo
E
% GC FI
Ecto TZ Endo

Figure 8. GC exhibit different levels of colonization and subepithelial penetration in the ectocervical, TZ, and endocervical epithelium.

Human cervical tissue explants were incubated with MS11 Pil+Opa+ for 24 h (MOI~10), washed at 6 and 12 h post-inoculation, and cryopreserved. Tissue sections were collected, processed, and analyzed using CFM. (A) Representative images of the three cervical regions with or without GC infection. Scale bar, 20 μm. Arrowheads, colonizing GC. Arrows, penetrating GC. (B and C) The level of GC colonization was quantified of by the percentage (±SEM) of luminal epithelial cells with GC attaching to the luminal surface (B) and by fluorescence intensity (FI) (±SEM) of GC staining per μm^2 at the luminal surface (C). (D and E) The level of GC penetration was quantified by the percentage (±SEM) of epithelial cells associating with GC at subepithelia (D) and by the percentage of GC FI (±SEM) at the subepithelia relative to the total GC FI at the epithelium (E). n=4. >20 randomly selected fields and >200 cells per cervix and condition. *p<0.05; **p<0.01; ***p<0.001.

2.4.2 Pili are required for GC colonization, and Opa phase variation regulates GC infectivity in the human cervix

Pili and Opa are major phase variable virulence determinants of GC. To examine the roles of Pili in GC infection in the cervical epithelium, I first compared the level of colonization and penetration of piliated (Pil+) and non-piliated (Pil-) MS11Opa+ in the cervical tissue explant. Compared to the MS11Pil+Opa+, MS11Pil-Opa+ failed to colonize efficiently in all three cervical regions (Fig. 9 A, B-D). And no penetration of MS11Pil-Opa+ in all three cervical regions was observed (Fig. 9. A, E-G). To examine the roles of Opa proteins in GC infectivity, I inoculated cervical tissue explants with Pil+ GC expressing phase variable Opa (Opa+) and all 11 Opa isoforms deleted (ΔOpa). The deletion of Opa significantly reduced the level of colonization in the ecto and endocervix, but not in the TZ (Fig. 9 A, B-D). In contrast, deletion of Opa significantly increased the level of penetration in the endocervix (Fig. 9 A, G). The above results indicate the Pili is essential to establish colonization in all three cervical regions; while the expression of phase variable Opa proteins regulates GC infectivity differently in the three cervical regions.

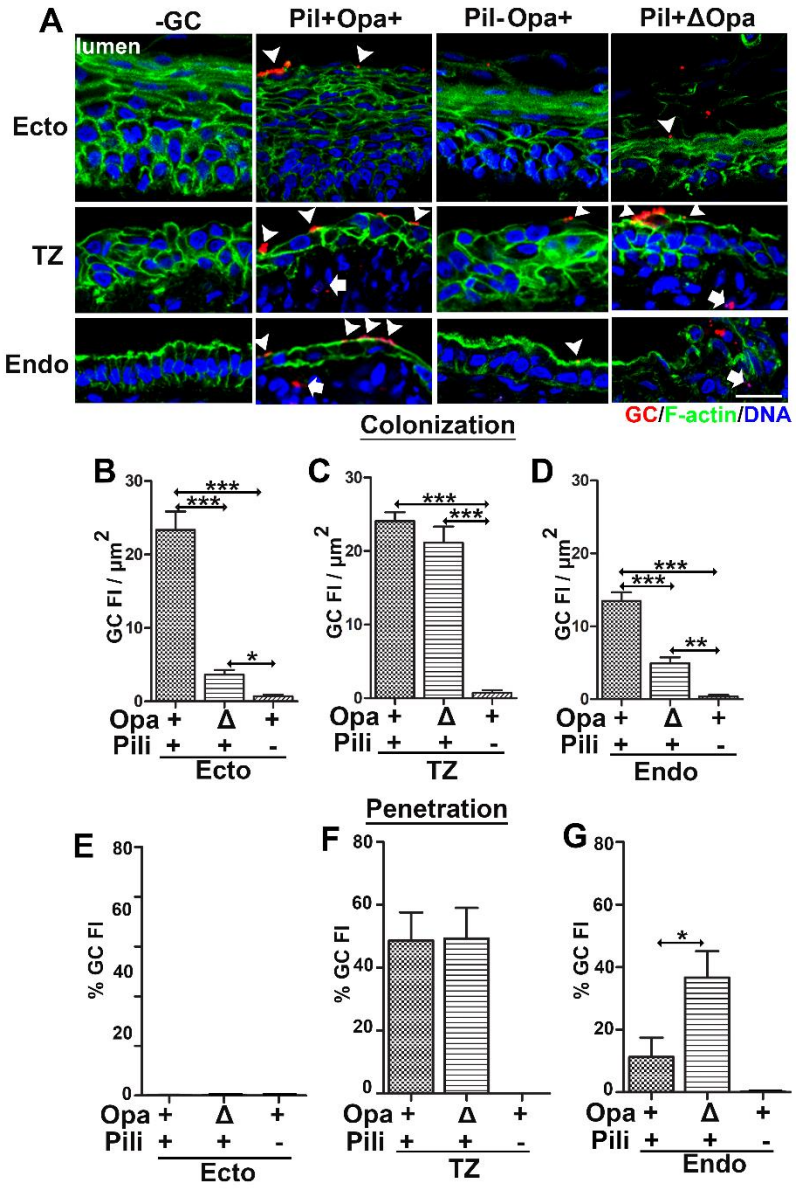
A
-GC
Pil+Opa+
Pil-Opa+
Pil+ΔOpa
lumen
Ecto
TZ
Endo
GC/F-actin/DNA
Colonization
B
C
D
GC FI / µm2
***
*
**
Opa + Δ +
Pili + + -
Ecto
TZ
Endo
Penetration
E
F
G
% GC FI

Figure 9. Pili are required for GC colonization, and Opa expression differentially regulates GC infectivity in the three cervical regions.

Human cervical tissue pieces were inoculated with GC MS11 Pil+Opa+, Pil+ΔOpa, or Pil-Opa+, processed and analyzed as described in Fig. 8. (A) Representative images of three cervical regions with or without GC infection. Arrowheads, colonizing GC. Arrows, penetrating GC. Scale bar, 20 μm. (B-D) Levels of GC colonization at the ectocervix (B), TZ (C), and endocervix (D) by GC FI per μm^2 (±SEM). (E-G) Levels of GC penetration into the subepithelia of the ectocervix (E), TZ (F), and endocervix (G) by the percentage of GC FI (±SEM) at the subepithelia relative to the total GC FI at the epithelium. n=2~4. >20 randomly selected fields and >200 cells per cervix and condition. *p<0.05; **p< 0.01; ***p<0.001.

One GC bacterium can express up to 11 different Opa isoforms, which can be categorized into two groups: 1) CEACAM-binding Opa_{CEA}, represented by OpaH, 2) HSPG-biding Opa_{HSPG}, represented by OpaC. Majority of Opa proteins expressed are CEACAM-binding Opa. I hypothesize that Opa proteins regulate GC infectivity in different cervical regions through phase variation, switch between dominant Opa_{CEA} and dominant Opa_{HSPG} expression. To test this hypothesis, I inoculated human cervical tissue explants with Pil+ MS11 expressing OpaH and OpaC that do not phase vary, as well as MS11Pil+ ΔOpa. Expression of OpaH but not OpaC significantly enhanced the level of colonization in the ecto and endocervix, but not in the TZ (Fig. 10 A, B-D). In contrast, expression of OpaH inhibited penetration only in the endocervix (Fig. 10 A, G). All three Opa isogenic strains did not penetrate in the ectocervix (Fig. 10 A, E); while penetrating at a high level in the TZ (Fig. 10 A, F). GC expressing OpaC show a similar level of colonization and penetration as GC ΔOpa. The above data suggest that Opa_{CEA} selectively enhanced the level of colonization in the ecto and endocervix, and inhibited the level of penetration solely in the endocervix. Expression of Opa_{HSPG} does not significantly affect GC infectivity in the human cervix. Intriguingly, expression of different Opa isoforms does not affect GC infectivity in TZ. Taken together, GC infectivity is regulated by both Opa phase variation and properties of different types of cervical epithelial cell.

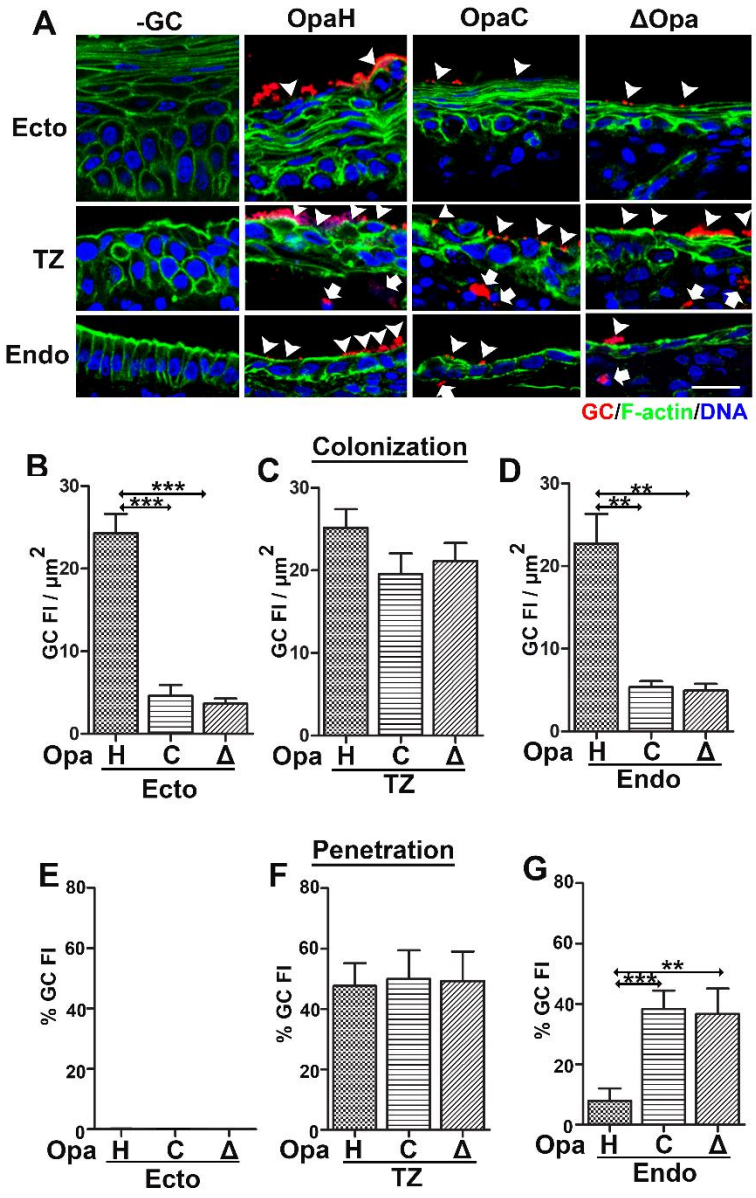
A
-GC
OpaH
OpaC
ΔOpa
Ecto
TZ
Endo
GC/F-actin/DNA
Colonization
B
C
D
GC FI / µm2
Opa H C Δ
Ecto
TZ
Endo
***
**
Penetration
E
F
G
% GC FI

Figure 10. **Opa variants differentially regulate GC colonization and penetration into the three cervical regions.**

Human cervical tissue pieces were incubated with piliated (Pil+) GC MS11 OpaH, OpaC, and ΔOpa, processed and analyzed as described in Fig. 8. (A) Representative images of three cervical regions with or without GC infection. Arrowheads, colonizing GC. Arrows, penetrating GC. Scale bar, 20 μm. (B-D) Levels of GC colonization at the ectocervix (B), TZ (C), and endocervix (D) by GC FI per μm^2 (±SEM). (E-G) Levels of GC penetration into the subepithelia of the ectocervix (E), TZ (F), and endocervix (G) by the percentage of GC FI (±SEM) at the subepithelia relative to the total GC FI at the epithelium. n=3~4. >20 randomly selected fields and >200 cells per cervix and condition. $^{**}p< 0.01$; $^{***}p<0.001$.

2.4.3 The OpaH-dependent regulation of GC infectivity involves CEACAM1L expression in cervical epithelial cells

My finding that OpaH expression affects GC infectivity in different cervical regions suggests the differential role of its epithelial receptor CEACAM in different cervical regions. To test this hypothesis, I first examined the expression and distribution of CEACAM by CEACAM fluorescence intensity (FI) per cell. I used an antibody cross react with CEACAM1, 3 and 6 (Fig. 11 A, B). Without inoculation with GC, the TZ epithelial cells express low-level CEACAM, with most puncta staining in the cytoplasma. The endocervical epithelial cells show strong staining at the apical surface. The ectocervical epithelial cells show strong staining at luminal surface and strong puncta staining in cytoplasma. The lack of CEACAM expression provides a potential explanation of the similar infectivity displayed by GC OpaH, OpaC and ΔOpa in the TZ.

To answer the question that whether the expression of Opa_{CEA} regulates GC infectivity through differential interaction with CEACAM in three cervical regions, I examined the recruitment of CEACAM by percentage of GC microcolonies colocalized with CEACAM staining underneath. In the endocervix, around 58% microcolonies of GC Pil+ OpaH colocalized with CEACAM staining (Fig. 11 C, D, arrowheads), significantly higher than the 20% in the TZ, which expresses low-level CEACAM. It is also significantly higher than the level induced by GC Pil+ΔOpa and GC Pil+OpaC, which displays less than 10% colocalization in both endocervix and TZ. These

observations indicate a direct interaction of Opa_{CEA} with CEACAM and its role in GC infectivity modulation.

To test the hypothesis further, I utilized a human endometrium epithelial cell line, HEC-1-B, which does not express endogenous CEACAM [153]. CEACAM1 is the only CEACAM expressed in epithelial cells that has a cytoplasmic domain. CEACAM1L harbors an ITIM motif in the cytoplasmic domain; while the isoform CEACAM1S lacks it. I transiently transfected HEC-1-B with CEACAM1L and CEACAM1S and inoculated transfected cells with MS11Pil+OpaH and ΔOpa for 6 h on transwell. I examined the level of adhesion of GC by the GC fluorescent intensity ratio (FIR) at the area with CEACAM1 expression to that without CEACAM1 expression using the same ROI in the same image with all z series slides projected onto it (Fig. 11 E, F). GC Pil+OpaH adhered to the CEACAM1L-expressing area twice as much as the area without CEACAM1L expression, while GC Pil+ΔOpa adhered to the area with or without CEACAM1L expression at a similar level. In the CEACAM1S transfected cells, both MS11Pil+OpaH and ΔOpa adhere to the area with or without CEACAM1S expression similarly (FIR ~ 1). Taken together, the above data suggest the Opa_{CEA}-dependent regulation of GC infectivity in different cervical regions involves CEACAM1L expression.

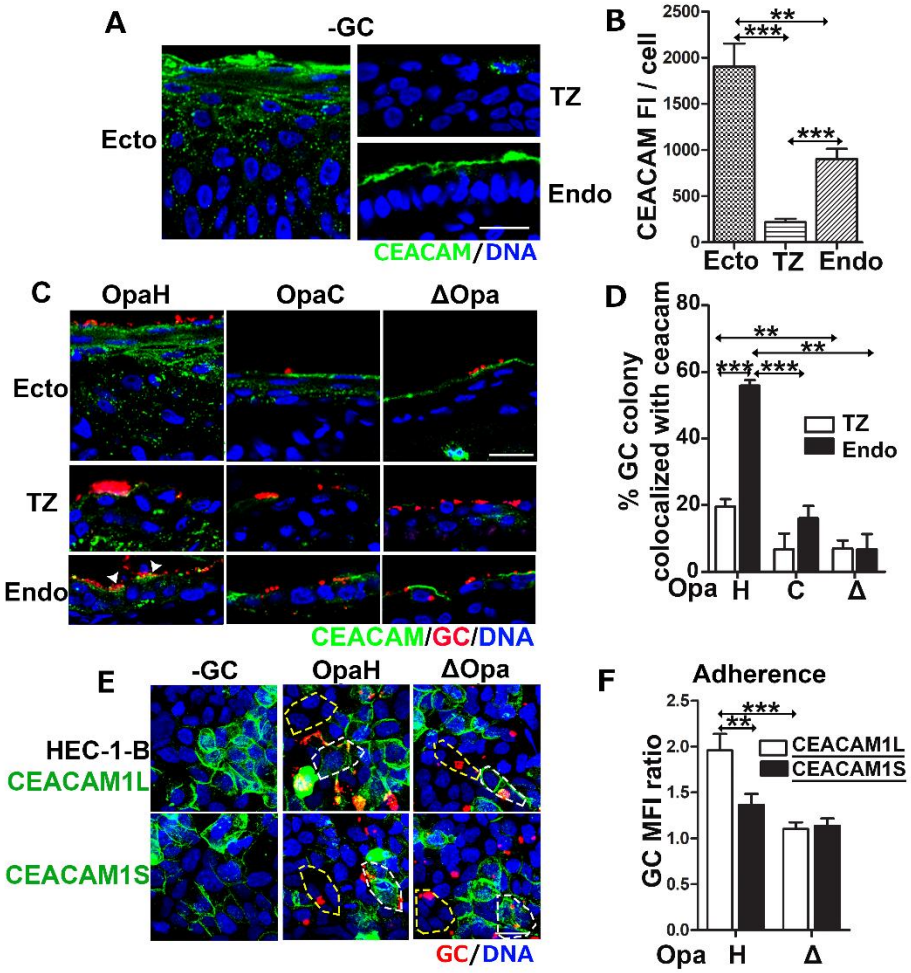
A
-GC
Ecto
TZ
Endo
CEACAM/DNA
B
CEACAM FI / cell
2500
2000
1500
1000
500
0
**
***
***
Ecto TZ Endo
C
OpaH
OpaC
ΔOpa
Ecto
TZ
Endo
CEACAM/GC/DNA
D
% GC colony colocalized with ceacam
80
60
40
20
0
**
**
***
***
TZ
Endo
Opa H C Δ
E
-GC
OpaH
ΔOpa
HEC-1-B
CEACAM1L
CEACAM1S
GC/DNA
F
Adherence
GC MFI ratio
2.5
2.0
1.5
1.0
0.5
0.0
***
**
CEACAM1L
CEACAM1S
Opa H Δ

Figure 11. Regulatory roles of OpaH depend on the expression of CEACAML in the human cervical epithelial cells.

(A) Representative CFM images of uninfected human cervical tissue explants stained with the anti-CEACAM antibody (reacting with CEACAM 1, 3, and 6). (B) Levels of CEACAM expression measured by the FI (±SEM) of CEACAM per cell. (C) Representative CFM images of human cervical tissue explants inoculated with GC MS11Pil+ OpaH, OpaC, and ΔOpa and stained for GC and CEACAMs. Arrowhead, GC microcolonies colocalizing with CEACAM staining. (D) The spatial relationship of GC with CEACAMs was quantified by the percentage of GC microcolonies colocalizing with CEACAM staining. (E) Representative CFM images of HEC-1-B cells transiently transfected with or without CEACAM1L or 1S and infected with GC MS11 Pil+ OpaH or Pil+ΔOpa GC. White dashed lines circle CEACAM-expressing cells. Yellow dashed lines circle cells that do not express CEACAMs. (F) Levels of GC adherence to CEACAM1L or 1S-expressing cells were compared to those that did not express CEACAMs by the FIR (±SEM) of GC on CEACAM-positive cells versus CEACAM-negative cells in the same images using the same ROI. Scale bar, 20 μm. n=3~4. >4 randomly selected fields and >200 cells per condition and cervixes. $**p < 0.01$; $***p<0.001$.

2.4.4 The OpaH-dependent regulation of GC infectivity involves activation of SHP

The enhanced adherence of MS11Pil+OpaH in CEACAM1L-expressing cells compared to CEACAM1S-expressing cells suggests the role of the ITIM motif in the cytoplasmic domain of CEACAM1L. CEACAM1L has been shown to recruit and activate the tyrosine phosphatase SHP1/2 [154]. Thus, I hypothesize that SHP1/2 play a role downstream of Opa_{CEA}-CEACAM1L dependent regulation of GC infectivity. I used an SHP1/2 enzymatic inhibitor NSC-87877 to test this hypothesis [155]. The treatment of GC alone with the inhibitor did not affect the growth rate of GC (Fig. 12). The treatment of the cervical tissue explant with SHP1/2 inhibitor significantly reduced the level of colonization of OpaH in the ecto and endocervix but not the TZ compared to the inoculation with GC Pil+OpaH alone (Fig. 14 A, B). Treatment with the inhibitor also enhanced the level of penetration of GC Pil+OpaH in the endocervix but had no effect on penetration in the ecto and TZ (Fig. 14 A, C). Similarly, treatment of polarized T84 cell monolayer with the inhibitor increase the level of GC Pil+OpaH transmigration (Fig. 14 D). These observations suggest that the Opa_{CEA}-CEACAM1L dependent regulation of GC infectivity involves the subsequent activation of SHP1/2.

To test whether the inoculation with MS11Pil+OpaH induces SHP1/2 activation in cervical epithelial cells, I examined the phosphorylation and redistribution of SHP1/2 with or without inoculation with GC Pil+OpaH with or without inhibitor. The staining of SHP1 in the cervical tissue showed little signal (Fig. 13), thus I focused on the phosphorylation of SHP2 (pSHP2) and its redistribution. I only detected a significant

signal of pSHP2 staining in the ectocervix inoculated with GC Pil+OpaH, which was abolished by the treatment with the inhibitor (Fig. 14 E). I quantified it by the fluorescence intensity (FI) of pSHP2 per cell in the three cervical regions (Fig. 14 F). Staining of SHP2 was detected in all three cervical regions (Fig. 14 G). The ectocervix displayed an overall cytoplasmic staining pattern with no significant difference detected with or without inoculation with GC Pil+ OpaH with or without inhibitor. In contrast, in the TZ and endocervix, SHP2 staining was observed both at the luminal surface and in cytoplasma, with the FIR of SHP2 at the luminal surface to cytoplasma around 2. Inoculation of GC Pil+OpaH increased the level of SHP2 staining at the luminal surface in the endocervix to FIR ~ 3, but not in the TZ. This was abolished by the treatment with NSC-87877 (Fig. 14 G, H). The above data indicate that GC Pil+OpaH can induce the activation of SHP2 in ecto and endocervical but not the TZ epithelial cells, and expression of Opa_{CEA} enhances GC colonization and inhibits penetration by inducing CEACAM1L-mediated SHP activation.

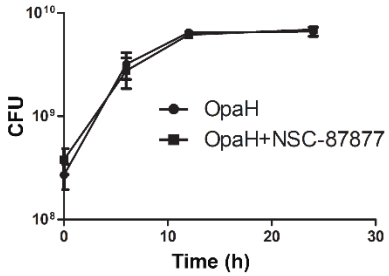

Figure 12. Treatment of the SHP inhibitor NSC-87877 has no significant effect on GC growth (Conducted by Sofia Di Benigno).

GC MS11 Pil+OpaH was cultured in GC media (with 1% Kellogg's supplement and 1% $NaHCO_3$) in the absence or presence of NSC-87877 (20 μM). The bacterial CFU was numerated at 6, 12 and 24 h. Shown are average CFU (±SEM) of three independent experiments.

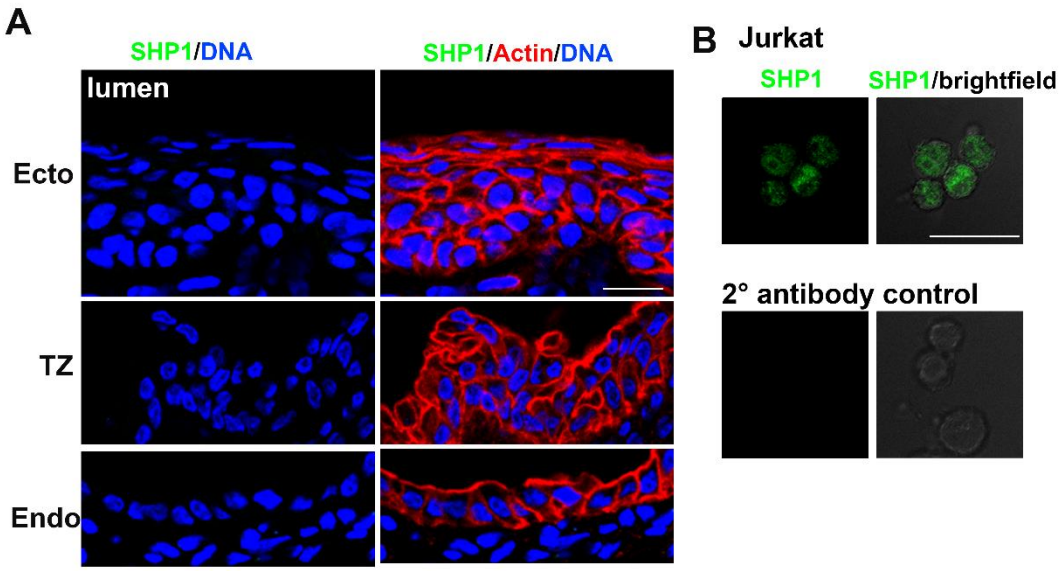

Figure 13. Human cervical tissue explants show no significant staining of SHP1.

Representative images of the three regions of uninfected cervical tissue explants stained for SHP1, F-actin, and DNA (A) and Jurkat human T cells stained for SHP1 as a positive control. Scale bar, 20 μm.

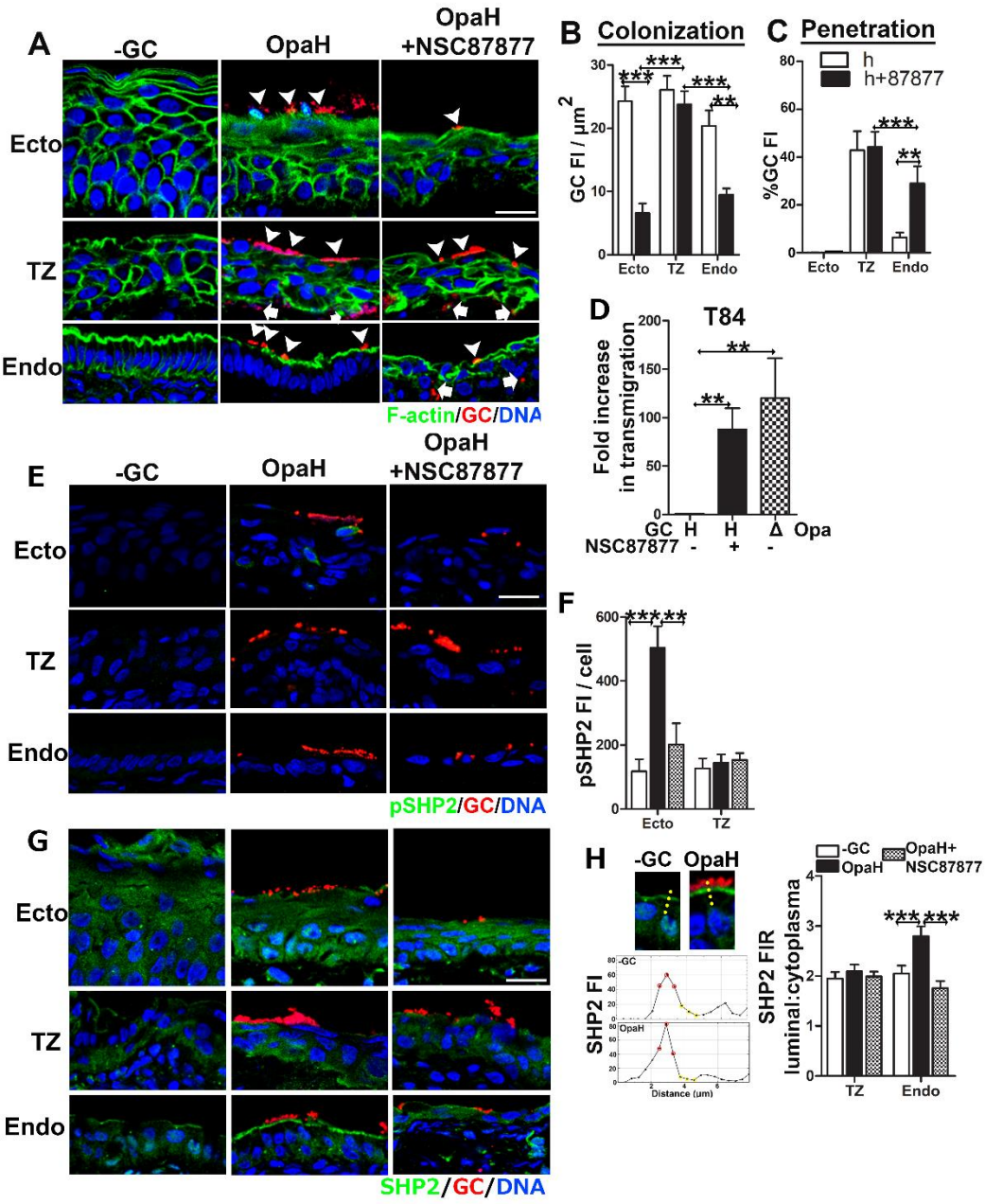
A
-GC
OpaH
OpaH +NSC87877
Ecto
TZ
Endo
F-actin/GC/DNA
B Colonization
GC FI / µm2
Ecto TZ Endo
C Penetration
h
h+87877
%GC FI
Ecto TZ Endo
D
T84
Fold increase in transmigration
GC H H Δ Opa
NSC87877 - + -
E
-GC
OpaH
OpaH +NSC87877
Ecto
TZ
Endo
pSHP2/GC/DNA
F
pSHP2 FI / cell
Ecto TZ
G
Ecto
TZ
Endo
SHP2/GC/DNA
H
-GC OpaH
SHP2 FI
-GC
OpaH
Distance (µm)
-GC
OpaH
OpaH+ NSC87877
SHP2 FIR luminal:cytoplasma
TZ Endo

Figure 14. SHP activation is involved in the regulatory role of OpaH in GC infectivity in the human cervix.

(A) Representative CFM images of human cervical tissue explants inoculated with GC MS11 Pil+OpaH with or without the SHP inhibitor NSC87877 (20 μM) and stained for GC, F-actin, and DNA. Arrowheads, colonizing GC. Arrows, penetrating GC. (B) Levels of GC colonization at the ectocervix, TZ and endocervix by GC FI per μm^2 (±SEM) of the luminal surface. (C) Levels of GC penetration into the subepithelia of the ectocervix, TZ and endocervix measured as the percentage of GC FI (±SEM) at the subepithelium. (D) The level of transmigration of GC Pil+OpaH and Pil+ΔOpa across polarized T84 epithelial cells treated with or without the SHP inhibitor NSC-87877 (20 μM) is showed as the fold increase of GC CFU in the basal medium compared to the CFU of transmigrated GC Pil+OpaH without SHP inhibitor treatment. (E and G) Representative CFM images of tissue explants inoculated with GC Pil+OpaH with or without the SHP inhibitor and stained for GC, DNA, SHP2, or pSHP2. (F) Levels of pSHP2 staining were quantified by pSHP2 FI per cells (±SEM). (H) The redistribution of SHP2 from the cytoplasm to the luminal surface quantified by the FIR (±SEM) at the luminal surface versus the cytoplasm using FI line profiles cross luminal surface (yellow dotted lines). Scale bar, 20 μm. n=3~4. >20 randomly selected fields and >200 cells per cervix and condition. *$p<0.05$; **$p< 0.01$; ***$p<0.001$.

2.4.5 OpaH expression inhibits GC-induced cervical epithelial exfoliation in a CEACAM1L and SHP-dependent manner

Clinical research shows that GC infection can induce cervical epithelial exfoliation. It has been shown that Opa_{CEA} inhibited epithelial exfoliation in CEACAM transfected cell line and mouse model [61, 62]. However, whether Opa_{CEA}-CEACAM interaction regulates epithelial exfoliation in the cervical epithelium in the same way or differently is unknown. To answer the questions, I first examined the level of exfoliation induced by GC Pil+OpaH, OpaC or ΔOpa in the three cervical regions. Inoculation with GC induced epithelial exfoliation in all three cervical regions (Fig. 15 A, E, H). The superficial stratified layers of epithelial cells in the ectocervix were exfoliated in layers (Fig. 15 A). I plot the line profile of F-actin staining across the ectocervical epithelium (Fig. 15 A, white dash lines, B), to measure the thickness (μm) and the number of layers of the ectocervical epithelial cells. I quantified the level of epithelial exfoliation in the TZ and ectocervix by the percentage of the thickness (Fig. 15 C), and the number of epithelial layers remained (Fig. 15 D), compared to the tissue without GC inoculation. In the ectocervix, expression of OpaH reduced the level of exfoliation by 50% comparing to OpaC, and ΔOpa. In contrast, all three Opa isogenic strains induced around 50% epithelial exfoliation in the TZ (Fig. 15 F, G). In the endocervix, epithelial cells were exfoliated as individual cells (Fig. 15 H, arrowhead), thus I quantified the level of exfoliation by the percentage of cells located above the epithelium versus total number of epithelial cells (Fig. 15 I). Inoculation of GC Pil+ OpaH induced 13% exfoliation, significantly lower than the 27% and 33% for GC Pil+ OpaC and ΔOpa. Inoculation with MS11 Pil-Opa+ did not induce significant

epithelial exfoliation in all three cervical regions (data not shown). Therefore, the expression of Opa_{CEA} inhibits GC-induced exfoliation in the endo and ectocervix, which may contribute to the enhanced, and the inhibited penetration in the endocervix. In the TZ, potentially due to the low level of CEACAM expression, the expression of Opa_{CEA} did not affect the level of epithelial exfoliation as with the infectivity.

To determine whether the inhibition of epithelial exfoliation by Opa_{CEA} involves CEACAM1L, I inoculated HEC-1-B cells transiently transfected with CEACAM1L and CEACAM1S with GC Pil+ OpaH and ΔOpa. Using the x-z view CFM images cutting across the luminal surface to the basal level, I quantified the level of exfoliation by the percentage of HEC-1-B cells located on top of the monolayer versus the total number of epithelial cells (Fig. 15 J, K). Without transfection, both OpaH and ΔOpa induced around 12% exfoliation. Without inoculation with GC, transfection of both constructs did not induce a significant basal level of exfoliation (around 4%). The transfection of CEACAM1S did not affect the level of exfoliation induced by both OpaH and ΔOpa, compared to the cells without transfection. In contrast, transfection of CEACAM1L reduced OpaH-induced exfoliation, but not ΔOpa-induced, to the basal level. Taken together, the inhibition of epithelial exfoliation by Opa_{CEA} expression depends on the CEACAM1L expression, thus potentially involves SHP as well.

To examine the role of SHP activation in the epithelial exfoliation, I quantified the level of exfoliation in the three cervical regions with or without NSC-87877 treatment, the SHP1/2 activation inhibitor. The treatment with inhibitor significantly increased the level of exfoliation induced by GC Pil+ OpaH in the ecto and endocervix, but not TZ (Fig. 15 L-O). Thus, the above data suggest that the Opa_{CEA}-dependent inhibition of epithelial exfoliation involves CEACAM1L and subsequent activation of SHP1/2.

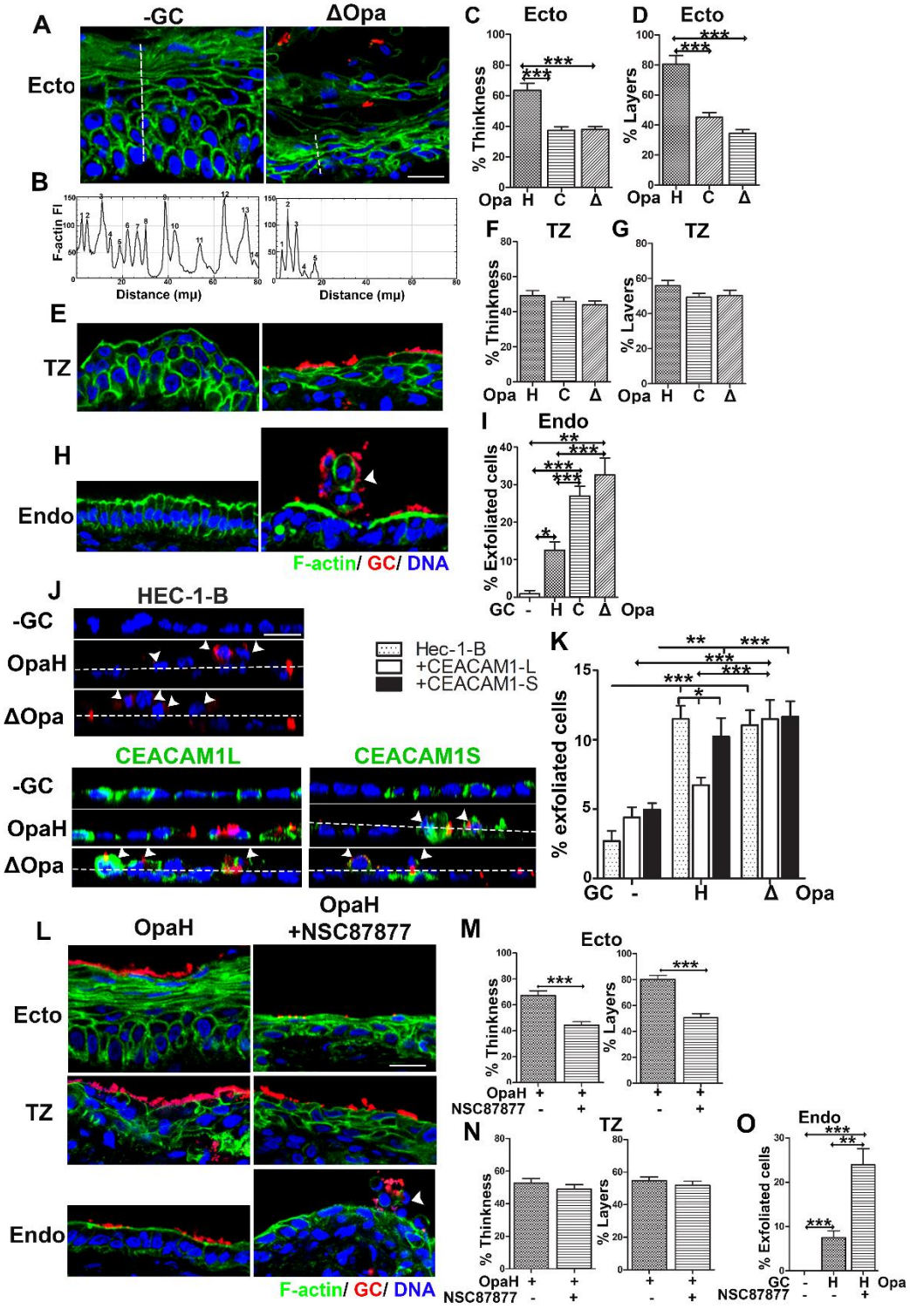
A
-GC
ΔOpa
Ecto
B
F-actin FI
Distance (mμ)
C
Ecto
% Thinkness
Opa H C Δ
D
Ecto
% Layers
E
TZ
F
TZ
% Thinkness
G
TZ
% Layers
H
Endo
F-actin/ GC/ DNA
I
Endo
% Exfoliated cells
GC - H C Δ Opa
J
HEC-1-B
-GC
OpaH
ΔOpa
Hec-1-B
+CEACAM1-L
+CEACAM1-S
CEACAM1L
CEACAM1S
K
% exfoliated cells
GC - H Δ Opa
L
OpaH
OpaH +NSC87877
Ecto
TZ
Endo
F-actin/ GC/ DNA
M
Ecto
% Thinkness
% Layers
OpaH
NSC87877
N
TZ
% Thinkness
% Layers
O
Endo
% Exfoliated cells
GC - H H Opa
NSC87877

Figure 15. OpaH inhibits GC-induced shedding of the cervical epithelial cells in a CEACAM1L and SHP-dependent manner.

(A, D, and F) Representative images of the ectocervical (A), TZ (D), and endocervical (F) regions of tissue explants inoculated with or without GC Pil+ OpaH, OpaC or ΔOpa. Arrowheads, shedding cells. (B) Representative line profiles of F-actin FI along dashed lines in A, indicating the number of epithelial layers and the thickness of the epithelium remained. (C and E) Levels of epithelial shedding in the ectocervix (C) and the TZ (E) quantified by the percentage (±SEM) of the thickness of the epithelium and the number of epithelial layers remained. (G) Levels of epithelial shedding in the endocervix quantified by the percentage (±SEM) of epithelial cells moving above the epithelial monolayer. (H) Representative images of HEC-1-B cell monolayers that transfected with or without CEACAM1L or 1S and inoculated with or without GC Pil+OpaH and Pil+ΔOpa. Dashed lines, the surface of monolayers. Arrowheads, cells moving above the epithelial monolayer. (I) Shedding of HEC-1-B cells quantified by the percentage (±SEM) of cells moving above the monolayers. (J) Representative CFM images of human cervical tissue explants inoculated with GC Pil+OpaH with or without the SHP inhibitor NSC-87877 (20 μM). Arrowheads, shedding cells. (K-M) Levels of epithelial shedding in the ectocervical (K), TZ (L), and endocervical (M) regions quantified as above. Scale bar, 20 μm. n=3~4. >20 randomly selected fields and >200 cells per condition and cervix. *p<0.05; **p< 0.01; ***p<0.001.

2.4.6 GC infection manipulates cell-cell junction in cervical epithelial cells in a CEACAM1L and SHP-dependent manner

Our lab has previously shown that inoculation of GC Pil+ΔOpa induced junction disassembly leading to epithelial exfoliation and GC penetration across polarized epithelial cells, and Opa expression inhibited these processes [95]. To determine whether Opa_{CEA} expression induces a similar effect on the cell-cell junction in the three cervical regions, I examined the distribution of adherens junction protein E-cadherin in the three cervical regions (Fig. 16 A, Fig. 17). I evaluated the integrity of E-cadherin based cell-cell junction by the FIR of E-cadherin at the cell-cell junction (average of the value of red dots) to that at the cytoplasm (average of the value of yellow dots) (Fig. 16 B). Without inoculation with GC, E-cadherin staining was primarily localized at the cell-cell junction in the intermedium and basal layers in the ectocervix (Fig. 16 A). Inoculation with all three Opa variants did not change the junction: cytoplasma FIR of E-cadherin significantly in the ectocervix (Fig. 16 C), indicating that ectocervical epithelium is organized and regulated by another mechanism. In the TZ, E-cadherin staining was localized at the cell-cell junction; in the endocervix, at the lateral surface of polarized endocervical epithelial cells. In both TZ and endocervix, inoculation with GC Pil+ΔOpa and OpaC induced a significant decrease of junction: cytoplasma FIR (~2) of E-cadherin compared to no inoculation control (~4). However, expression of OpaH restored the junction: cytoplasma FIR of E-cadherin only in the endocervix (~3.5) but not in TZ (~2) (Fig. 16 C). The above data suggest that the expression of Opa_{CEA} inhibited cell-cell junction disruption in the endocervix, but not in TZ, and ectocervix.

To determine whether the Opa_{CEA}-mediated inhibition of cell-cell junction disruption also involves CEACAM1L, I examined the redistribution of β-catenin, an adaptor protein associated with E-cadherin in adherens junction, in the HEC-1-B cells transfected with CEACAM1L and CEACAM1S (Fig. 16 D). Using the same method as to quantify redistribution of E-cadherin, inoculation of both CEACAM1S and CEACAM1L transfected cells with GC Pil+ ΔOpa significant decreased the FIR, indicating cell-cell junction disruption. In contrast, inoculation of CEACAM1L transfected cells with GC Pil+ OpaH restored the FIR in the CEACAM1L-expressing cells alone (Fig. 16 E), indicating the inhibition of cell-cell junction disruption requires both Opa_{CEA} and CEACAM1L.

To determine whether the Opa_{CEA}- CEACAM1L dependent inhibition of cell-cell junction disruption involves SHP1/2 activation, I examined E-cadherin distribution in the cervical tissue treated with or without NSC-87877 using the same method. With or without the treatment with inhibitor, GC Pil+ OpaH inoculation did not affect the E-cadherin distribution in the ectocervix and TZ. In contrast, in the endocervix, treatment with the inhibitor-induced a significant decrease of E-cadherin FIR, indicating the OpaH-CEACAM1L dependent inhibition of junction disruption involves SHP (Fig. 16 F, G).

Taking together, the above data suggest that the inhibition of cell-cell junction disruption by Opa_{CEA} involves CEACAM1 and subsequent SHP1/2 activation. In the

endocervix, the inhibited junction disruption by Opa_{CEA} can lead to the decrease epithelial exfoliation, thus decreased penetration, and increased colonization. In the TZ, the low level of CEACAM expression abolishes the Opa_{CEA}-CEACAM pathway and subsequent SHP1/2 activation, thus the expression of which Opa or no Opa does not affect GC infectivity. In the ectocervix, the luminal expression of CEACAM1L and SHP activation may contribute to the enhanced colonization and inhibited exfoliation mediated by Opa_{CEA}, but not through inhibition of junction disruption.

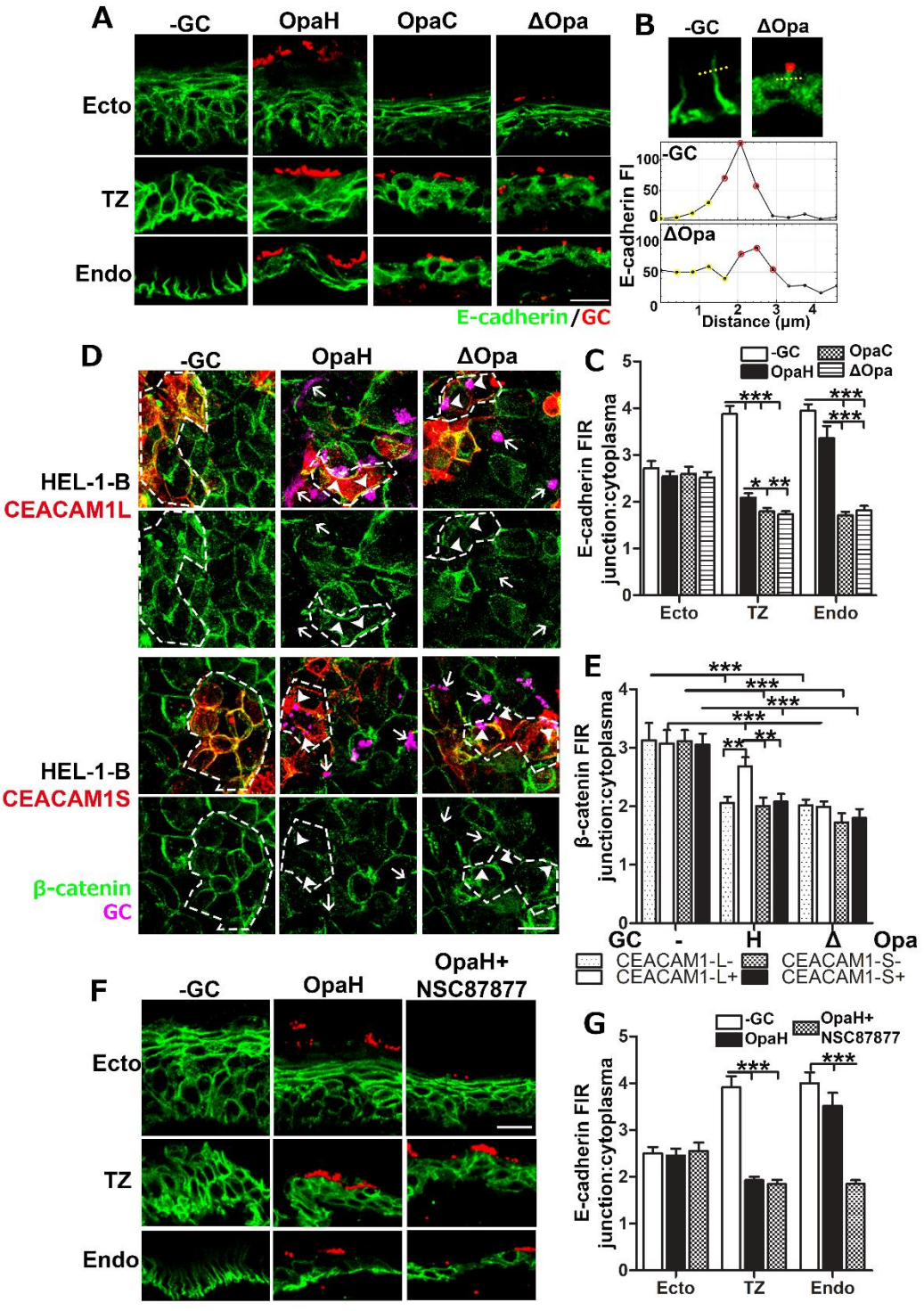
A
-GC
OpaH
OpaC
ΔOpa
Ecto
TZ
Endo
E-cadherin / GC
B
-GC
ΔOpa
-GC
ΔOpa
E-cadherin FI
Distance (μm)
C
-GC
OpaH
OpaC
ΔOpa
E-cadherin FIR junction:cytoplasma
Ecto
TZ
Endo
D
-GC
OpaH
ΔOpa
HEL-1-B CEACAM1L
HEL-1-B CEACAM1S
β-catenin
GC
E
β-catenin FIR junction:cytoplasma
GC - H Δ Opa
CEACAM1-L-
CEACAM1-L+
CEACAM1-S-
CEACAM1-S+
F
-GC
OpaH
OpaH+ NSC87877
Ecto
TZ
Endo
G
-GC
OpaH
OpaH+ NSC87877
E-cadherin FIR junction:cytoplasma
Ecto
TZ
Endo

Figure 16. OpaH inhibits GC-induced junction disruption in the cervical epithelial cells in a CEACAM1L and SHP-dependent manner.

(A) Representative CFM images of human cervical tissue explants inoculated with GC Pil+ OpaH, OpaC or ΔOpa and stained for GC and E-cadherin (E-cad). (B and C) Disruption of cell-cell junctions was determined by the FIR (±SEM) of E-cad at the cell-cell border (average of red dots in B) relative to the cytoplasm (average of yellow dots in B) using FI line profiles crossing cell-cell junction (B). (D) Representative CFM images of HEC-1-B cells transfected with or without CEACAM1L or 1S, inoculated with GC Pil+OpaH or Pil+ΔOpa, and stained for GC, CEACAM, and β-catenin. Dashed lines, cells expressing CEACAM1L or 1S. (E) Disruption of cell-cell junctions was determined by the FIR (±SEM) of β-catenin at the cell-cell border to the cytoplasm. (F) Representative CFM images of human cervical tissue explants inoculated with GC Pil+OpaH with or without the SHP inhibitor (20 μM). (G) Disruption of cell-cell junctions was determined by the FIR (±SEM) of E-cad at the cell-cell border to the cytoplasm. Scale bar, 20 μm. n=3~4. >20 randomly selected fields and >50 cells per condition and per cervix. $^{**}p< 0.01$; $^{***}p<0.001$.

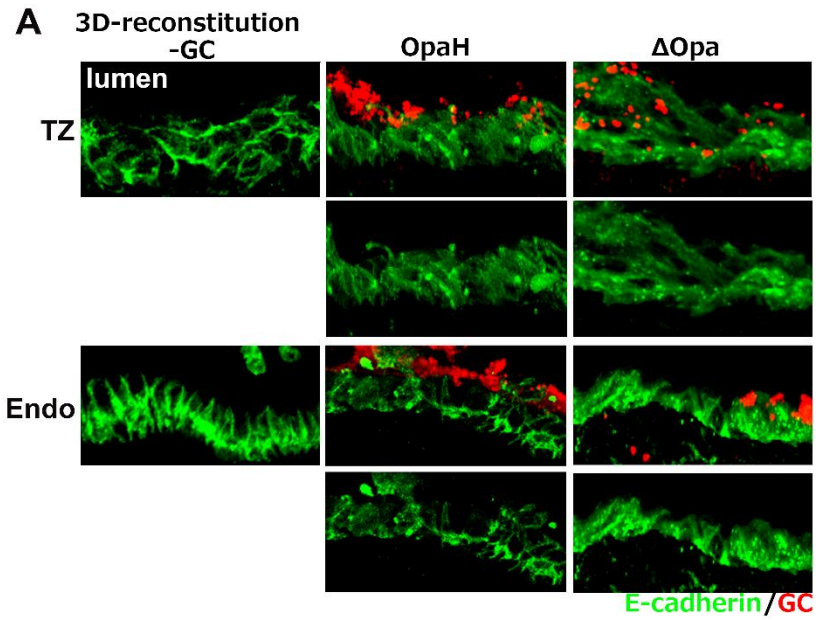

Figure 17. GC inoculation disrupts E-cadherin-based cell-cell junction.

Representative 3D reconstruction images of the TZ and endocervical epithelium in human cervical tissue explants that were inoculated with or without Pil+OpaH or Pil+ΔOpa GC and stained for GC and E-cadherin. Scale bar, 20 μm.

2.5 Discussion

To study the GC infection in the female reproductive tract, I first developed a human cervical tissue explant model, which not only closely mimics *in vivo* morphology of cervical epithelium, but mimics the *in vivo* GC infectivity as well. Using this model, I showed that GC modifies infectivity based on the different properties of cervical epithelial cells they encounter by phase varying bacterial surface molecules. When exposed to all three cervical regions, GC colonize more in the ectocervix and TZ than endocervix; while only penetrate in the TZ and endocervix. Pili are required for colonization in all three cervical regions. Expression of Opa_{CEA} enhances colonization in ecto and endocervix, where CEACAM is abundantly expressed at the luminal surface of the epithelial cells. Expression of Opa_{CEA} inhibits penetration in the endocervix, by engaging CEACAMs, leading to subsequent activation of SHP1/2 and inhibition of junction disruption. The unresponsiveness of TZ to Opa phase variation can be accounted for by the lack of CEACAM expression. The enhanced colonization by Opa_{CEA} expression in the ecto and endocervix can enhance the localized asymptomatic infection; while the high penetration in the TZ and enhanced penetration by the lack of Opa_{CEA} in endocervix provides an explanation for the switch to the penetrating symptomatic GC infection which may further lead to DGI.

Transformation zone (TZ) of the cervix is a specialized region in between the ecto and endocervix. The formation of TZ starts at the puberty when the endocervix invades into the ectocervix. The invasion triggers metaplasia of the part of endocervical tissue now located in the ectocervical region to gradually transform into ectocervix. Two

theories of the morphology of TZ are available. The first theory calls TZ the squamocolumnar junction (SCJ) instead. It shows as an abrupt junction where the polarized endocervical epithelium meets with multiple layered squamous ectocervical epithelium. The small region flanks the squamocolumnar junction is defined as TZ. In this theory the boundary between the ectocervix and TZ, and TZ and the endocervix are blurry. In other words, the range of the region flanks squamocolumnar junction is not defined. The second theory shows a region going through metaplasia where the epithelium is composed of multiple layers of epithelial cells. And the TZ epithelial cells are neither as polarized and columnar as in the endocervix nor as stratified and squamous as in the ectocervix. Based on this theory, the TZ is easy to define based on the morphology of epithelial cells. I also observe a junction between the TZ and ectocervix in this model. Out of the total 22 samples I used for this research, the morphology of the TZ in two samples fits the first theory, where the boundary of the TZ is hard to define. Thus, data of these two samples were not included. The rest 20 samples have TZ with the morphology described in the second theory. Although the length the TZ varies based on the age of the patients, a clear region of TZ can be defined. Thus, data presented here can be applied to the GC infection in the cervix with a gradual change of epithelial morphology from the ecto to endocervix.

I showed that TZ is the most vulnerable cervical region to GC infection with a high level of colonization and penetration. The Opa phase variation fails to regulate infectivity in this region, which can be explained by the lack of CEACAM expression. The similar behavior of Opa_{HSPG} and ΔOpa eliminates the role of HSPG as well. These

observations led me to ask the question that what the mechanism of the strong infectivity of GC in TZ is. One possibility is the signaling triggered by pili through its receptor CR3. The non-piliated GC fails to colonize all three cervical regions, making it difficult to study the detailed role of pili in GC infection. The other possibility is the dynamics of epithelial turnover in TZ. TZ is known to be a dynamic region, where the reserve cells proliferate and differentiate. This dynamic nature of TZ can be utilized by GC to infect. Although the data presented here obtained from the cervix with the morphology of TZ fitting the second theory, the results may be also applicable to the first theory, with the squamocolumnar junction a soft spot for GC infection.

I observed both a strong luminal expression of CEACAM and puncta staining in the intermedium layers of the ectocervix. The luminal expression provides an explanation of the enhanced colonization by Opa_{CEA} expression. The lack of Opa_{CEA} expression reduced the level of colonization but enhanced exfoliation without inducing any penetration. This can be explained by the multiple-layered structure of the ectocervical epithelium. Of all the samples, despite the dramatic exfoliation induced by Opa_{HSPG} and ΔOpa, and the thinness of the ectocervical epithelium left, I have never observed a breach of the ectocervical epithelium. It reinforces my central hypothesis that both the properties of cervical epithelium and GC phase variable surface molecules affect infectivity. It also agrees with the asymptomatic GC infection in ectocervix. *In vivo*, ectocervix is covered by dense normal microbiota. When first deposited, GC need to first compete with the normal microbiota to establish a niche, in other words,

colonization, and to proliferate. The successful colonization in ectocervix provides the opportunity for GC to ascend to the upper genital tract.

The upper genital tract, the upper portion of TZ and endocervix, is sterile. Thus, when GC make it to the TZ and endocervix along the continuity of cervical epithelium, the possibility of a small amount of pathogens present causing infection increases. The relatively low level of colonization and penetration presented in endocervix agrees with the clinical observation. The inhibition of exfoliation and further penetration by Opa_{CEA} expression indicates the role of Opa phase variation in regulation of switch between localized colonization to disseminated penetration, thus switch between asymptomatic to symptomatic infection.

The Opa_{CEA}-CEACAM interaction has long been established, but its role in GC infection in the female reproductive tract is not completely understood. Islem et al. showed differential expression of CEACAM1, 5, 6, three epithelial CEACAM, in the female reproductive tract, indicating the role of CEACAM in the regulation of GC infectivity in the three cervical regions. Here, I used an antibody reacting with CEACAM1, 3, 6. CEACAM3 is expressed in neutrophil exclusively. CEACAM1 is the only one has a cytoplasmic domain and harbors an ITIM motif in the cytoplasmic domain, which makes it a perfect candidate for signaling transduction. I used the CEACAM1L and CEACAM1S transfected Hec-1-B cells. The enhanced adherence and inhibited exfoliation requires both Opa_{CEA} and CEACAM1L, which confirms the

CEACAM1L-dependent regulatory role of Opa_{CEA} of GC infectivity in three cervical regions. It has been shown that the ITIM motif of CEACAM1L recruits and activates SHP1/2. The treatment of SHP inhibitor, NSC-87877, abolished the Opa_{CEA}-dependent enhancement of colonization and the inhibition of exfoliation in the ecto and endocervix. It also abolishes the inhibition of penetration in endocervix. Overall data suggest the engagement of Opa_{CEA}-induced CEACAM1L-SHP pathway in the regulation of GC infectivity.

The invasion of GC into epithelial cells intracellularly has been shown in various cell line models by invasion assay and by TEM as well. However, using the human cervical tissue explants together with the confocal microscopy, it remains technically difficult to distinguish intracellular and extracellular bacteria. On the other hand, I rarely observed intracellular GC staining, which does not agree with the previous observation. However, the ability of GC to disruption cell-cell junction in various cell line models as well as in the human cervical tissue explant model indicates that GC is also capable of transmigration or penetration across epithelial cells paracellularly, without entering into cytoplasma.

My data showed the different organization of E-cadherin based cell-cell junction in the three cervical regions, and the differential effect of GC inoculation on E-cadherin redistribution. The disruption of the cell-cell junction has been shown in a close relationship with epithelial exfoliation [99]. In the ectocervix, E-cadherin is expressed

at the cell-cell junction in the intermedium and basal layers, but not in the superficial layers. Despite the dramatic exfoliation induced by Opa_{HSPG} and ΔOpa and the thinness of the ectocervical epithelium left, the very superficial layers were always devoid of E-cadherin staining and the no redistribution of E-cadherin is detected. These data indicated that the exfoliation and response of cell-cell junction to GC inoculation in the ectocervical epithelium is mediated by other mechanisms. In TZ, E-cadherin is expressed at cell-cell junction throughout all the layers. GC inoculation induced redistribution of E-cadherin protein into cytoplasma, indicating the junction disassembly and junction disruption. Because of the lack of CEACAM expression in TZ, Opa phase variation did not affect the level of E-cadherin redistribution, and a potentially similar level of exfoliation. In endocervix, E-cadherin based adhesion junction is part of the apical junction. Expression of Opa_{CEA} inhibited E-cadherin redistribution into cytoplasma, restoring the integrity of cell-cell junction, thus inhibited exfoliation and penetration. Since endocervical epithelium is only composed of one layer of epithelial cells, the exfoliation induced by GC inoculation can potentially create breach on the epithelial layer, thus a portal for GC to penetrate into subepithelial tissue and triggers immune response causing symptomatic infection and DGI.

Based on the data presented in this chapter, I propose the following working model. GC colonize at a high level in the ectocervix without penetration thus result in the localized asymptomatic infection. The Opa phase variation favors Opa_{CEA} expression in response to the high expression of CEACAM at the luminal surface to enhance the

colonization and the chance to get into the upper genital tract. Once in the endocervix, the colonization level is relatively low, but penetration across the single layer of epithelial cells occurs. Opa phase variation regulates the infectivity between colonization and penetration, thus asymptomatic and symptomatic, localized and disseminated gonococcal infection. Opa_{CEA} expression enhances colonization and inhibits exfoliation and penetration by engaging CEACAM1L-SHP pathway with subsequent inhibited junction disruption. TZ is localized between the ecto and endocervix and does not express very much CEACAM, thus did not respond to Opa phase variation, and is the most vulnerable to colonization and penetration.

Chapter 3: The polarity of epithelial cells regulates *Neisseria gonorrhoeae* infectivity

3.1 Abstract

To establish infection in the female reproductive tract from the cervix, GC encounter both non-polarized stratified ectocervical epithelial cells and polarized columnar endocervical epithelial cells. The studies presented in Chapter two have shown that distinct properties of cervical epithelial cells affect GC infectivity. However, whether the different polarity of epithelial cells, which associates with cell morphology and actin cytoskeleton organization, contribute to the differential infectivity of GC in the ecto and endocervix is unknown. To address this question, I utilized a non-polarized and polarized epithelial cell model generated from the same cell line. While GC adhered to both non-polarized and polarized epithelial cells to a similar level. GC invasion into non-polarized epithelial cells was more efficient than into polarized epithelial cells. The expression of phase variable Opa (Opa+) enhanced GC adhesion and invasion, compared to an Opa deletion mutant (ΔOpa). Electron microscopy observed microvilli elongation in non-polarized epithelial cells inoculated with Opa+ GC, which was concurrent with F-actin recruitment at GC adherent sites. In contrast, massive disruption of microvilli was observed in polarized epithelial cells inoculated with GC ΔOpa, which was concurrent with NMII-dependent reduction of F-actin at GC adherent sites. GC inoculation only induced intracellular calcium in polarized, but not in non-polarized epithelial cells. Overall, my data demonstrated that the level of

epithelial cell polarity regulates GC infectivity and the function of Opa in GC infection.

3.2 Introduction

Successful colonization at the mucosal surface is the first step for microbial pathogens to establish infection. The epithelium is the first line of defense to protect the host against the microbial pathogens. *Neisseria gonorrhoeae* (GC), the pathogen causing the sexually transmitted infection (STI) gonorrhea, initiates infection from the mucosal surface of the human cervix, the gate of the female reproductive tract (FRT). The human cervical epithelia are composed of multiple-layered non-polarized stratified epithelial cells at the ectocervix and single-layered polarized columnar epithelial cells at the endocervix. The polarity of epithelial cells is an essential property distinguishing the ecto and endocervical epithelial cells. However, whether the epithelial cell polarity affects GC infection in the non-polarized ecto and polarized endocervical epithelial cells is unknown.

The polarity of polarized epithelial cells is maintained and regulated by the apical junction (AJ) and the perijunctional actomyosin ring [117]. One essential component of the perijunctional actomyosin ring is the actin motor protein non-muscle myosin II (NMII), which regulates the dynamics of the apical junction by contracting the perijunctional actin cytoskeleton [156]. The role of the actin-nucleating factor Arp2/3 in regulating the dynamics of the apical junction through perijunctional actin

cytoskeleton has been suggested [121]. In the non-polarized epithelial cells, the Arp2/3 complex mediates the polymerization of branched actin filament and plays an essential role in remodeling of the plasma membrane in response to pathogens [135]. Furthermore, polarized epithelial cells are known to form densely packed microvilli at the apical surface, which is supported by the bundled F-actin [141]. Similarly, in the human cervix, the polarized columnar endocervical epithelial cells form the apical junction between neighboring cells [123] and densely packed microvilli at the apical surface [124]. In contrast, the mucosal surface of non-polarized ectocervical epithelium appears smooth [124].

It has been shown that GC can induce membrane ruffling, microvilli elongation and the rearrangement of the actin cytoskeleton at the plasma membrane in multiple non-polarized epithelial cell lines [130, 131, 133]. Our lab has previously shown that GC can induce cell-cell junction disassembly in both polarized epithelial cell line [76] and the human endocervical tissue explant [95]. However, whether GC induce the similar response of actin cytoskeleton and the underlying mechanism in the non-polarized ecto and polarized endocervical epithelial cells are unknown.

Here, I used a non-polarized and polarized epithelial cell model generated from the same cell line to study the impact of epithelial cell polarity on GC infection processes and its underlying mechanism. I found that GC invade into non-polarized epithelial cells more efficiently than into polarized epithelial cells without changing the level of

GC adhesion. And the expression of Opa enhances GC adhesion and invasion compared to an Opa deletion mutant (ΔOpa). Such differential GC infectivity is concurrent with differential morphology change of plasma membrane and F-actin reorganization induced by GC in the non-polarized and polarized epithelial cells.

3.2 Materials and Methods

Neisseria Strains

N. gonorrhoeae strain MS11 that expressed both phase variable Pili and Opa (Pil+ Opa+) and the MS11 *opa* deletion mutant (Pil+ ΔOpa) were used [149]. GC were grown on GC media plates supplemented with 1% Kellogg's supplement (GCK) for 16–18 h before inoculation. Pil+ colonies were identified based on colony morphology using a dissecting light microscope. GC was suspended and the concentration of bacteria was determined by using a spectrophotometer. GC were inoculated with epithelial cells at MOI ~10.

Epithelial Cells

Human colorectal carcinoma cell line T84 cells (ATCC) was maintained in Dulbecco's modified Eagle's medium: Ham F12 (1:1) supplemented with 7% heat-inactivated FBS. Cells were maintained at 37°C with 5% CO_2. Cells were seeded at $6x10^4$ (6.5 mm diameter transwell inserts, Corning, Lowell, MA, USA) and cultured for ~10 days until transepithelial electrical resistance (TEER) reached ~2000 Ω for polarized epithelial cells. Cells were seeded at 1.2 $x10^5$ (6.5 mm diameter transwell inserts) and

cultured for ~2 days for non-polarized epithelial cells. TEER was measured using a Millicell ERS volt-ohm meter (Millipore, Bedford, MA, USA).

Immunofluorescence analysis of epithelial cells

Non-polarized and polarized T84 cells were inoculated with GC for 6 h. Cells were rinsed, fixed with 4% paraformaldehyde, permeabilized, and stained with phalloidin (Life Technology, Grand Island, NY, USA), anti-GC antibodies, and hoechst for nuclei (Life Technologies). Cells were analyzed by confocal fluorescence microscopy (Zeiss LSM 710, Carl Zeiss Microscopy LLC, Thornwood, NY, USA). Z-series of images were obtained in 0.57 μm slices from the apical to the basal of the monolayer, and three-dimensional (3D) composites obtained.

The redistribution of F-actin induced by GC inoculation at the luminal surface was examined by using the x-z view images cutting across the luminal surface to the basal level. Fluorescence intensity (FI) profiles of F-actin were generated by drawing a line underneath GC microcolonies using the ImageJ software. The fluorescence intensity ratio (FIR) of F-actin underneath GC microcolonies to the neighboring area without GC was quantified.

Human cervical tissue explants

The tissue explants were cultured using a previously published protocol [152]. Briefly, cervical tissues were obtained from patients undergoing voluntary hysterectomies and received within 24 h post-surgery. Age of patients ranges from 28 to 40. Supporting muscle tissue was removed by using a carbon steel surgical blade. Remaining cervical tissue samples were cut into ~2.5 cm (L) X 0.6 cm (W) X 0.3 cm (H) pieces, incubated in 6-well tissue culture plate in cervical tissue culture media conataining CMRL-1066 (GIBCO), with 5% heat-inactivated fetal bovine serum, 2 mM L-glutamine, bovine insulin (1 μg/ml, Akron Biotech) and penicillin/streptomycin for 24 h and then in antibiotic-free media for another 24 h, before inoculation with GC as previously described.

Immunofluorescence analysis of human cervical tissue explants

Individual pieces of cervical tissue explants were inoculated with GC at MOI ~10. The number of epithelial cells at the mucosal surface was determined by the area of the mucosal surface of the individual piece and the average luminal area of individual cervical epithelial cells. When indicated, the tissue explants were pretreated with MLC kinase inhibitor ML-7 (10 μM, Calbiochem, San Diego, CA, USA) for 1 h, and inoculated with GC with or without the inhibitors for 24 h as previously described. Briefly, GC were collected by using a sterile applicator to swab GC from the plate and re-suspend GC in pre-warmed antibiotic-free cervical tissue culture media. An aliquot of the GC suspension was added directly onto each tissue piece to make an MOI = 10

bacteria to 1 epithelial cell. The cervical tissue explants were incubate at 37 °C with 5% CO2 with gentle shaking for 24 h. The infected cervical tissue explants were rinsed with antibiotic-free cervical tissue culture medium at 6 and 12 h to remove un-adhered bacteria and replace with fresh media without bacteria. Tissue explants were then fixed 24 h post inoculation, embedded in 20% gelatin, cryopreserved, sectioned by cryostat across the luminal and basal surfaces of the epithelium, stained for F-actin (Cytoskeleton), Arp2 (Santa Cruz Biotechnology), GC by specific antibodies, and nuclei by Hoechst (Life Technologies), and analyzed using confocal fluorescence microscope (Zeiss LSM 710, Carl Zeiss Microscopy LLC) as previously described [95]. Images of the luminal surface were randomly acquired in the endocervix as single images or Z-series of 0.57 μm/image, and 3D composites obtained using Zeiss Zen software.

The redistribution of F-actin induced by MS11 Pil+Opa+ and ΔOpa was evaluated by two methods: 1) the percentage of GC microcolonies with decrease F-actin staining underneath versus total number of GC microcolonies, 2) the fluorescence intensity ratio (FIR) of F- actin at the apical surface to the lateral surface in individual endocervical epithelial cells. The redistribution of Arp2 induced by MS11 Pil+ ΔOpa was evaluated by the fluorescence intensity ratio (FIR) of Arp2 at the apical surface to the lateral surface in individual endocervical epithelial cells.

GC adherence and invasion assays

Non-polarized and polarized T84 cells were inoculated apically with GC for 3 h for adherence assay and 6 h for invasion assays. For adherence, cells were intensively rinsed, lysed and plated on GCK plates to determine the CFU. For invasion, cells were treated with gentamicin (100 μg/ml) for 2 h, rinsed, lysed and plated. Cell-associated bacteria that were resistant to gentamicin treatment were counted as invaded GC.

Calcium imaging

Non-polarized and polarized T84 cells were seeded at 1×10^5 per transwell on the underside of transwells [95] and cultured for ~2 days for non-polarized, and ~10 days for polarized epithelial cells. Cells were pretreated with or without the intracellular Ca^{2+} inducer thapsigargin (10 μM, Sigma) for 1 h and incubated with GC (MOI ~10) apically with or without the inhibitors for 4 h. Cells were incubated with the fluorescent calcium indicator Fluo-4 (100 μM, Life Technologies) for 1 h. Confocal x-z view images were acquired with the membrane dye CellMask (5 mg/ml, Life Technology) using Leica TCS SP5X confocal microscope (Leica Microsystems, Buffalo Grove, IL).

To quantify the level of intracellular calcium, the cytoplasmic area of the individual cell was manually selected based on the Cell Mask staining in randomly acquired confocal images, and the mean fluorescent intensity (MFI) of Fluo-4 in the cytoplasmic region was measured using the NIH ImageJ software.

Ultrastructure analysis

For transmitted electron microscopy (TEM), non-polarized and polarized T84 cells were apically incubated with GC for 6 h with MOI ~50. The monolayer of epithelial cells on the transwell inserts was first fixed with 2% glutaraldehyde, and secondary fixed with 1% osmium tetroxide. Samples were rinsed with distilled water and post-fixed with 2% uranyl acetate. The samples were dehydrated in a 35% to 100% graded ethanol series, and infiltrated with graded EPON 812 resin (Araldite/Medcast; Ted Pella, Redding, Ca.) series. The transwell membranes were embedded in flat silicone molds (Polyscience, Inc. Warrington, PA) overnight at 60°C. Cross sections of the cells were obtained by sectioning through the embedded transwell membranes. Sections were placed on bare 150-mesh copper grids, stained with uranyl acetate and lead citrate, and viewed with a ZEISS 10CA electron microscope (ZEISS, Thornwood, NY).

For scanning electron microscopy (SEM), non-polarized and polarized T84 cells were apically incubated with GC for 6 h with MOI ~50. The monolayer of epithelial cells on the transwell inserts was first fixed with 2% glutaraldehyde, and secondary fixed with 1% osmium tetroxide. The samples were dehydrated in a graded ethanol series, dried by critical point drying method, and coated with gold-palladium alloy. Samples were visualized with Amray 1820D microscope (20 kV) and Hitachi S4700 microscope (5 kV).

Statistical analysis

Statistical significance was assessed by using Student's t-test by Prism software (GraphPad Software, San Diego, CA). P-values were determined using unpaired t test with Welch's correction in comparison with no infection controls.

Ethics statement

Human cervical tissue explants were obtained from the National Disease Research Interchange (NDRI, Philadelphia, PA). Human cervical tissues used were anonymized. The use of human tissues has been approved by the Institution Review Board of the University of Maryland.

3.4 Results

3.4.1 GC invade into non-polarized epithelial cells more efficiently than into polarized epithelial cells without altering the level of GC adhesion

To mimic the non-polarized and polarized nature of the ecto and endocervical epithelial cells, I established the non-polarized and polarized epithelial cell model using human colonic epithelial cell line T84. T84 is the only cell line that can be polarized to the level similar to that of endocervical epithelial cells in *vivo.* And none of available female genital epithelial cell line can be polarized to that level. T84 cells also express the host receptors for GC Opa proteins as well [93, 157]. T84 cells were cultured on transwells for ~10 days, when the transepithelial resistance reached 2000, to mimic polarized epithelial cells and for two days (transepithelial resistance <300) to mimic non-polarized epithelial cells. While the 2-day culture of T84 cells showed flat

morphology and non-polarized staining of junction proteins E-cadherin and ZO-1, the 10-day culture of T84 cells displayed columnar morphology and polarized staining of E-cadherin and ZO-1 staining at the apical junction.

To answer the question whether GC infect non-polarized and polarized epithelial cells in the same way, I compared the level of adhesion and invasion of piliated Opa phase variable MS11 (Pil+Opa+) and its Opa deletion mutant (Pil+ΔOpa) in non-polarized and polarized epithelial cells. To measure GC adherence, epithelial cells were incubated with GC for 3 h. Epithelial cells were intensively washed to remove non-adhered GC, lysed, and the lysates were cultured to numerated the colony forming units (CFU). Both Pil+Opa+ and Pil+ ΔOpa Opa adhered to the non-polarized and polarized epithelial cells at the same level (Fig. 18 A). GC invasion was determined using gentamicin resistant assay post 6 h inoculation. In contrast to GC adhesion, there were significantly more gentamicin resistant Pil+Opa+ and Pil+ ΔOpa GC in the non-polarized than the polarized epithelial cells (Fig. 18 B). This suggests that GC invade into the non-polarized epithelial cells more efficiently than into polarized epithelial cells independently of GC adhesion.

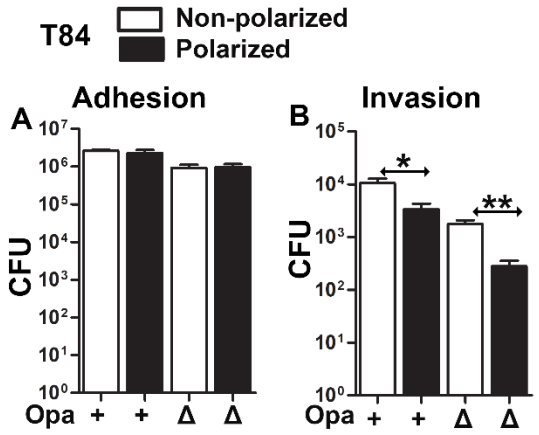

Figure 18. GC invade into non-polarized epithelial cells more efficiently than into polarized epithelial cells without altering the level of GC adhesion.

Two-day non-polarized and 10-day polarized T84 cells were apically inoculated with Pil+Opa+ or ΔOpa GC (MOI~10). (A) Adherent GC (±SEM) were quantified by culturing the lysates of infected epithelial cells 3 h post incubation. (B) Invaded GC (±SEM) were quantified by gentamicin resistance assay 6 h post inoculation. The results were generated from 4–6 independent experiments. *p<0.05; **p< 0.01; ***p<0.001.

3.4.2 Expression of Opa enhances GC adhesion and invasion in both non-polarized and polarized epithelial cells

Chapter 2 has shown that both properties of epithelial cells and the phase variable GC surface molecules affect GC infectivity. To determine if Opa expression differentially affected GC infectivity in non-polarized and polarized epithelial cells, I compared the level of adhesion and invasion of Pil+ Opa+ and Pil+ΔOpa GC in non-polarized and polarized epithelial cells. Pil+ Opa+ GC exhibited a significantly higher level of adhesion and invasion in both non-polarized and polarized T84 cells than Pil+ΔOpa GC (Fig. 19 A, B). In addition, both GC strains adhered to and invade into non-polarized epithelial cells much more efficiently than into polarized epithelial cells (Fig. 19 A). The above results indicate that Opa proteins play a similar role in GC infection of non-polarized and polarized epithelial cells.

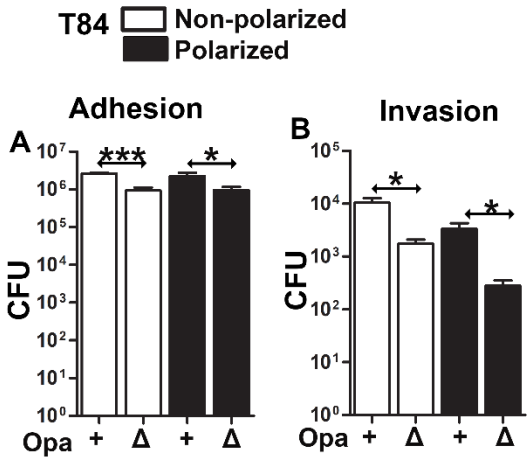

Figure 19. Expression of Opa enhances the level of adhesion and invasion in non-polarized and polarized epithelial cells.

Two-day non-polarized and 10-day polarized T84 cells were apically inoculated with Pil+ Opa+ or Pil+ ΔOpa for 3 or 6 h (MOI~10), and the numbers of adherent GC (±SEM) (A) and invading GC (±SEM) (B) were determined as described above. n=4–6. *p<0.05; **p< 0.01; ***p<0.001.

3.4.3 GC inoculation induces differential membrane remodeling in non-polarized and polarized epithelial cells

Previous studies showed that GC inoculation can induce membrane ruffling and microvilli elongation in primary cervical epithelial cell culture [130], patient biopsies [130], and cell lines [39, 131, 132, 134]. This membrane remodeling has been implicated for GC invasion. The different levels of GC adhesion and invasion in non-polarized and polarized epithelial cells lead to a hypothesis that Opa can regulate GC infectivity by inducing differential membrane remodeling in non-polarized and polarized epithelial cells. To test this hypothesis, I conducted transmitted electron microscopy (TEM) (Fig. 20 A) and scanning electron microscopy (SEM) (Fig. 20 B) of non-polarized T84 cells to compare with polarized T84 cell images obtained by previous graduate students Liang-Chun Wang (TEM) and Senthil V. Bhoopalan (SEM). Without GC inoculation, non-polarized T84 cells possess short irregular membrane protrusions on their luminal membrane (Fig. 20 A, arrows), while polarized T84 cells have densely packed microvilli at the apical surface (Fig. 20). The inoculation of GC Pil+Opa+ induced elongation of membrane protrusions in non-polarized cells (Fig. 20 open arrows) but did not change the morphology of microvilli of the polarized cell. Pil+Opa+ appeared to establish intimate interaction with the surface of non-polarized but only sat on the top of microvilli at the apical surface of polarized epithelial cells (Fig. 20 arrowheads). In contrast to GC Pil+Opa+, GC Pil+ΔOpa did not induce membrane protrusion in non-polarized cells or sit on the top of microvilli of polarized cells. Instead, GC Pil+ ΔOpa inoculation abolished microvilli of both non-polarized and polarized epithelial cells, enabling Pil+ΔOpa to

form intimate interactions with the luminal membrane of epithelial cells as well (Fig. 20 arrowheads). Thus, the expression of Opa induces membrane remodeling in non-polarized epithelial cells but inhibits GC-induced disruption of microvilli in polarized epithelial cells.

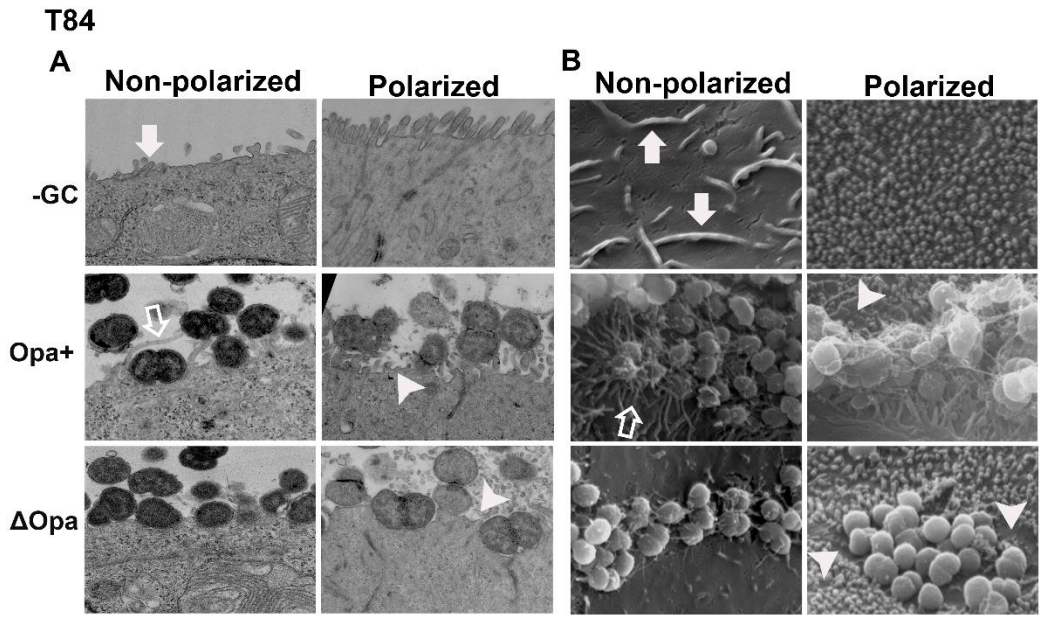

Figure 20. GC inoculation induces differential remodeling of the plasma membrane of non-polarized and polarized epithelial cells.

Two-day non-polarized and 10-day polarized T84 cells were apically incubated with Pil+Opa+ or ΔOpa for 6 h (MOI~50). Cells were fixed and processed for transmitted electron microscopy (TEM) (A) and scanning electron microscopy (SEM) (B). Shown are representative images. (TEM of polarized T84 cells was obtained by Liang-Chun Wang, and SEM of polarized T84 cells was obtained by Senthil Velan Bhoopalan).

3.4.4 GC inoculation induces differential redistribution of F-actin at the luminal surface of non-polarized and polarized epithelial cells

Disruption of the actin cytoskeleton by cytochalasin D inhibited GC invasion into but not adhesion to Chang epithelial cells [132]. I postulated that GC induce different morphological changes in the plasma membrane of non-polarized and polarized epithelial cells by differentially remodeling the actin cytoskeleton underneath, which leads to different levels of GC adhesion and invasion. To test this, I inoculated non-polarized and polarized T84 cells with GC Pil+Opa+ and Pil+ΔOpa, for 6 h. Infected cells were fixed, stained for F-actin, GC, and nuclei, and analyzed by confocal fluorescence microscopy (CFM). The remodeling of the actin cytoskeleton was evaluated by the mean fluorescent intensity ratio (FIR) of F-actin staining underneath GC microcolonies to the immediately neighboring region at the cell surface. In non-polarized T84 cells, the FIRs of F-actin staining underneath both Pil+Opa+ and Pil+ΔOpa microcolonies were significantly bigger than 1 (Fig. 21 A, open arrows), indicating the recruitment of the actin cytoskeleton to GC adherent sites. The FIR of F-actin underneath Pil+Opa+ GC (FIR~ 1.5) was significantly higher than that underneath Pil+ΔOpa (FIR~ 1.2) (Fig. 21 B), indicating that Opa expression enhances F-actin accumulation in non-polarized epithelial cells. In contrast, in polarized T84 cells, the FIRs of F-actin staining underneath both Pil+Opa+ and Pil+ΔOpa GC microcolonies at the apical surface were smaller than one and significantly lower than those in non-polarized epithelial cells (Fig. 21 A, stars in x-y view, arrows in x-z view). Furthermore, the F-actin FIR in Pil+ΔOpa-infected cells (~ 0.5) was significantly lower than that of Pil+Opa+ infected polarized epithelial cells (~ 0.7)

(Fig. 21 B). Taken together, these data suggest that GC induce F-actin recruitment to adherent sites in non-polarized epithelial cells, which is associated with microvilli elongation, but F-actin reduction at GC adherent sites in polarized epithelial cells, which is associated with microvilli damaging. Opa expression enhances F-actin recruitment and reduction at GC adherent sites of non-polarized and polarized epithelial cells respectively.

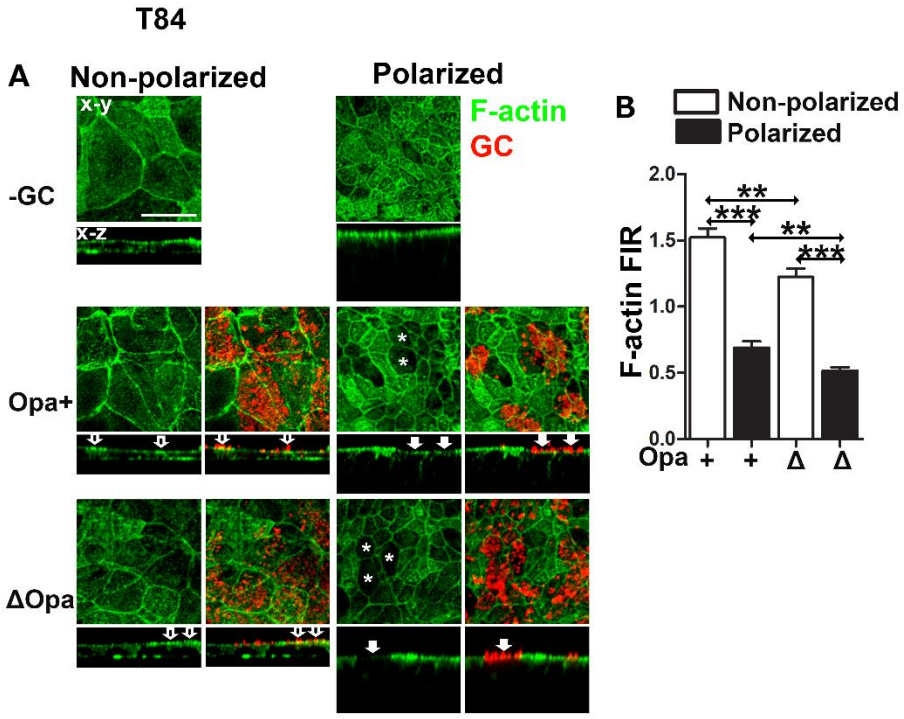

Figure 21. GC inoculation induces differential redistribution of F-actin at GC adherent sites in non-polarized and polarized epithelial cells.

Two-day non-polarized and 10-day polarized T84 cells were apically incubated with Pil+Opa+ or ΔOpa for 6 h (MOI~10). Cells were fixed and stained for F-actin and GC, and analyzed using 3D-CFM. (A) Representative images of x-y views of the luminal surface and x-z views of sections cross the luminal to the basal surface are shown. (B) The level of F-actin redistribution was quantified by mean fluorescence intensity ratio (FIR) (±SEM) of F-actin underneath GC microcolony to the adjacent luminal area. n=3, *p<0.05; **p< 0.01; ***p<0.001.

3.4.5 GC induce F-actin redistribution in endocervical epithelial cells, which involves NMII

To determine if GC-induced differential actin reorganization in non-polarized and polarized epithelial cells occurs in the human cervix, I used the human cervical tissue explant model. Without GC inoculation, F-actin staining is evenly distributed under the plasma membrane of individual epithelial cells across all the layers in the ectocervix (Fig. 22). In contrast, F-actin staining in the endocervical epithelium is highly polarized to the apical surface with much less staining at the lateral and basal surface (Fig. 23 A). Unlike in the non-polarized T84 cells, GC inoculation (both Pil+Opa+ and Pil+ΔOpa) had no significant effect on F-actin redistribution in ectocervical epithelial cells (Fig. 22). In contrast, decreased F-actin staining was observed underneath GC microcolonies in endocervical epithelial cells (Fig. 23 A, arrows). By visual inspection, I found ~70% Pil+ΔOpa but ~40% Pil+Opa+ microcolonies with decreased F-actin staining underneath (Fig. 23 B).

In addition to the reduction of F-actin staining underneath GC microcolonies, the level of F-actin staining under the lateral membrane increased, which was concurrent with a decrease in the height of endocervical columnar epithelial cells inoculated with Pil+ΔOpa. These observations suggest a decrease in the polarity of endocervical epithelial cells. To quantify this decrease, I measured the FIR of F-actin at the apical surface (Fig. 23 C, yellow dotted line) relatively to the lateral surface (Fig. 23 C, yellow dotted line). Inoculation of both Pil+Opa+ and Pil+ΔOpa induced significant decreases in the F-actin apical to the lateral FIR, compared to no inoculation control.

Furthermore, the apical to lateral F-actin FIR in Pil+ΔOpa GC-infected endocervical epithelial cells (~2) was significantly lower than Pil+Opa+ GC-infected cells (~3) (Fig. 23 C). Taking together, my data suggest that GC can induce actin depolarization beneath their contact sites and disrupt the polarized actin organization in the endocervical epithelial cells, but do not significantly change actin organization in ectocervical epithelial cells. Opa expression weakens the ability of GC to remodel the actin cytoskeleton.

Previous studies from our lab showed that GC induced activation of the actin motor protein NMII through its light chain kinase (MLCK) and NMII activation involved in GC-induced exfoliation and penetration in the human endocervix [95]. To address the question if NMII activation plays any role in the GC-induced actin redistribution in polarized epithelial cells, I examined F-actin distribution in epithelial cells of cervical tissue explants treated with the MLCK inhibitor ML-7. The treatment with ML-7 significantly decreased the percentage of Pil+ΔOpa microcolonies with decreased F-actin underneath (from ~70% to ~ 40%) (Fig. 23 A, B, arrowheads). The apical polarity of F-actin, measured by F-actin apical to the lateral FIR, and columnar morphology of endocervical epithelial cells were also partially restored by ML-7 (Fig. 23 C). These results indicate that GC-induced actin remodeling in the columnar endocervical epithelial cells involves NMII activation. The inhibition of NMII activation can be a potential mechanism by which Opa inhibits actin remodeling in polarized endocervical epithelial cells.

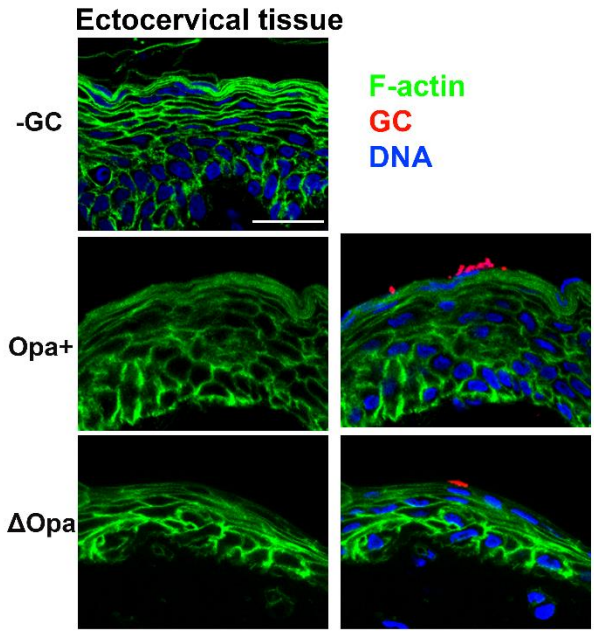

Figure 22. GC inoculation had no significant effect on F-actin redistribution in ectocervical epithelial cells.

Human ectocervical tissue pieces were incubated with Pil+Opa+ and Pil+ΔOpa (MOI~10) for 24 h, with unassociated GC washed off at 6 and 12 h. Tissues were fixed, stained for F-actin, DNA, and GC, and analyzed using 3D-CFM. Representative images that intercept both the apical and basolateral surfaces are shown (Scale bar, 20 μm). n=3, *p<0.05; **p< 0.01; ***p<0.001.

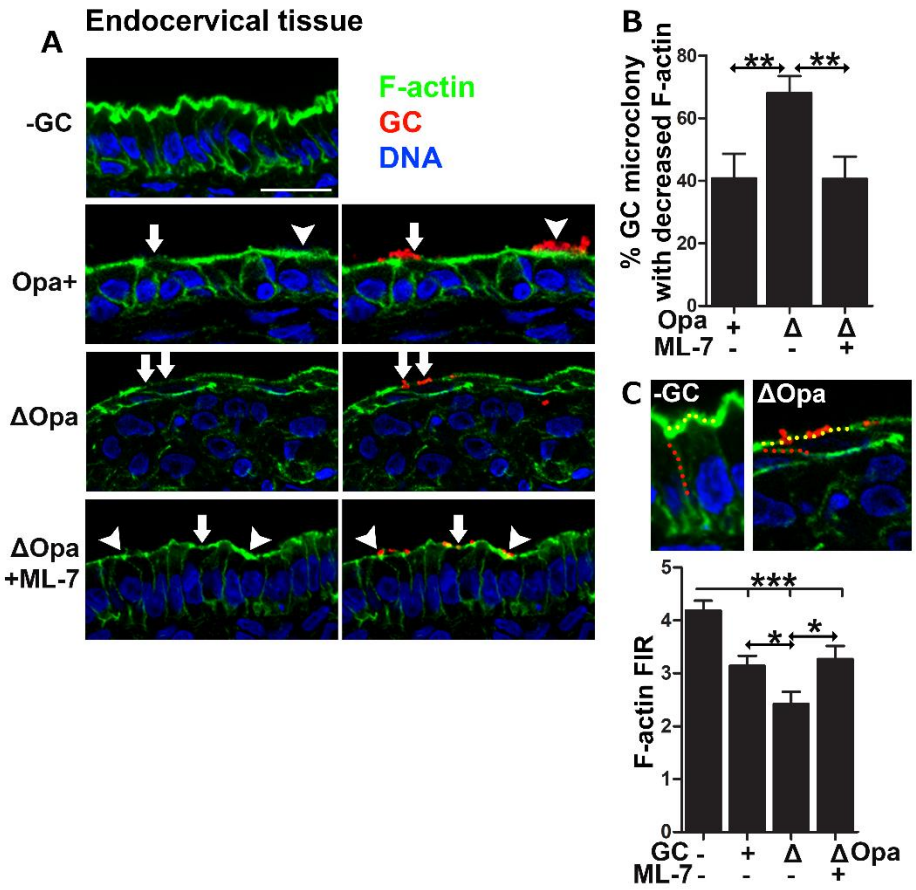

Figure 23. GC induce F-actin redistribution in endocervical epithelial cells, which involves NMII.

Human endocervical tissue pieces were untreated or pretreated with ML-7 for 1 h and incubated with Pil+Opa+ and ΔOpa (MOI~10) with or without inhibitor for 24 h at 37˚C, with unassociated GC washed off at 6 and 12 h. Tissues were fixed, stained for F-actin, DNA, and GC, and analyzed using 3D-CFM. (A) Representative images that intercept both the apical and basolateral surfaces are shown (Scale bar, 20 μm). The level of F-actin redistribution was quantified by the percentage of GC microcolonies with decreased F-actin staining (±SEM) (B), and by the FIR of F-actin at the apical surface to the lateral surface of endocervical epithelial cells (±SEM) (C). n=2, *p<0.05; **p< 0.01; ***p<0.001.

3.4.6 GC induce the redistribution of the actin nucleation factor Arp2/3 in endocervical epithelial cells, which involves NMII

Arp2/3 complex, which mediates polymerization of branched actin filaments, has been implicated for the uptake of various pathogens [135]. I hypothesize that GC regulate actin remodeling in polarized endocervical epithelial cells through the Arp2/3 complex. To test this hypothesis, I inoculated human endocervical tissue explants with Pil+Opa+ and Pil+ΔOpa GC for 24 h and stained tissue sections for Arp2. The Arp2 distribution in columnar endocervical epithelial cells was quantified by the Arp2 FIR at the apical to the lateral membrane as described in Figure 23 C. Without infection, Arp2 staining concentrated beneath the apical membrane, with an FIR >2 (Fig. 24 A, B). Inoculation with GC Pil+ΔOpa significantly decreased the apical polarization of Arp2 (FIR< 1.5). Inoculation with GC Pil+Opa+ also decreased the Arp2 polarity (FIR~ 1.7), but the decrease was significantly lower than that induced by GC Pil+ΔOpa (Fig. 24 A arrowheads, B). The treatment of the MLCK inhibitor ML-7 inhibited Arp2 redistribution induced by Pil+ΔOpa back to the level of Pil+ Opa+ infected cells (FIR~ 2)(Fig. 24 A, arrowheads). My data indicate that GC disrupt the apical polarized distribution of Arp2/3 in endocervical epithelial cells, which depends on GC-induced NMII activation. Opa expression inhibits GC-induced redistribution of Arp2/3

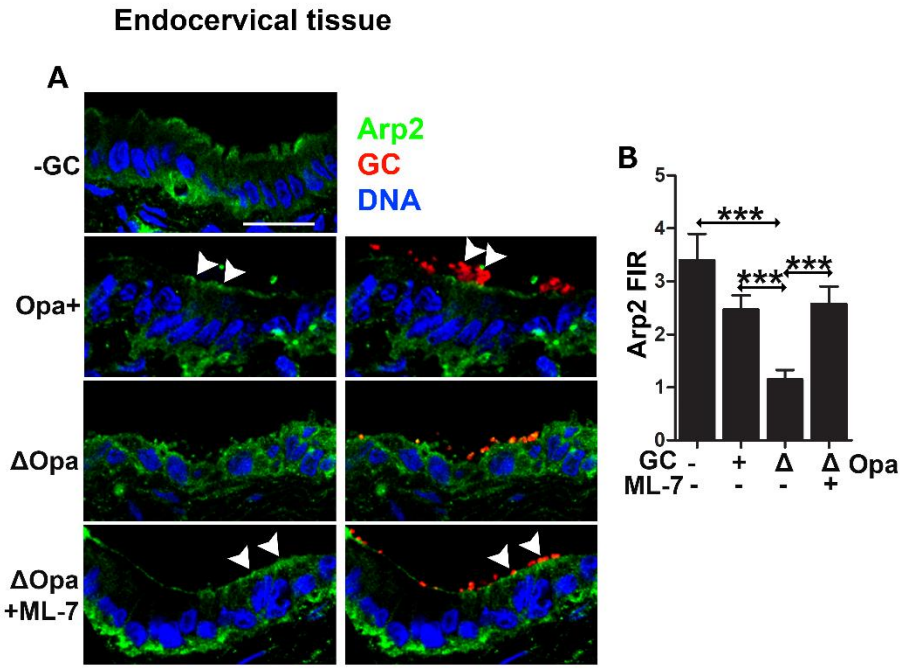

Figure 24. GC induce Arp2/3 redistribution in endocervical epithelial cells, which involves NMII.

Human endocervical tissue explants were untreated or pretreated with ML-7 for 1 h and incubated with Pil+Opa+ and Pil+ΔOpa (MOI~10) with or without inhibitor for 24 h at 37˚C, with unassociated GC washed off at 6 and 12 h. Tissues were fixed, sectioned, stained for Arp2, DNA and GC, and analyzed using CFM. (A) Representative images that intercept both the apical and basolateral surfaces are shown (Scale bar, 20 μm). (B) The level of Arp2 redistribution was quantified by the FIR of Arp2 staining at the apical relative to the lateral surface (±SEM). n=2 *p<0.05; **p< 0.01; ***p<0.001.

3.3.7 GC inoculation induces the elevation of the intracellular calcium level in polarized but not non-polarized epithelial cells

Data from my experiments and previous lab members have shown that GC inoculation induces the increase of intracellular calcium level in polarized T84, which leads to the NMII activation, apical junction disruption, epithelial exfoliation, and eventually penetration into the subepithelium. Opa expression inhibits these processes [95]. However, whether GC also induce the calcium flux similarly in non-polarized epithelial cells is unknown. To address this question, I compared the intracellular calcium levels in non-polarized and polarized T84 cells with or without inoculation with GC Pil+Opa+ and Pil+ΔOpa by the mean fluorescence intensity (MFI) of Fluo-4, a calcium dye, in the cytoplasma region of individual cells (Fig. 25 A). Epithelial cells treated with thapsigargin, which induces intracellular calcium by inhibition of calcium pumping into endoplasmic reticula, serves as a positive control. Consistent with my previous results, inoculation with GC Pil+Opa+ and Pil+ΔOpa both increased the intracellular calcium level in polarized epithelial cells, with the level in Pil+ΔOpa-infected cells significantly higher than Pil+Opa+-infected cells (Fig. 25 B). In contrast, in non-polarized epithelial cells, cells inoculated with both Pil+Opa+ and Pil+ΔOpa did not show significant changes in the level of the intracellular calcium (Fig. 25 B). This result suggests that GC induce different upstream signaling which triggers distinct actin reorganization and leads to different infectivity of GC in non-polarized and polarized epithelial cells.

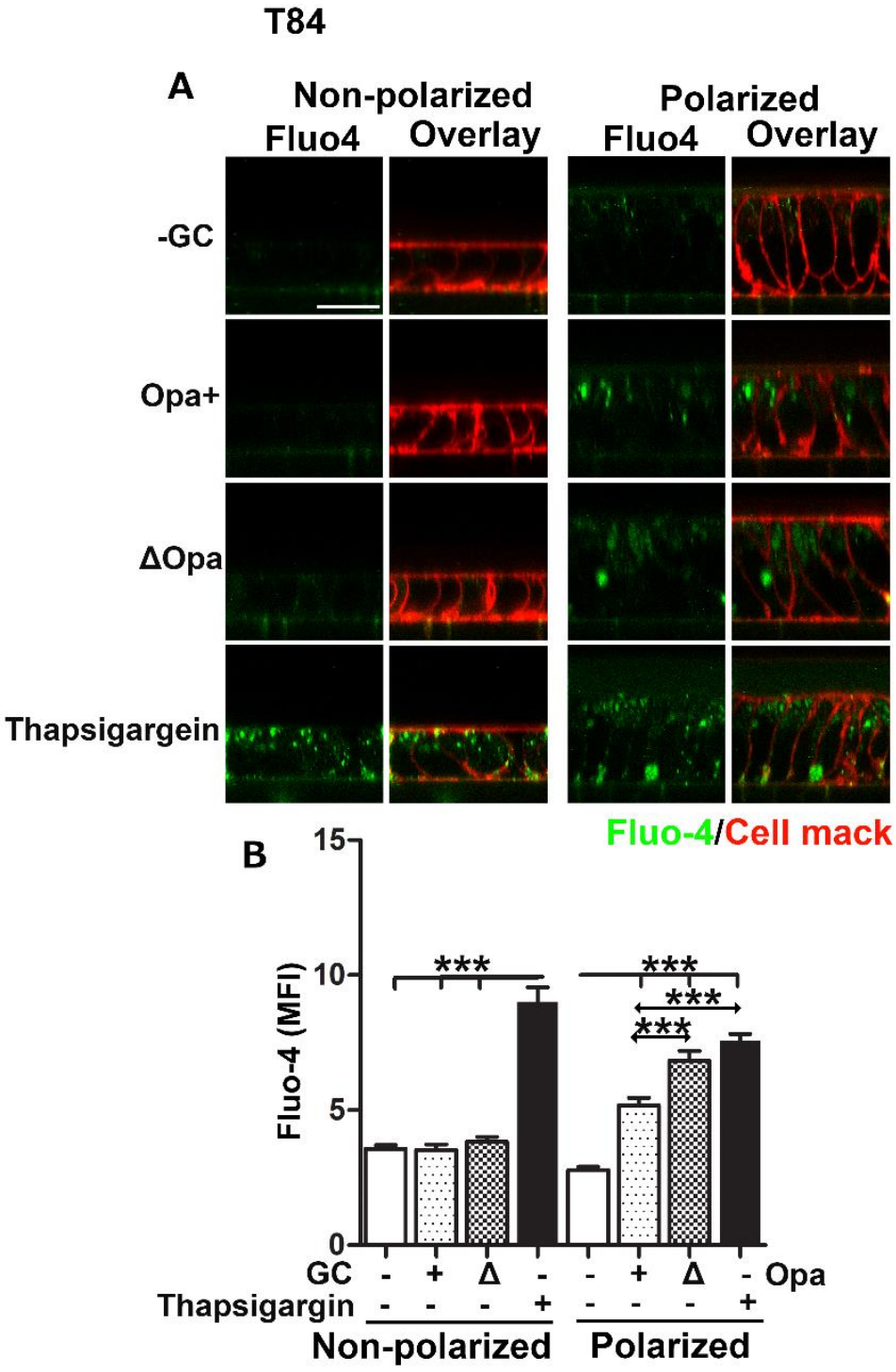
T84
A
Non-polarized
Polarized
Fluo4
Overlay
Fluo4
Overlay
-GC
Opa+
ΔOpa
Thapsigargein
Fluo-4/Cell mack
B
Fluo-4 (MFI)
15
10
5
0
***
***
***
***
GC - + Δ - - + Δ - Opa
Thapsigargin - - - + - - - +
Non-polarized
Polarized

Figure 25. GC inoculation induces the elevation of intracellular calcium levels in polarized but not in non-polarized T84 cells.

Two-day non-polarized and 10-day polarized T84 cells were incubated apically with or without GC Pil+Opa+ or Pil+ΔOpa with or without thapsigargin (10 μM), for 4 h. Cells were incubated with the calcium indicator Fluo-4 and the membrane dye CellMask and analyzed using 3D-CFM. (A) Representative images of x-z view are shown. Scale bar, 20 μm. (B) The level of intracellular calcium was quantified by MFI (±SEM) of Fluo-4 in the cytoplasmic region of >50 cells from three independent experiments. n=3, *p<0.05; **p< 0.01; ***p<0.001.

3.5 Discussion

Cell polarity is the key difference in the properties of epithelial cells in the human cervix. This study utilized non-polarized and polarized epithelial cell model generated from the same cell line to study the impact of cell polarity on GC infectivity and GC-induced actin cytoskeleton remodeling. I found that GC invade more efficiently into non-polarized than polarized epithelial cells, but cell polarity does not significantly affect GC of adhesion despite their different surface morphology. GC remodel the actin cytoskeleton in non-polarized and polarized epithelial cells in the opposite way, accumulating and reducing F-actin underneath GC adherent sites, respectively. The F-actin accumulation in non-polarized epithelial cells is concurrent with microvilli elongation, and the F-actin reduction, which also occurs in GC-infected endocervix, is concurrent with microvilli demolishment. These results demonstrate that the epithelial cell polarity can significantly impact GC infectivity, and the non-polarized and polarized organization of the actin cytoskeleton is a critical underlying factor.

By comparing GC strains expressing phase variable Opa and no Opa, I found that Opa expression enhanced the level of adhesion in both non-polarized and polarized epithelial cells. This observation is consistent with what I have seen in the human cervical tissue explants where expression of CEACAM- binding Opa (Opa_{CEA}) enhanced GC colonization in both non-polarized ectocervical and polarized endocervical epithelial cells. These findings suggest that epithelial cell polarity does not significantly change the regulatory effect of Opa on GC infectivity, and the non-polarized and polarized epithelial cell model mimics a certain aspect of GC infection

processes *in vivo*. However, there is an inconsistency in our observation between the two models. In the cell line model, GC adhered to non-polarized and polarized epithelial cells at a similar level. But GC colonized the ectocervix at a higher level than the endocervix. Such differences could be caused by a differential expression level of GC host receptors in the ecto and endocervical epithelial cells. Chapter 2 has shown a higher level of CEACAM expression in ectocervical than endocervical epithelial cells. In contrast, non-polarized and polarized cell model was derived from the same cell line and unlikely had different expression level of the host receptors due to polarization. Technical differences may also contribute to the inconsistency. In the tissue explant model, GC had access to all three cervical regions, but in the cell line model, GC were incubated with non-polarized and polarized epithelial cells separately.

It is technically difficult to identify GC inside epithelial cells in human cervical tissue explants using confocal fluorescence microscopy, thus GC invasion into epithelial cells in tissue explants cannot be examined. However, I did not observe significant GC staining between the luminal surface and the basal membrane of the cervical epithelium. This is not surprising as only 0.1-1% of adhered GC invade into epithelial cells using a cell line model and gentamicin resistance assay. The non-polarized and polarized epithelial cell line model enabled me to examine the impact of epithelial polarity on GC invasion. I found that GC invade more efficiently into the non-polarized than polarized epithelial cells, which is consistent with the clinical observation of GC inside cervical epithelial cells shed off the epithelium [20].

Furthermore, I found that Opa expression enhanced invasion into both types of epithelial cells. Published data from Song lab [95] and the results presented in Chapter 2 showed that Pil+ΔOpa GC transmigrate across polarized epithelial cells and penetrate into the subepithelium of the polarized endocervical epithelial cells more efficiently than Pil+Opa+. However, none of the GC strains used penetrate into the subepithelium of non-polarized ectocervical epithelial cells. These findings together suggest that Opa expression differentially regulates GC infectivity in different types of epithelial cells. In non-polarized epithelial cells and the ectocervix, Opa expression enhanced GC colonization and invasion, but in polarized epithelial cells and the endocervix, inhibited GC penetration. Consequently, expression of Opa drives GC infectivity to colonization and invasion but not penetration.

Non-polarized and polarized epithelial cells have different morphology (stratified with sparse microvilli or columnar with dense microvilli at the apical membrane) and actin organization (non-polarized or apical polarized distribution). Apical polarized F-actin generates and maintains the apical microvilli of polarized epithelial cells. It is expected that GC can induce different changes in the morphology and actin organization in non-polarized and polarized epithelial cells. It is surprising that GC modify actin organization in non-polarized and polarized epithelial cells in the opposite way, increasing or decreasing F-actin underneath GC adherent sites, which may lead to different morphological changes in non-polarized and polarized epithelial cells, microvilli elongation and demolishment respectively. Pil+Opa+ GC induce microvilli elongation in non-polarized epithelial cells, which may contribute to

enhanced GC invasion by wrapping GC with host cell membranes. The extensive membrane protrusion induced by GC Pil+Opa+ is potentially mediated by actin polymerization underneath GC microcolonies, demonstrated by the recruitment of F-actin. In contrast, GC Pil+ΔOpa+ induce microvilli demolishment at the apical surface of polarized epithelial cells probably by inhibiting actin polymerization or enhancing actin depolymerization. Microvilli demolishment appears to allow GC to interact with the apical membrane intimately, probably facilitating GC invasion by the zipper mechanism, which requires membrane ruffling [130-132]. However, as Opa expression reduces the level of Arp2/3 and F-actin exclusion but enhances GC invasion into polarized epithelial cells, the reduction of Arp2/3 and F-actin is not essential for GC invasion. These data demonstrate that GC differentially modify the morphology and actin organization of non-polarized and polarized epithelial cells to promote adhesion and invasion. The mechanism by which GC modulate actin organization in epithelial cells is unknown. Unlike those well-studied actin modulating pathogens [135], no secreted effector proteins have been found in GC. The potential mechanisms include the interactions of GC surface molecules with host receptors and the downstream signaling of host receptors. For example, the host receptors for Opa, CEACAM, have been shown to direct or indirect interaction with actin regulators [59, 158].

GC-induced actin recruitment to GC adherent sites was observed in non-polarized T84 cells but was not observed in the GC-inoculated ectocervical epithelial cells in tissue explants. The ectocervical epithelium has a much more complicated cytoarchitecture

than non-polarized epithelial monolayers. The superficial layers of multiple-layered ectocervical epithelial cells are highly differentiated and cornified. Cornified cells eventually lose nuclei and die, consequently lacking the actin cytoskeleton response to GC infection. However, the inner layers of the ectocervical epithelium, when are exposed to GC due to GC-induced exfoliation of the superficial layers, may be able to mount actin remodeling response to GC.

The decrease of Arp2/3 in the apical surface of polarized epithelial cells is a potential cause of F-actin exclusion underneath GC adherent sites. The exclusion of F-actin provides an explanation for the massive microvilli demolishment induced by GC Pil+ΔOpa. GC Pil+Opa+ induce the above phenotypes to a significantly less degree, suggesting that the Opa expression inhibits GC-induced actin reorganization and morphological changes in polarized epithelial cells. In addition, to support microvilli, the actin cytoskeleton is a critical support for the apical junction. The perijunctional actomyosin ring regulates the stability and permeability of the apical junction [137]. Song lab previously showed that GC induce the activation of NMII, which leads to the disassembly of the apical junction [95]. Here, I show that inhibition of GC-induced NMII activation restores the polarized distribution of Arp2/3 and the actin cytoskeleton. My data suggest that GC-induced NMII activation is also involved in actin reorganization in response to GC infection.

The GC-induced microvilli elongation and F-actin accumulation in non-polarized epithelial cells indicate actin polymerization. In contrast, the GC-induced microvilli demolishment and F-actin exclusion in polarized epithelial cells indicate actin depolymerization. NMII has been shown to play a role in both polymerization and depolymerization of the actin filament [156]. The role of Arp2/3 has been implicated in the polarized endocervical epithelial cells. Further experiments need to be done on the effect of NMII and Arp2/3 inhibitors on the plasma membrane remodeling and actin reorganization induced by GC Pil+Opa+ and Pil+ΔOpa in non-polarized and polarized epithelial cells. Data presented in Chapter 2 show that Opa expression regulates these processes differently in non-polarized and polarized epithelial cells, and the role of Opa interaction with its host receptors has been implicated. To test this hypothesis, further studies need to done on the plasma membrane remodeling and actin reorganization induced by different Opa isoforms in non-polarized and polarized epithelial cells.

In summary, the data presented in this chapter demonstrate that GC induced differential remodeling of the actin cytoskeleton, which leads to the differential membrane remodeling and infectivity in non-polarized and polarized epithelial cells. Expression of Opa regulates these processes differently in non-polarized and polarized epithelial cells. These data suggest that the polarity of epithelial cells is one of the critical factors that regulate GC infectivity.

Chapter 4: Conclusions, discussion, and future direction

4.1 Summary

Gonorrhea, caused by *Neisseria gonorrhoeae* (GC), is the second most common sexually transmitted infection (STI) in the United States. GC is a gram-negative bacteria and a human exclusive pathogen. More than 50% GC infection in females is asymptomatic, which delays treatments and, leads to severe complications, including pelvic inflammatory disease (PID), fallopian tube scarring and blockage with subsequent ectopic pregnancy and infertility. The asymptomatic female infection can also lead to disseminated gonococcal infection (DGI) and increase the possibility of getting coinfection with HIV and other sexually transmitted infections. The continuous raising of antibiotic-resistant strains makes gonorrhea public health and women's health crisis.

The cervix is the gate of the female reproductive tract (FRT) and the initiation site of GC infection. The epithelium is the first line of defense GC need to overcome to establish infection. The cervical epithelium is heterogeneous and has distinct properties in different anatomical regions. The ectocervix is line with multiple-layered non-polarized epithelial cells; the endocervix, single-layered polarized columnar epithelial cells; and the transformation zone (TZ), epithelial cells that gradually transformed from multiple-layered to single-layered and from non-polarized to

polarized columnar epithelial cells. However, whether GC infect the heterogeneous cervical epithelium in the same way or differently is unknown.

A major barrier to the research of GC infection in women is the lack of experimental model mimicking the heterogeneous cervical epithelium. To overcome this barrier, I established a human cervical tissue explant model, which maintains the *in vivo* cytoarchitecture of the cervical epithelium. This model enables us to observe that GC change their infectivity in different cervical regions based on phase variable virulence determinants on the bacterial surface and differential availability of host receptors on the cervical epithelial cells. GC colonize the ectocervical and TZ more efficiently than the endocervical epithelial cells. In contrast, GC only penetrate into sub-epithelial tissue in TZ and the endocervix, with a higher level of penetration in TZ. Pili are required for GC colonization in all three cervical regions. Expression of Opa_{CEA} enhances colonization in the ecto and endocervix, where CEACAM is abundantly expressed at the luminal surface, but only inhibits GC penetration in the endocervix. Expression of different Opa proteins does not affect GC infectivity in the TZ, where CEACAM is expressed at a low level. The regulatory effect of Opa_{CEA} is dependent on the expression of CEACAM1 and the ITIM domain in its cytoplasmic domain, potentially also its downstream SHP activation. GC-induced junction disruption and epithelial exfoliation in the TZ that expresses low levels of CEACAMs are not regulated by Opa_{CEA} expression on GC. The inhibition of GC penetration in the endocervix by Opa_{CEA}-CEACAM1 interaction involves SHP activation, which inhibits cell-cell junction disruption and subsequent inhibition of epithelial exfoliation.

The level of cell polarity is the most prominent difference between the ecto and endocervical epithelial cells. The non-polarized and polarized epithelial cell line model enables us to examine the impact of epithelial polarity alone on GC infectivity, particularly GC invasion that is difficult to study using tissue explants. GC exhibit a higher level of invasion into non-polarized than into polarized epithelial cells, but similar levels of adhesion to non-polarized cells as to polarized epithelial cells. The expression of phase variable Opa enhances both adhesion and invasion in both non-polarized and polarized epithelial cells, suggesting the cell polarity is the main factor influencing GC invasion. GC with phase variable Opa induce microvilli elongation exclusively in non-polarized cells, which is mediated by F-actin accumulation to facilitate GC adhesion and invasion. In contrast, GC lacking Opa expression induce massive disruption of microvilli in the apical surface of polarized epithelial cells, by a reduction of the actin cytoskeleton at GC adherent sites, observed in both polarized cell line model and endocervical tissue explant model. Such actin cytoskeleton exclusion may result from the redistribution of Arp2 and the activation of NMII. Furthermore, GC inoculation only induces an increase in intracellular calcium levels in polarized, but not in non-polarized epithelial cells. These data suggest that GC induces different signaling and actin reorganization in non-polarized and polarized epithelial cells, which alter GC infectivity and infection mechanisms.

Taking together, GC modulate its infectivity, colonization, invasion and penetration and infection mechanisms, based on both the properties of cervical epithelial cells

(host receptor expression and cell polarity) and the phase variable bacterial surface structure.

4.2 Working Model

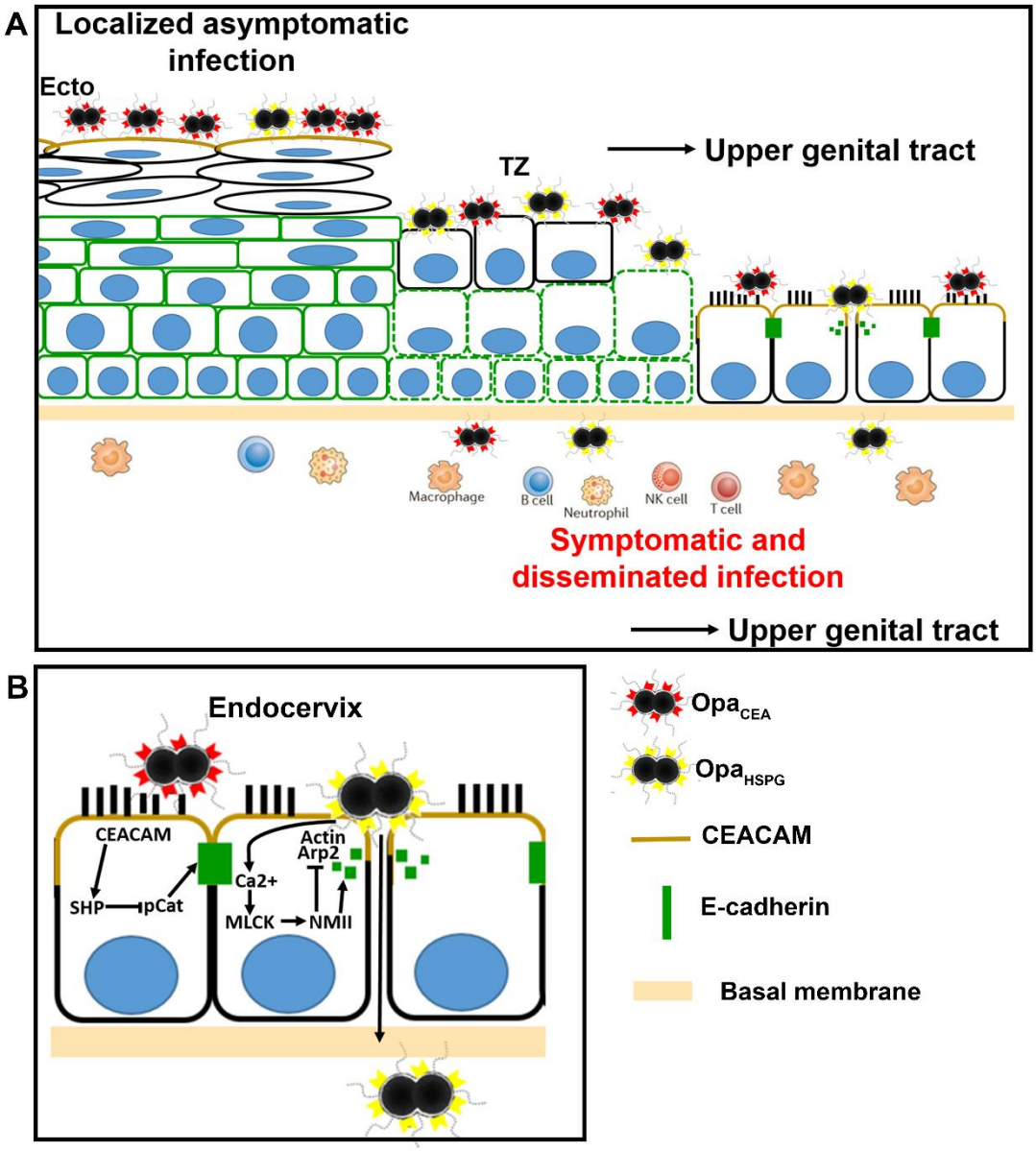

Figure 26. Working model for *Neisseria gonorrhoeae* interaction with the three cervical regions, the ectocervix, transformation zone (TZ), and endocervix [159].

(A) A schematic diagram of GC infectivity in the three cervical regions. The level of GC colonization at the luminal surface of the ecto and TZ epithelia is higher than in the endocervix. GC can only penetrate into the subepithelial tissue of the TZ and endocervix, with a higher level of GC penetration into the TZ epithelium. The Opa_{CEA} expressing GC dominate the colonizing GC community at the luminal surface of the ecto and endocervical epithelia by interacting with its epithelial receptor CEACAM. In the endocervix, Opa_{HSPG} expressing GC penetrate more into the subepithelial tissue by disrupting the apical junction. The TZ epithelium expresses CEACAM at a low level, thus both the colonizing and penetrating bacterial community is a mixture of GC expressing different Opa proteins.

(B) A schematic diagram of the signaling pathway induced by GC Opa_{CEA} and Opa_{HSPG} in the endocervical epithelial cells. GC Opa_{CEA} interact with its receptor CEACAM at the apical surface of the endocervical epithelial cells, which potentially activates the tyrosine phosphatase SHP, leading to inhibition of the apical junction disassembly and subsequent GC penetration. In contrast, GC Opa_{HSPG} infection increases intracellular calcium level, leading to NMII activation through MLCK. The NMII activation can lead to the apical junction disassembly and consequently GC penetration. The NMII activation can also potentially lead to the redistribution of the Arp2/3 complex and F-actin from the apical surface of the polarized endocervical epithelial cells.

My thesis project used the human cervical tissue explant model, non-polarized and polarized epithelial cell line model and GC expressing different Opa proteins to study the effect of phase variable bacterial surface structures and the heterogeneity of cervical epithelium on GC infectivity in the human cervical epithelial cells. Based on my results and previously published studies, I propose the following working model.

GC are first deposited onto the vaginal and ectocervical epithelium through sex with an infected partner. The vaginal and ectocervical epithelium is colonized by dense commensal microbiota creating a unique microenvironment at the mucosal surface [11, 160]. To establish infection, successful colonization at the mucosal surface is the first step for GC. A higher level of colonization of GC in the vaginal and ectocervical epithelium has been reported clinically [15, 20], but GC induced vaginitis is rare [4], indicating GC colonization fails to induce immune response in the vagina and ectocervix. My results show higher levels of GC colonization in the ectocervix without any penetration, consistent with previous clinical observations of no symptomatic infection in the vagina and the ectocervix. My finding that pili are essential for GC colonization in all anatomic regions of the human cervix indicates that pili-mediated interaction of GC with the luminal surface of cervical epithelial cells is the essential first step to establish infection in the human cervix. In contrast, Opa expression is not essential for GC infection but can regulate GC infectivity. The expression of CEACAM-binding Opa (Opa_{CEA}), enhances GC colonization in both non-polarized ectocervical epithelial cells and polarized endocervical epithelial cells, through interaction with CEACAMs, which is expressed at the luminal surface of the

ectocervical and endocervical but not TZ epithelium. Such Opa-CEACAM interaction enhances colonization through the inhibition of GC-induced epithelial shedding. Opa$_{CEA}$ inhibit shedding of non-polarized epithelial cells by activation of integrin and CD105 showed by Dr. Hauck's group using cell line and mouse model [61, 62]. In the absence of Opa$_{CEA}$, GC induce higher levels of epithelial shedding, which shed off GC colonized epithelial cells resulting in the low level of colonization. Consequently, the community of GC colonizing the ectocervical epithelium is dominated by the Opa$_{CEA}$ expressing bacteria, given that the Opa$_{HSPG}$ expressing bacteria are shed and the majority of 11 Opa proteins interact with CEACAMs. Despite the exfoliation, GC do not penetrate into the ectocervical epithelium, may be due to the incapability of GC to disrupt the of E-cadherin-based adherens junction in the remaining epithelial layers after infection. The failure of GC to penetrate across the ectocervical epithelium provides a potential explanation for the localized and asymptomatic vaginal and ectocervical infection. GC expressing phase variable Opa adhere and invade more efficiently into non-polarized epithelial cells compared to GC expressing no Opa and GC invasion into polarized epithelial cells. Concurrent with the enhanced invasion of Opa-expressing GC, the F-actin accumulation and microvilli elongation at GC adherent sites was observed exclusively in non-polarized epithelial cells. These data obtained from the non-polarized epithelial cell line model suggest that GC, particularly those expressing phase variable Opa, can invade into non-polarized epithelial cells, such as ectocervical epithelial cells and exfoliated cervical epithelial cells, by inducing actin cytoskeleton mediated bacterial uptake.

The transformation zone (TZ) is a unique area between the ecto and endocervix. The low level of CEACAM expression in TZ epithelial cells provides an explanation for the similar level of colonization, penetration, and exfoliation induced by GC expressing different isoforms of Opa or no Opa. The level of GC colonization in the TZ is similar to that in the ectocervix that expresses CEACAMs, suggesting that Opa proteins do not play a significant role in GC colonization in TZ. The high level of penetration across TZ epithelium is mediated by the disruption of E-cadherin based cell-cell adhesion, which also leads to epithelial exfoliation. The multiple-layered structure of TZ epithelium indicates that the number of layers is not a major factor that deters GC from penetration. The similar infectivity displayed by GC expressing Opa_{CEA} and Opa_{HSPG} indicates that the bacteria community infecting the TZ is a mixture of GC expressing different Opa proteins. The penetration of GC into subepithelial tissue will increase the chance of GC being exposed to immune cells, which potentially cause inflammation and symptomatic infection.

The TZ epithelium gradually transforms into the endocervix, which leads to the upper genital tract. The level of GC colonization and penetration in the endocervix are generally lower than those in the ectocervix (colonization only) and TZ (colonization and penetration). However, Opa_{CEA} expression increases the level of colonization in the endocervical epithelial cells, which is mediated by CEACAMs expressed on the apical surface of the endocervical epithelial cells. Opa-CEACAM interaction inhibits the disruption of E-cadherin-based adherens junction, consequently decreasing epithelial exfoliation and penetration, and increasing colonization. Consistently, Song

lab has previously shown that Opa_{CEA} expression interferes with GC transmigration across polarized T84 epithelial cells, that express CEACAMs [94, 95]. In contrast, in the absence of Opa-CEACAM interaction (Opa_{HSPG} GC and TZ epithelial cells), GC disrupt the adherens junction, leading to epithelial shedding and GC penetration, and colonization reduction. Previously published data from Song lab demonstrate that GC disrupt the apical junction through increasing intracellular calcium level and calcium-dependent activation of NMII [95], providing a mechanistic explanation for the distinct behavior of GC in polarized endocervical epithelial cells. Data from both epithelial cell line model and cervical tissue explant mode suggest the invasion into epithelial cells is not the major mechanism used by GC to infect polarized endocervical epithelial cells. GC invade into polarized epithelial cells even less than into non-polarized epithelial cells. The invasion of GC into polarized epithelial cells involves in the demolishment of microvilli at the apical surface probably by activation of NMII and redistribution of the actin nucleator Arp2/3 away from the apical surface of polarized epithelial cells. Taking together, in the endocervix, colonizing GC at the mucosal surface predominantly express Opa_{CEA}, which can potentially ascend to the upper genital tract through the continuity of the epithelium, causing pelvic inflammatory disease. Penetrating GC predominantly express Opa_{HSPG}. They penetrate through the paracellular space between neighboring epithelial cells by disassembling cell-cell junction complex creating breaches in this physical protective barrier. GC penetrating into subepithelial tissues potentially induce inflammation and causing disseminated gonococcal infection (DGI).

In summary, my Ph.D. research focused on the mechanism by which GC cope with the heterogeneous mucosal surface of the human cervix to initiate infection. The differential infectivity of GC, preferring colonization or penetration, in different cervical regions is the first direct evidence for that GC use different mechanisms to infect different types of cervical epithelial cells. The infection mechanism changes depending on both the bacterial phase variation of bacterial surface structures and the distinct properties of cervical epithelial cells.

4.3 Future Direction

4.3.1 Highlights

We are the first to study the mechanism of GC infection in the cervical epithelium using human cervical tissue explants. Using this model, I showed that GC switch the mode of infectivity, colonization or penetration by Opa phase variation in response to the heterogeneous cervical epithelium they encounter. The results from my thesis research indicate that Opa_{CEA} expression specifically promotes colonization in the ecto and endocervix, which expresses CEACAMs. GC colonization my mainly lead to localized, asymptomatic infection. In contrast, the expression of Opa_{HSPG} and low level of CEACAM expression all GC penetration into the endocervix and TZ respectively, which potentially leads to symptomatic infection and disseminated gonococcal infection (DGI).

My thesis research enables us to reconcile conflicting results of previous research based on cell line and the mouse model, which do not fully represent the characteristics of the human cervix *in vivo*. No previous model mimics the heterogeneity of cervical epithelium, and thus, this important factor was largely disregarded previously. The results from my thesis research emphasize the impact of the heterogeneous cervical epithelium on the outcomes of GC infection in women and raise the importance for the field to take this factor into consideration in GC pathogenesis research.

4.3.2 Question 1. Does the mucosal microenvironment of the human cervix affect GC infectivity and how?

In my thesis project, I focused on the impact of different types of cervical epithelial cells on GC infectivity. However, the environment of the mucosal surface along the three cervical regions is another layer of complication that GC have to deal with during infection. First, microbiota in the ectocervix, where the *Lactobacillus* species is the major commensal species, creating an acidic environment [11]. Second, the endocervix secrets a great amount of mucus, forming mucus plug to block the gate of the female reproductive tract [18]. Third, the properties of the cervical epithelial cells, including their morphology and mucus secretion, are under the influence of the periodic change of the sex hormones progestogen and estrogen [161]. All the above environmental factors along the mucosal surface of the cervix can potentially affect GC infectivity, but very limited research has been done on these subjects. The human cervical tissue explant model provides us a great opportunity to examine the impact of these mucosal environment factors on GC infectivity.

4.3.3 Question 2. Does GC infection induce differential immune responses in different cervical regions?

The asymptomatic and symptomatic infection caused by GC is directly linked to the ability of GC to evade or activate immune responses. Neutrophils have been detected in the cervical papsmear from infected patients. The alternative complement pathway has been shown involved in the female gonococcal infection [3]. These data suggest that GC infection induces immune responses to a certain level. However, does GC infection induce differential immune responses in different cervical regions is unknown. How GC manipulate host immune response to suppress symptomatic infection in the human cervix is not clear. To test the hypothesis that GC colonization in the ectocervix leads to asymptomatic infection and GC penetration into the subepithelium of the TZ and endocervix leads to symptomatic infection, the immune response induced by GC in different cervical regions should be examined.

4.3.4 Question 3. How to reconstruct the heterogeneous cervical *in vitro*?

Although the human cervix tissue explant model maintains the *in vivo* cytoarchitecture of cervical epithelium, it has some drawbacks. Although the overall structure of the cervical epithelium is consistent from one human subject to another, the ethnicity, age, menstrual cycle, and overall health condition are highly variable. Human cervical tissue explants cannot be manipulated *in vitro* as easily as cell lines and other models. Techniques, such as RNAi and transfection, are not readily available to be performed in tissue explants. Thus, we sought to mimic the cervical epithelium using cell lines as what I showed in Chapter 3 of my thesis. However, the non-polarized cells do not form a multiple-layered structure on transwells, and no method is currently available to mimics the unique structure of the TZ epithelium. It is important to develop a system to mimic all the three types of cervical epithelial cells, which can be manipulated easily *in vitro*, which will allow us to dissect the molecular and cellular mechanisms by which GC infect the human cervix in a more detailed way.

Bibliography

1.Report on global sexually transmitted infection surveillance 2015.

2.Workowski KA, Bolan GA. Sexually transmitted diseases treatment guidelines, 2015. MMWR Recomm Rep. 2015;64(RR-03):1-137. PubMed PMID: 26042815.

3.Edwards JL, Butler EK. The Pathobiology of *Neisseria gonorrhoeae* Lower Female Genital Tract Infection. Front Microbiol. 2011;2:102. doi: 10.3389/fmicb.2011.00102. PubMed PMID: 21747805; PubMed Central PMCID: PMCPMC3129011.

4.Edwards JL, Apicella MA. The molecular mechanisms used by *Neisseria gonorrhoeae* to initiate infection differ between men and women. Clin Microbiol Rev. 2004;17(4):965-81, table of contents. doi: 10.1128/CMR.17.4.965-981.2004. PubMed PMID: 15489357; PubMed Central PMCID: PMCPMC523569.

5.Rice PA, Shafer WM, Ram S, Jerse AE. *Neisseria gonorrhoeae*: Drug Resistance, Mouse Models, and Vaccine Development. Annu Rev Microbiol. 2017;71:665-86. doi: 10.1146/annurev-micro-090816-093530. PubMed PMID: 28886683.

6.(CDC) CfDCaP. Update to CDC's Sexually transmitted diseases treatment guidelines, 2010: oral cephalosporins no longer a recommended treatment for gonococcal infections. MMWR Morb Mortal Wkly Rep. 2012;61(31):590-4. PubMed PMID: 22874837.

7.Fairley CK, Hocking JS, Zhang L, Chow EP. Frequent Transmission of Gonorrhea in Men Who Have Sex with Men. Emerg Infect Dis. 2017;23(1):102-4. doi: 10.3201/eid2301.161205. PubMed PMID: 27983487; PubMed Central PMCID: PMCPMC5176237.

8.Fleming DT, Wasserheit JN. From epidemiological synergy to public health policy and practice: the contribution of other sexually transmitted diseases to sexual transmission of HIV infection. Sex Transm Infect. 1999;75(1):3-17. PubMed PMID: 10448335; PubMed Central PMCID: PMCPMC1758168.

9.Draper DL, James JF, Brooks GF, Sweet RL. Comparison of virulence markers of peritoneal and fallopian tube isolates with endocervical *Neisseria gonorrhoeae* isolates from women with acute salpingitis. Infect Immun. 1980;27(3):882-8. PubMed PMID: 6769811; PubMed Central PMCID: PMCPMC550857.

10.Bhattacharyya MN, Jephcott AE, Morton RS. Diagnosis of gonorrhoea in women: comparison of sampling sites. Br Med J. 1973;2(5869):748-50. PubMed PMID: 4736958; PubMed Central PMCID: PMCPMC1589763.

11.Ling Z, Liu X, Chen X, Zhu H, Nelson KE, Xia Y, et al. Diversity of cervicovaginal microbiota associated with female lower genital tract infections.

Microb Ecol. 2011;61(3):704-14. Epub 2011/02/02. doi: 10.1007/s00248-011-9813-z. PubMed PMID: 21287345.

12.Ghosh M, Shen Z, Fahey JV, Crist SG, Patel M, Smith JM, et al. Pathogen recognition in the human female reproductive tract: expression of intracellular cytosolic sensors NOD1, NOD2, RIG-1, and MDA5 and response to HIV-1 and *Neisseria gonorrhea*. Am J Reprod Immunol. 2013;69(1):41-51. Epub 2012/09/17. doi: 10.1111/aji.12019. PubMed PMID: 22984986; PubMed Central PMCID: PMCPMC3518676.

13.Chen C, Song X, Wei W, Zhong H, Dai J, Lan Z, et al. The microbiota continuum along the female reproductive tract and its relation to uterine-related diseases. Nat Commun. 2017;8(1):875. Epub 2017/10/17. doi: 10.1038/s41467-017-00901-0. PubMed PMID: 29042534; PubMed Central PMCID: PMCPMC5645390.

14.Mitchell CM, Haick A, Nkwopara E, Garcia R, Rendi M, Agnew K, et al. Colonization of the upper genital tract by vaginal bacterial species in nonpregnant women. Am J Obstet Gynecol. 2015;212(5):611.e1-9. Epub 2014/12/16. doi: 10.1016/j.ajog.2014.11.043. PubMed PMID: 25524398; PubMed Central PMCID: PMCPMC4754962.

15.HARKNESS AH. The pathology of gonorrhoea. Br J Vener Dis. 1948;24(4):137-47. PubMed PMID: 18099876; PubMed Central PMCID: PMCPMC1053606.

16.Rice PA. Gonococcal arthritis (disseminated gonococcal infection). Infect Dis Clin North Am. 2005;19(4):853-61. doi: 10.1016/j.idc.2005.07.003. PubMed PMID: 16297736.

17.Wu Z, Xu L, Tu Y, Chen R, Yu Y, Li J, et al. The relationship between the symptoms of female gonococcal infections and serum progesterone level and the genotypes of *Neisseria gonorrhoeae* multi-antigen sequence type (NG-MAST) in Wuhan, China. Eur J Clin Microbiol Infect Dis. 2011;30(1):113-6. Epub 2010/09/04. doi: 10.1007/s10096-010-1040-x. PubMed PMID: 20820835; PubMed Central PMCID: PMCPMC2998644.

18.Gipson IK. Mucins of the human endocervix. Front Biosci. 2001;6:D1245-55. Epub 2001/10/01. PubMed PMID: 11578960.

19.Hladik F, McElrath MJ. Setting the stage: host invasion by HIV. Nat Rev Immunol. 2008;8(6):447-57. doi: 10.1038/nri2302. PubMed PMID: 18469831; PubMed Central PMCID: PMCPMC2587276.

20.Evans BA. Ultrastructural study of cervical gonorrhea. J Infect Dis. 1977;136(2):248-55. PubMed PMID: 408425.

21.Plant L, Jonsson AB. Contacting the host: insights and implications of pathogenic Neisseria cell interactions. Scand J Infect Dis. 2003;35(9):608-13. PubMed PMID: 14620143.

22.Haas R, Meyer TF. The repertoire of silent pilus genes in *Neisseria gonorrhoeae*: evidence for gene conversion. Cell. 1986;44(1):107-15. PubMed PMID: 2866848.

23.Jonsson AB, Nyberg G, Normark S. Phase variation of gonococcal pili by frameshift mutation in pilC, a novel gene for pilus assembly. EMBO J. 1991;10(2):477-88. PubMed PMID: 1671354; PubMed Central PMCID: PMCPMC452669.

24.Rudel T, Scheurerpflug I, Meyer TF. Neisseria PilC protein identified as type-4 pilus tip-located adhesin. Nature. 1995;373(6512):357-9. doi: 10.1038/373357a0. PubMed PMID: 7830772.

25.Rudel T, Boxberger HJ, Meyer TF. Pilus biogenesis and epithelial cell adherence of *Neisseria gonorrhoeae* pilC double knock-out mutants. Mol Microbiol. 1995;17(6):1057-71. PubMed PMID: 8594326.

26.Rudel T, van Putten JP, Gibbs CP, Haas R, Meyer TF. Interaction of two variable proteins (PilE and PilC) required for pilus-mediated adherence of *Neisseria gonorrhoeae* to human epithelial cells. Mol Microbiol. 1992;6(22):3439-50. PubMed PMID: 1362447.

27.Wolfgang M, Park HS, Hayes SF, van Putten JP, Koomey M. Suppression of an absolute defect in type IV pilus biogenesis by loss-of-function mutations in pilT, a twitching motility gene in *Neisseria gonorrhoeae*. Proc Natl Acad Sci U S A. 1998;95(25):14973-8. PubMed PMID: 9844000; PubMed Central PMCID: PMCPMC24560.

28.Dietrich M, Mollenkopf H, So M, Friedrich A. Pilin regulation in the pilT mutant of *Neisseria gonorrhoeae* strain MS11. FEMS Microbiol Lett. 2009;296(2):248-56. Epub 2009/05/08. doi: 10.1111/j.1574-6968.2009.01647.x. PubMed PMID: 19486161; PubMed Central PMCID: PMCPMC4428587.

29.Edwards JL, Brown EJ, Ault KA, Apicella MA. The role of complement receptor 3 (CR3) in *Neisseria gonorrhoeae* infection of human cervical epithelia. Cell Microbiol. 2001;3(9):611-22. PubMed PMID: 11553013.

30.Stern A, Brown M, Nickel P, Meyer TF. Opacity genes in *Neisseria gonorrhoeae*: control of phase and antigenic variation. Cell. 1986;47(1):61-71. PubMed PMID: 3093085.

31.Bhat KS, Gibbs CP, Barrera O, Morrison SG, Jähnig F, Stern A, et al. The opacity proteins of *Neisseria gonorrhoeae* strain MS11 are encoded by a family of 11 complete genes. Mol Microbiol. 1991;5(8):1889-901. PubMed PMID: 1815562.

32.Billker O, Popp A, Gray-Owen SD, Meyer TF. The structural basis of CEACAM-receptor targeting by neisserial Opa proteins. Trends Microbiol. 2000;8(6):258-60; discussion 60-1. PubMed PMID: 10838580.

33.van Putten JP, Paul SM. Binding of syndecan-like cell surface proteoglycan receptors is required for *Neisseria gonorrhoeae* entry into human mucosal cells. EMBO J. 1995;14(10):2144-54. PubMed PMID: 7774572; PubMed Central PMCID: PMCPMC398320.

34.Cole JG, Fulcher NB, Jerse AE. Opacity proteins increase *Neisseria gonorrhoeae* fitness in the female genital tract due to a factor under ovarian control. Infect Immun. 2010;78(4):1629-41. doi: 10.1128/IAI.00996-09. PubMed PMID: 20100859; PubMed Central PMCID: PMCPMC2849431.

35.Yamasaki R, Bacon BE, Nasholds W, Schneider H, Griffiss JM. Structural determination of oligosaccharides derived from lipooligosaccharide of *Neisseria gonorrhoeae* F62 by chemical, enzymatic, and two-dimensional NMR methods. Biochemistry. 1991;30(43):10566-75. PubMed PMID: 1931980.

36.Danaher RJ, Levin JC, Arking D, Burch CL, Sandlin R, Stein DC. Genetic basis of *Neisseria gonorrhoeae* lipooligosaccharide antigenic variation. J Bacteriol. 1995;177(24):7275-9. PubMed PMID: 8522539; PubMed Central PMCID: PMCPMC177611.

37.Banerjee A, Wang R, Uljon SN, Rice PA, Gotschlich EC, Stein DC. Identification of the gene (lgtG) encoding the lipooligosaccharide beta chain synthesizing glucosyl transferase from *Neisseria gonorrhoeae*. Proc Natl Acad Sci U S A. 1998;95(18):10872-7. PubMed PMID: 9724797; PubMed Central PMCID: PMCPMC27988.

38.Harvey HA, Jennings MP, Campbell CA, Williams R, Apicella MA. Receptor-mediated endocytosis of *Neisseria gonorrhoeae* into primary human urethral epithelial cells: the role of the asialoglycoprotein receptor. Mol Microbiol. 2001;42(3):659-72. PubMed PMID: 11722733.

39.Song W, Ma L, Chen R, Stein DC. Role of lipooligosaccharide in Opa-independent invasion of *Neisseria gonorrhoeae* into human epithelial cells. J Exp Med. 2000;191(6):949-60. PubMed PMID: 10727457; PubMed Central PMCID: PMCPMC2193109.

40.Weel JF, Hopman CT, van Putten JP. Bacterial entry and intracellular processing of *Neisseria gonorrhoeae* in epithelial cells: immunomorphological evidence for alterations in the major outer membrane protein P.IB. J Exp Med. 1991;174(3):705-15. PubMed PMID: 1908511; PubMed Central PMCID: PMCPMC2118933.

41.Deo P, Chow SH, Hay ID, Kleifeld O, Costin A, Elgass KD, et al. Outer membrane vesicles from *Neisseria gonorrhoeae* target PorB to mitochondria and induce apoptosis. PLoS Pathog. 2018;14(3):e1006945. Epub 2018/03/30. doi: 10.1371/journal.ppat.1006945. PubMed PMID: 29601598; PubMed Central PMCID: PMCPMC5877877.

42.Mosleh IM, Huber LA, Steinlein P, Pasquali C, Günther D, Meyer TF. *Neisseria gonorrhoeae* porin modulates phagosome maturation. J Biol Chem. 1998;273(52):35332-8. PubMed PMID: 9857075.

43.Müller A, Günther D, Brinkmann V, Hurwitz R, Meyer TF, Rudel T. Targeting of the pro-apoptotic VDAC-like porin (PorB) of *Neisseria gonorrhoeae* to mitochondria of infected cells. EMBO J. 2000;19(20):5332-43. doi: 10.1093/emboj/19.20.5332. PubMed PMID: 11032801; PubMed Central PMCID: PMCPMC314008.

44.Kozjak-Pavlovic V, Dian-Lothrop EA, Meinecke M, Kepp O, Ross K, Rajalingam K, et al. Bacterial porin disrupts mitochondrial membrane potential and sensitizes host cells to apoptosis. PLoS Pathog. 2009;5(10):e1000629. Epub 2009/10/23. doi: 10.1371/journal.ppat.1000629. PubMed PMID: 19851451; PubMed Central PMCID: PMCPMC2759283.

45.Binnicker MJ, Williams RD, Apicella MA. Gonococcal porin IB activates NF-kappaB in human urethral epithelium and increases the expression of host antiapoptotic factors. Infect Immun. 2004;72(11):6408-17. doi: 10.1128/IAI.72.11.6408-6417.2004. PubMed PMID: 15501771; PubMed Central PMCID: PMCPMC523018.

46.Dupuy AG, Caron E. Integrin-dependent phagocytosis: spreading from microadhesion to new concepts. J Cell Sci. 2008;121(11):1773-83. doi: 10.1242/jcs.018036. PubMed PMID: 18492791.

47.Edwards JL, Apicella MA. The role of lipooligosaccharide in *Neisseria gonorrhoeae* pathogenesis of cervical epithelia: lipid A serves as a C3 acceptor molecule. Cell Microbiol. 2002;4(9):585-98. PubMed PMID: 12390351.

48.Edwards JL, Brown EJ, Uk-Nham S, Cannon JG, Blake MS, Apicella MA. A co-operative interaction between *Neisseria gonorrhoeae* and complement receptor 3 mediates infection of primary cervical epithelial cells. Cell Microbiol. 2002;4(9):571-84. PubMed PMID: 12390350.

49.Edwards JL, Entz DD, Apicella MA. Gonococcal phospholipase d modulates the expression and function of complement receptor 3 in primary cervical epithelial cells. Infect Immun. 2003;71(11):6381-91. PubMed PMID: 14573659; PubMed Central PMCID: PMCPMC219594.

50.Bos MP, Kuroki M, Krop-Watorek A, Hogan D, Belland RJ. CD66 receptor specificity exhibited by neisserial Opa variants is controlled by protein determinants in CD66 N-domains. Proc Natl Acad Sci U S A. 1998;95(16):9584-9. PubMed PMID: 9689124; PubMed Central PMCID: PMCPMC21382.

51.Beauchemin N, Arabzadeh A. Carcinoembryonic antigen-related cell adhesion molecules (CEACAMs) in cancer progression and metastasis. Cancer Metastasis Rev. 2013;32(3-4):643-71. doi: 10.1007/s10555-013-9444-6. PubMed PMID: 23903773.

52.Gray-Owen SD, Blumberg RS. CEACAM1: contact-dependent control of immunity. Nat Rev Immunol. 2006;6(6):433-46. doi: 10.1038/nri1864. PubMed PMID: 16724098.

53.Sadarangani M, Pollard AJ, Gray-Owen SD. Opa proteins and CEACAMs: pathways of immune engagement for pathogenic Neisseria. FEMS Microbiol Rev. 2011;35(3):498-514. doi: 10.1111/j.1574-6976.2010.00260.x. PubMed PMID: 21204865.

54.Lee HS, Ostrowski MA, Gray-Owen SD. CEACAM1 dynamics during *neisseria gonorrhoeae* suppression of CD4+ T lymphocyte activation. J Immunol. 2008;180(10):6827-35. PubMed PMID: 18453603.

55.Hauck CR, Grassmé H, Bock J, Jendrossek V, Ferlinz K, Meyer TF, et al. Acid sphingomyelinase is involved in CEACAM receptor-mediated phagocytosis of *Neisseria gonorrhoeae*. FEBS Lett. 2000;478(3):260-6. PubMed PMID: 10930579.

56.McCaw SE, Schneider J, Liao EH, Zimmermann W, Gray-Owen SD. Immunoreceptor tyrosine-based activation motif phosphorylation during engulfment of *Neisseria gonorrhoeae* by the neutrophil-restricted CEACAM3 (CD66d) receptor. Mol Microbiol. 2003;49(3):623-37. PubMed PMID: 12864848.

57.Booth JW, Telio D, Liao EH, McCaw SE, Matsuo T, Grinstein S, et al. Phosphatidylinositol 3-kinases in carcinoembryonic antigen-related cellular adhesion molecule-mediated internalization of *Neisseria gonorrhoeae*. J Biol Chem. 2003;278(16):14037-45. Epub 2003/02/05. doi: 10.1074/jbc.M211879200. PubMed PMID: 12571236.

58.Sarantis H, Gray-Owen SD. The specific innate immune receptor CEACAM3 triggers neutrophil bactericidal activities via a Syk kinase-dependent pathway. Cell Microbiol. 2007;9(9):2167-80. Epub 2007/05/15. doi: 10.1111/j.1462-5822.2007.00947.x. PubMed PMID: 17506820.

59.Billker O, Popp A, Brinkmann V, Wenig G, Schneider J, Caron E, et al. Distinct mechanisms of internalization of *Neisseria gonorrhoeae* by members of the CEACAM receptor family involving Rac1- and Cdc42-dependent and -independent pathways. EMBO J. 2002;21(4):560-71. PubMed PMID: 11847104; PubMed Central PMCID: PMCPMC125849.

60.Voges M, Bachmann V, Naujoks J, Kopp K, Hauck CR. Extracellular IgC2 constant domains of CEACAMs mediate PI3K sensitivity during uptake of pathogens. PLoS One. 2012;7(6):e39908. doi: 10.1371/journal.pone.0039908. PubMed PMID: 22768164; PubMed Central PMCID: PMCPMC3386982.

61.Muenzner P, Bachmann V, Zimmermann W, Hentschel J, Hauck CR. Human-restricted bacterial pathogens block shedding of epithelial cells by stimulating integrin activation. Science. 2010;329(5996):1197-201. doi: 10.1126/science.1190892. PubMed PMID: 20813953.

62.Muenzner P, Rohde M, Kneitz S, Hauck CR. CEACAM engagement by human pathogens enhances cell adhesion and counteracts bacteria-induced detachment of epithelial cells. J Cell Biol. 2005;170(5):825-36. doi: 10.1083/jcb.200412151. PubMed PMID: 16115956; PubMed Central PMCID: PMCPMC2171332.

63.Islam EA, Anipindi VC, Francis I, Shaik-Dasthagirisaheb Y, Xu S, Leung N, et al. Specific Binding to Differentially Expressed Human Carcinoembryonic Antigen-Related Cell Adhesion Molecules Determines the Outcome of *Neisseria gonorrhoeae* Infections along the Female Reproductive Tract. Infect Immun. 2018;86(8). Epub 2018/07/23. doi: 10.1128/IAI.00092-18. PubMed PMID: 29760215; PubMed Central PMCID: PMCPMC6056862.

64.Dehio C, Gray-Owen SD, Meyer TF. The role of neisserial Opa proteins in interactions with host cells. Trends Microbiol. 1998;6(12):489-95. PubMed PMID: 10036728.

65.Hauck CR, Meyer TF. 'Small' talk: Opa proteins as mediators of Neisseria-host-cell communication. Curr Opin Microbiol. 2003;6(1):43-9. PubMed PMID: 12615218.

66.van Putten JP, Duensing TD, Cole RL. Entry of OpaA+ gonococci into HEp-2 cells requires concerted action of glycosaminoglycans, fibronectin and integrin receptors. Mol Microbiol. 1998;29(1):369-79. PubMed PMID: 9701828.

67.Duensing TD, van Putten JP. Vitronectin mediates internalization of *Neisseria gonorrhoeae* by Chinese hamster ovary cells. Infect Immun. 1997;65(3):964-70. PubMed PMID: 9038304; PubMed Central PMCID: PMCPMC175076.

68.Gómez-Duarte OG, Dehio M, Guzmán CA, Chhatwal GS, Dehio C, Meyer TF. Binding of vitronectin to opa-expressing *Neisseria gonorrhoeae* mediates invasion of HeLa cells. Infect Immun. 1997;65(9):3857-66. PubMed PMID: 9284164; PubMed Central PMCID: PMCPMC175551.

69.Grassmé H, Gulbins E, Brenner B, Ferlinz K, Sandhoff K, Harzer K, et al. Acidic sphingomyelinase mediates entry of N. gonorrhoeae into nonphagocytic cells. Cell. 1997;91(5):605-15. PubMed PMID: 9393854.

70.Freissler E, Meyer auf der Heyde A, David G, Meyer TF, Dehio C. Syndecan-1 and syndecan-4 can mediate the invasion of OpaHSPG-expressing *Neisseria gonorrhoeae* into epithelial cells. Cell Microbiol. 2000;2(1):69-82. PubMed PMID: 11207564.

71.Naumann M, Rudel T, Meyer TF. Host cell interactions and signalling with *Neisseria gonorrhoeae*. Curr Opin Microbiol. 1999;2(1):62-70. PubMed PMID: 10047561.

72.Stockert RJ. The asialoglycoprotein receptor: relationships between structure, function, and expression. Physiol Rev. 1995;75(3):591-609. doi: 10.1152/physrev.1995.75.3.591. PubMed PMID: 7624395.

73.Porat N, Apicella MA, Blake MS. *Neisseria gonorrhoeae* utilizes and enhances the biosynthesis of the asialoglycoprotein receptor expressed on the surface of the hepatic HepG2 cell line. Infect Immun. 1995;63(4):1498-506. PubMed PMID: 7890416; PubMed Central PMCID: PMCPMC173181.

74.Harvey HA, Ketterer MR, Preston A, Lubaroff D, Williams R, Apicella MA. Ultrastructural analysis of primary human urethral epithelial cell cultures infected with *Neisseria gonorrhoeae*. Infect Immun. 1997;65(6):2420-7. PubMed PMID: 9169783; PubMed Central PMCID: PMCPMC175335.

75.Swanson KV, Griffiss JM, Edwards VL, Stein DC, Song W. *Neisseria gonorrhoeae*-induced transactivation of EGFR enhances gonococcal invasion. Cell Microbiol. 2011;13(7):1078-90. doi: 10.1111/j.1462-5822.2011.01603.x. PubMed PMID: 21501367.

76.Edwards VL, Wang LC, Dawson V, Stein DC, Song W. *Neisseria gonorrhoeae* breaches the apical junction of polarized epithelial cells for transmigration by activating EGFR. Cell Microbiol. 2013;15(6):1042-57. doi: 10.1111/cmi.12099. PubMed PMID: 23279089.

77.Howie HL, Shiflett SL, So M. Extracellular signal-regulated kinase activation by *Neisseria gonorrhoeae* downregulates epithelial cell proapoptotic proteins Bad and Bim. Infect Immun. 2008;76(6):2715-21. Epub 2008/04/07. doi: 10.1128/IAI.00153-08. PubMed PMID: 18391004; PubMed Central PMCID: PMCPMC2423055.

78.Howie HL, Glogauer M, So M. The N. gonorrhoeae type IV pilus stimulates mechanosensitive pathways and cytoprotection through a pilT-dependent mechanism. PLoS Biol. 2005;3(4):e100. Epub 2005/03/22. doi: 10.1371/journal.pbio.0030100. PubMed PMID: 15769184; PubMed Central PMCID: PMCPMC1065265.

79.Citri A, Yarden Y. EGF-ERBB signalling: towards the systems level. Nat Rev Mol Cell Biol. 2006;7(7):505-16. doi: 10.1038/nrm1962. PubMed PMID: 16829981.

80.Merz AJ, Enns CA, So M. Type IV pili of pathogenic Neisseriae elicit cortical plaque formation in epithelial cells. Mol Microbiol. 1999;32(6):1316-32. PubMed PMID: 10383771.

81.Lee SW, Higashi DL, Snyder A, Merz AJ, Potter L, So M. PilT is required for PI(3,4,5)P3-mediated crosstalk between *Neisseria gonorrhoeae* and epithelial cells. Cell Microbiol. 2005;7(9):1271-84. doi: 10.1111/j.1462-5822.2005.00551.x. PubMed PMID: 16098215.

82.Higashi DL, Zhang GH, Biais N, Myers LR, Weyand NJ, Elliott DA, et al. Influence of type IV pilus retraction on the architecture of the *Neisseria gonorrhoeae*-infected cell cortex. Microbiology. 2009;155(Pt 12):4084-92. Epub 2009/09/17. doi: 10.1099/mic.0.032656-0. PubMed PMID: 19762436; PubMed Central PMCID: PMCPMC2889423.

83.Ison CA. Sexually Transmitted Infections and Sexually Transmitted Diseases. Springer-Verlag Berlin Heidelberg2011.

84.Fichorova RN, Desai PJ, Gibson FC, Genco CA. Distinct proinflammatory host responses to *Neisseria gonorrhoeae* infection in immortalized human cervical and vaginal epithelial cells. Infect Immun. 2001;69(9):5840-8. PubMed PMID: 11500462; PubMed Central PMCID: PMCPMC98702.

85.McGee ZA, Johnson AP, Taylor-Robinson D. Pathogenic mechanisms of *Neisseria gonorrhoeae*: observations on damage to human fallopian tubes in organ culture by gonococci of colony type 1 or type 4. J Infect Dis. 1981;143(3):413-22. PubMed PMID: 6785363.

86.McCaw SE, Liao EH, Gray-Owen SD. Engulfment of *Neisseria gonorrhoeae*: revealing distinct processes of bacterial entry by individual carcinoembryonic antigen-related cellular adhesion molecule family receptors. Infect Immun. 2004;72(5):2742-52. PubMed PMID: 15102784; PubMed Central PMCID: PMCPMC387857.

87.Dehio M, Gómez-Duarte OG, Dehio C, Meyer TF. Vitronectin-dependent invasion of epithelial cells by *Neisseria gonorrhoeae* involves alpha(v) integrin receptors. FEBS Lett. 1998;424(1-2):84-8. PubMed PMID: 9537520.

88.Lin L, Ayala P, Larson J, Mulks M, Fukuda M, Carlsson SR, et al. The Neisseria type 2 IgA1 protease cleaves LAMP1 and promotes survival of bacteria within epithelial cells. Mol Microbiol. 1997;24(5):1083-94. PubMed PMID: 9220014.

89.Edwards JL. *Neisseria gonorrhoeae* survival during primary human cervical epithelial cell infection requires nitric oxide and is augmented by progesterone. Infect Immun. 2010;78(3):1202-13. Epub 2010/01/04. doi: 10.1128/IAI.01085-09. PubMed PMID: 20048043; PubMed Central PMCID: PMCPMC2825954.

90.McGee ZA, Stephens DS, Hoffman LH, Schlech WF, Horn RG. Mechanisms of mucosal invasion by pathogenic Neisseria. Rev Infect Dis. 1983;5 Suppl 4:S708-14. PubMed PMID: 6415784.

91.Ilver D, Källström H, Normark S, Jonsson AB. Transcellular passage of *Neisseria gonorrhoeae* involves pilus phase variation. Infect Immun. 1998;66(2):469-73. PubMed PMID: 9453597; PubMed Central PMCID: PMCPMC107929.

92.Wang JA, Meyer TF, Rudel T. Cytoskeleton and motor proteins are required for the transcytosis of *Neisseria gonorrhoeae* through polarized epithelial cells. Int J Med Microbiol. 2008;298(3-4):209-21. doi: 10.1016/j.ijmm.2007.05.004. PubMed PMID: 17683982.

93.Wang J, Gray-Owen SD, Knorre A, Meyer TF, Dehio C. Opa binding to cellular CD66 receptors mediates the transcellular traversal of *Neisseria gonorrhoeae* across polarized T84 epithelial cell monolayers. Mol Microbiol. 1998;30(3):657-71. PubMed PMID: 9822830.

94.Stein DC, LeVan A, Hardy B, Wang LC, Zimmerman L, Song W. Expression of Opacity Proteins Interferes with the Transmigration of *Neisseria gonorrhoeae* across Polarized Epithelial Cells. PLoS One. 2015;10(8):e0134342. Epub 2015/08/05. doi: 10.1371/journal.pone.0134342. PubMed PMID: 26244560; PubMed Central PMCID: PMCPMC4526573.

95.Wang LC, Yu Q, Edwards V, Lin B, Qiu J, Turner JR, et al. *Neisseria gonorrhoeae* infects the human endocervix by activating non-muscle myosin II-mediated epithelial exfoliation. PLoS Pathog. 2017;13(4):e1006269. Epub 2017/04/13. doi: 10.1371/journal.ppat.1006269. PubMed PMID: 28406994; PubMed Central PMCID: PMCPMC5391109.

96.Ward ME, Watt PJ, Robertson JN. The human fallopian tube: a laboratory model for gonococcal infection. J Infect Dis. 1974;129(6):650-9. PubMed PMID: 4209721.

97.Mosleh IM, Boxberger HJ, Sessler MJ, Meyer TF. Experimental infection of native human ureteral tissue with *Neisseria gonorrhoeae*: adhesion, invasion, intracellular fate, exocytosis, and passage through a stratified epithelium. Infect Immun. 1997;65(8):3391-8. PubMed PMID: 9234803; PubMed Central PMCID: PMCPMC175480.

98.McGee ZA, Jensen RL, Clemens CM, Taylor-Robinson D, Johnson AP, Gregg CR. Gonococcal infection of human fallopian tube mucosa in organ culture: relationship of mucosal tissue TNF-alpha concentration to sloughing of ciliated cells. Sex Transm Dis. 1999;26(3):160-5. PubMed PMID: 10100774.

99.Kim M, Ashida H, Ogawa M, Yoshikawa Y, Mimuro H, Sasakawa C. Bacterial interactions with the host epithelium. Cell Host Microbe. 2010;8(1):20-35. doi: 10.1016/j.chom.2010.06.006. PubMed PMID: 20638639.

100.Mulvey MA, Schilling JD, Martinez JJ, Hultgren SJ. Bad bugs and beleaguered bladders: interplay between uropathogenic Escherichia coli and innate host defenses. Proc Natl Acad Sci U S A. 2000;97(16):8829-35. PubMed PMID: 10922042; PubMed Central PMCID: PMCPMC34019.

101.Mulvey MA, Schilling JD, Hultgren SJ. Establishment of a persistent Escherichia coli reservoir during the acute phase of a bladder infection. Infect Immun. 2001;69(7):4572-9. doi: 10.1128/IAI.69.7.4572-4579.2001. PubMed PMID: 11402001; PubMed Central PMCID: PMCPMC98534.

102.Coradini D, Casarsa C, Oriana S. Epithelial cell polarity and tumorigenesis: new perspectives for cancer detection and treatment. Acta Pharmacol Sin. 2011;32(5):552-64. Epub 2011/04/18. doi: 10.1038/aps.2011.20. PubMed PMID: 21499288; PubMed Central PMCID: PMCPMC4002515.

103.Meng W, Takeichi M. Adherens junction: molecular architecture and regulation. Cold Spring Harb Perspect Biol. 2009;1(6):a002899. Epub 2009/08/05. doi: 10.1101/cshperspect.a002899. PubMed PMID: 20457565; PubMed Central PMCID: PMCPMC2882120.

104.Hartsock A, Nelson WJ. Adherens and tight junctions: structure, function and connections to the actin cytoskeleton. Biochim Biophys Acta. 2008;1778(3):660-9. Epub 2007/07/27. doi: 10.1016/j.bbamem.2007.07.012. PubMed PMID: 17854762; PubMed Central PMCID: PMCPMC2682436.

105.Huber AH, Weis WI. The structure of the beta-catenin/E-cadherin complex and the molecular basis of diverse ligand recognition by beta-catenin. Cell. 2001;105(3):391-402. PubMed PMID: 11348595.

106.Lickert H, Bauer A, Kemler R, Stappert J. Casein kinase II phosphorylation of E-cadherin increases E-cadherin/beta-catenin interaction and strengthens cell-cell adhesion. J Biol Chem. 2000;275(7):5090-5. PubMed PMID: 10671552.

107.Nelson WJ. Regulation of cell-cell adhesion by the cadherin-catenin complex. Biochem Soc Trans. 2008;36(Pt 2):149-55. doi: 10.1042/BST0360149. PubMed PMID: 18363555; PubMed Central PMCID: PMCPMC3368607.

108.Rhee J, Mahfooz NS, Arregui C, Lilien J, Balsamo J, VanBerkum MF. Activation of the repulsive receptor Roundabout inhibits N-cadherin-mediated cell adhesion. Nat Cell Biol. 2002;4(10):798-805. doi: 10.1038/ncb858. PubMed PMID: 12360290.

109.Roura S, Miravet S, Piedra J, García de Herreros A, Duñach M. Regulation of E-cadherin/Catenin association by tyrosine phosphorylation. J Biol Chem. 1999;274(51):36734-40. PubMed PMID: 10593980.

110.Piedra J, Miravet S, Castaño J, Pálmer HG, Heisterkamp N, García de Herreros A, et al. p120 Catenin-associated Fer and Fyn tyrosine kinases regulate beta-catenin Tyr-142 phosphorylation and beta-catenin-alpha-catenin Interaction. Mol Cell Biol. 2003;23(7):2287-97. PubMed PMID: 12640114; PubMed Central PMCID: PMCPMC150740.

111.Balsamo J, Leung T, Ernst H, Zanin MK, Hoffman S, Lilien J. Regulated binding of PTP1B-like phosphatase to N-cadherin: control of cadherin-mediated adhesion by dephosphorylation of beta-catenin. J Cell Biol. 1996;134(3):801-13. PubMed PMID: 8707857; PubMed Central PMCID: PMCPMC2120944.

112.Winter MC, Shasby S, Shasby DM. Compromised E-cadherin adhesion and epithelial barrier function with activation of G protein-coupled receptors is rescued by Y-to-F mutations in beta-catenin. Am J Physiol Lung Cell Mol Physiol. 2008;294(3):L442-8. Epub 2007/12/14. doi: 10.1152/ajplung.00404.2007. PubMed PMID: 18083766.

113.Timmerman I, Hoogenboezem M, Bennett AM, Geerts D, Hordijk PL, van Buul JD. The tyrosine phosphatase SHP2 regulates recovery of endothelial adherens junctions through control of β-catenin phosphorylation. Mol Biol Cell. 2012;23(21):4212-25. Epub 2012/09/05. doi: 10.1091/mbc.E12-01-0038. PubMed PMID: 22956765; PubMed Central PMCID: PMCPMC3484100.

114.Huber AH, Stewart DB, Laurents DV, Nelson WJ, Weis WI. The cadherin cytoplasmic domain is unstructured in the absence of beta-catenin. A possible mechanism for regulating cadherin turnover. J Biol Chem. 2001;276(15):12301-9. Epub 2000/12/19. doi: 10.1074/jbc.M010377200. PubMed PMID: 11121423.

115.Van Itallie CM, Anderson JM. Architecture of tight junctions and principles of molecular composition. Semin Cell Dev Biol. 2014;36:157-65. Epub 2014/08/27. doi: 10.1016/j.semcdb.2014.08.011. PubMed PMID: 25171873; PubMed Central PMCID: PMCPMC4254347.

116.Harhaj NS, Antonetti DA. Regulation of tight junctions and loss of barrier function in pathophysiology. Int J Biochem Cell Biol. 2004;36(7):1206-37. doi: 10.1016/j.biocel.2003.08.007. PubMed PMID: 15109567.

117.Ulluwishewa D, Anderson RC, McNabb WC, Moughan PJ, Wells JM, Roy NC. Regulation of tight junction permeability by intestinal bacteria and dietary components. J Nutr. 2011;141(5):769-76. Epub 2011/03/23. doi: 10.3945/jn.110.135657. PubMed PMID: 21430248.

118.Tanos B, Rodriguez-Boulan E. The epithelial polarity program: machineries involved and their hijacking by cancer. Oncogene. 2008;27(55):6939-57. doi: 10.1038/onc.2008.345. PubMed PMID: 19029936.

119.Capaldo CT, Macara IG. Depletion of E-cadherin disrupts establishment but not maintenance of cell junctions in Madin-Darby canine kidney epithelial cells. Mol Biol Cell. 2007;18(1):189-200. Epub 2006/11/08. doi: 10.1091/mbc.e06-05-0471. PubMed PMID: 17093058; PubMed Central PMCID: PMCPMC1751327.

120.Fukuyama T, Ogita H, Kawakatsu T, Inagaki M, Takai Y. Activation of Rac by cadherin through the c-Src-Rap1-phosphatidylinositol 3-kinase-Vav2 pathway. Oncogene. 2006;25(1):8-19. doi: 10.1038/sj.onc.1209010. PubMed PMID: 16170364.

121.Miyoshi J, Takai Y. Structural and functional associations of apical junctions with cytoskeleton. Biochim Biophys Acta. 2008;1778(3):670-91. doi: 10.1016/j.bbamem.2007.12.014. PubMed PMID: 18201548.

122.Baum B, Georgiou M. Dynamics of adherens junctions in epithelial establishment, maintenance, and remodeling. J Cell Biol. 2011;192(6):907-17. doi: 10.1083/jcb.201009141. PubMed PMID: 21422226; PubMed Central PMCID: PMCPMC3063136.

123.Blaskewicz CD, Pudney J, Anderson DJ. Structure and function of intercellular junctions in human cervical and vaginal mucosal epithelia. Biol Reprod. 2011;85(1):97-104. Epub 2011/04/06. doi: 10.1095/biolreprod.110.090423. PubMed PMID: 21471299; PubMed Central PMCID: PMCPMC3123383.

124.Draper DL, Donegan EA, James JF, Sweet RL, Brooks GF. Scanning electron microscopy of attachment of *Neisseria gonorrhoeae* colony phenotypes to surfaces of

human genital epithelia. Am J Obstet Gynecol. 1980;138(7 Pt 1):818-26. PubMed PMID: 6108716.

125.Sobel G, Szabó I, Páska C, Kiss A, Kovalszky I, Kádár A, et al. Changes of cell adhesion and extracellular matrix (ECM) components in cervical intraepithelial neoplasia. Pathol Oncol Res. 2005;11(1):26-31. Epub 2005/03/31. doi: PAOR.2005.11.1.0026. PubMed PMID: 15800679.

126.Ponce de León-Rodríguez MDC, Guyot JP, Laurent-Babot C. Intestinal in vitro cell culture models and their potential to study the effect of food components on intestinal inflammation. Crit Rev Food Sci Nutr. 2018:1-19. Epub 2018/10/02. doi: 10.1080/10408398.2018.1506734. PubMed PMID: 30277794.

127.Dean P, Kenny B. Intestinal barrier dysfunction by enteropathogenic Escherichia coli is mediated by two effector molecules and a bacterial surface protein. Mol Microbiol. 2004;54(3):665-75. doi: 10.1111/j.1365-2958.2004.04308.x. PubMed PMID: 15491358.

128.Weflen AW, Alto NM, Hecht GA. Tight junctions and enteropathogenic *E. coli*. Ann N Y Acad Sci. 2009;1165:169-74. doi: 10.1111/j.1749-6632.2009.04060.x. PubMed PMID: 19538303; PubMed Central PMCID: PMCPMC3325541.

129.Simovitch M, Sason H, Cohen S, Zahavi EE, Melamed-Book N, Weiss A, et al. EspM inhibits pedestal formation by enterohaemorrhagic Escherichia coli and enteropathogenic *E. coli* and disrupts the architecture of a polarized epithelial monolayer. Cell Microbiol. 2010;12(4):489-505. Epub 2009/11/12. doi: 10.1111/j.1462-5822.2009.01410.x. PubMed PMID: 19912240.

130.Edwards JL, Shao JQ, Ault KA, Apicella MA. *Neisseria gonorrhoeae* elicits membrane ruffling and cytoskeletal rearrangements upon infection of primary human endocervical and ectocervical cells. Infect Immun. 2000;68(9):5354-63. PubMed PMID: 10948165; PubMed Central PMCID: PMCPMC101799.

131.Griffiss JM, Lammel CJ, Wang J, Dekker NP, Brooks GF. *Neisseria gonorrhoeae* coordinately uses Pili and Opa to activate HEC-1-B cell microvilli, which causes engulfment of the gonococci. Infect Immun. 1999;67(7):3469-80. PubMed PMID: 10377128; PubMed Central PMCID: PMCPMC116533.

132.Grassmé HU, Ireland RM, van Putten JP. Gonococcal opacity protein promotes bacterial entry-associated rearrangements of the epithelial cell actin cytoskeleton. Infect Immun. 1996;64(5):1621-30. PubMed PMID: 8613370; PubMed Central PMCID: PMCPMC173971.

133.Higashi DL, Lee SW, Snyder A, Weyand NJ, Bakke A, So M. Dynamics of *Neisseria gonorrhoeae* attachment: microcolony development, cortical plaque formation, and cytoprotection. Infect Immun. 2007;75(10):4743-53. doi: 10.1128/IAI.00687-07. PubMed PMID: 17682045; PubMed Central PMCID: PMCPMC2044525.

134.Merz AJ, So M. Attachment of piliated, Opa- and Opc- gonococci and meningococci to epithelial cells elicits cortical actin rearrangements and clustering of tyrosine-phosphorylated proteins. Infect Immun. 1997;65(10):4341-9. PubMed PMID: 9317047; PubMed Central PMCID: PMCPMC175623.

135.Haglund CM, Welch MD. Pathogens and polymers: microbe-host interactions illuminate the cytoskeleton. J Cell Biol. 2011;195(1):7-17. doi: 10.1083/jcb.201103148. PubMed PMID: 21969466; PubMed Central PMCID: PMCPMC3187711.

136.Goley ED, Welch MD. The ARP2/3 complex: an actin nucleator comes of age. Nat Rev Mol Cell Biol. 2006;7(10):713-26. doi: 10.1038/nrm2026. PubMed PMID: 16990851.

137.Ivanov AI. Actin motors that drive formation and disassembly of epithelial apical junctions. Front Biosci. 2008;13:6662-81. Epub 2008/05/01. PubMed PMID: 18508686.

138.Georgiou M, Marinari E, Burden J, Baum B. Cdc42, Par6, and aPKC regulate Arp2/3-mediated endocytosis to control local adherens junction stability. Curr Biol. 2008;18(21):1631-8. Epub 2008/10/30. doi: 10.1016/j.cub.2008.09.029. PubMed PMID: 18976918.

139.Ivanov AI, Parkos CA, Nusrat A. Cytoskeletal regulation of epithelial barrier function during inflammation. Am J Pathol. 2010;177(2):512-24. Epub 2010/06/25. doi: 10.2353/ajpath.2010.100168. PubMed PMID: 20581053; PubMed Central PMCID: PMCPMC2913378.

140.Fedwick JP, Lapointe TK, Meddings JB, Sherman PM, Buret AG. *Helicobacter pylori* activates myosin light-chain kinase to disrupt claudin-4 and claudin-5 and increase epithelial permeability. Infect Immun. 2005;73(12):7844-52. doi: 10.1128/IAI.73.12.7844-7852.2005. PubMed PMID: 16299274; PubMed Central PMCID: PMCPMC1307049.

141.Crawley SW, Mooseker MS, Tyska MJ. Shaping the intestinal brush border. J Cell Biol. 2014;207(4):441-51. doi: 10.1083/jcb.201407015. PubMed PMID: 25422372; PubMed Central PMCID: PMCPMC4242837.

142.Iizumi Y, Sagara H, Kabe Y, Azuma M, Kume K, Ogawa M, et al. The enteropathogenic *E. coli* effector EspB facilitates microvillus effacing and antiphagocytosis by inhibiting myosin function. Cell Host Microbe. 2007;2(6):383-92. doi: 10.1016/j.chom.2007.09.012. PubMed PMID: 18078690.

143.McGee ZA, Johnson AP, Taylor-Robinson D. Human fallopian tubes in organ culture: preparation, maintenance, and quantitation of damage by pathogenic microorganisms. Infect Immun. 1976;13(2):608-18. PubMed PMID: 816745; PubMed Central PMCID: PMCPMC420652.

144.Jerse AE. Experimental gonococcal genital tract infection and opacity protein expression in estradiol-treated mice. Infect Immun. 1999;67(11):5699-708. PubMed PMID: 10531218; PubMed Central PMCID: PMCPMC96944.

145.Eades-Perner AM, van der Putten H, Hirth A, Thompson J, Neumaier M, von Kleist S, et al. Mice transgenic for the human carcinoembryonic antigen gene maintain its spatiotemporal expression pattern. Cancer Res. 1994;54(15):4169-76. PubMed PMID: 8033149.

146.Apicella MA, Shero M, Jarvis GA, Griffiss JM, Mandrell RE, Schneider H. Phenotypic variation in epitope expression of the *Neisseria gonorrhoeae* lipooligosaccharide. Infect Immun. 1987;55(8):1755-61. PubMed PMID: 2440807; PubMed Central PMCID: PMCPMC260597.

147.Swanson J. Studies on gonococcus infection. IV. Pili: their role in attachment of gonococci to tissue culture cells. J Exp Med. 1973;137(3):571-89. PubMed PMID: 4631989; PubMed Central PMCID: PMCPMC2139381.

148.Chen T, Grunert F, Medina-Marino A, Gotschlich EC. Several carcinoembryonic antigens (CD66) serve as receptors for gonococcal opacity proteins. J Exp Med. 1997;185(9):1557-64. PubMed PMID: 9151893; PubMed Central PMCID: PMCPMC2196295.

149.LeVan A, Zimmerman LI, Mahle AC, Swanson KV, DeShong P, Park J, et al. Construction and characterization of a derivative of Neisseria gonorrhoeae strain MS11 devoid of all opa genes. J Bacteriol. 2012;194(23):6468-78. doi: 10.1128/JB.00969-12. PubMed PMID: 23002223; PubMed Central PMCID: PMCPMC3497525.

150.White LA, Kellogg DS. An improved fermentation medium for *Neisseria gonorrhoeae* and other Neisseria. Health Lab Sci. 1965;2(4):238-41. PubMed PMID: 4953822.

151.Schürch W, McDowell EM, Trump BF. Long-term organ culture of human uterine endocervix. Cancer Res. 1978;38(11 Pt 1):3723-33. PubMed PMID: 698932.

152.Wang LC, Yu Q, Stein DC, Song W. Immunofluorescence Analysis of Human Endocervical Tissue Explants Infected with. Bio Protoc. 2018;8(3). doi: 10.21769/BioProtoc.2720. PubMed PMID: 29780854; PubMed Central PMCID: PMCPMC5959038.

153.Swanson KV, Jarvis GA, Brooks GF, Barham BJ, Cooper MD, Griffiss JM. CEACAM is not necessary for *Neisseria gonorrhoeae* to adhere to and invade female genital epithelial cells. Cell Microbiol. 2001;3(10):681-91. PubMed PMID: 11580753.

154.Muenzner P, Bachmann V, Kuespert K, Hauck CR. The CEACAM1 transmembrane domain, but not the cytoplasmic domain, directs internalization of human pathogens via membrane microdomains. Cell Microbiol. 2008;10(5):1074-92. doi: 10.1111/j.1462-5822.2007.01106.x. PubMed PMID: 18081725.

155.Chen L, Sung SS, Yip ML, Lawrence HR, Ren Y, Guida WC, et al. Discovery of a novel shp2 protein tyrosine phosphatase inhibitor. Mol Pharmacol. 2006;70(2):562-70. Epub 2006/05/22. doi: 10.1124/mol.106.025536. PubMed PMID: 16717135.

156.Vicente-Manzanares M, Ma X, Adelstein RS, Horwitz AR. Non-muscle myosin II takes centre stage in cell adhesion and migration. Nat Rev Mol Cell Biol. 2009;10(11):778-90. doi: 10.1038/nrm2786. PubMed PMID: 19851336; PubMed Central PMCID: PMCPMC2834236.

157.Day RM, Mitchell TJ, Knight SC, Forbes A. Regulation of epithelial syndecan-1 expression by inflammatory cytokines. Cytokine. 2003;21(5):224-33. PubMed PMID: 12824007.

158.Pils S, Kopp K, Peterson L, Delgado Tascón J, Nyffenegger-Jann NJ, Hauck CR. The adaptor molecule Nck localizes the WAVE complex to promote actin polymerization during CEACAM3-mediated phagocytosis of bacteria. PLoS One. 2012;7(3):e32808. doi: 10.1371/journal.pone.0032808. PubMed PMID: 22448228; PubMed Central PMCID: PMCPMC3308951.

159.Wira CR, Rodriguez-Garcia M, Patel MV. The role of sex hormones in immune protection of the female reproductive tract. Nat Rev Immunol. 2015;15(4):217-30. doi: 10.1038/nri3819. PubMed PMID: 25743222.

160.Kyrgiou M, Mitra A, Moscicki AB. Does the vaginal microbiota play a role in the development of cervical cancer? Transl Res. 2017;179:168-82. Epub 2016/07/15. doi: 10.1016/j.trsl.2016.07.004. PubMed PMID: 27477083; PubMed Central PMCID: PMCPMC5164950.

161.Van Kooij RJ, Roelofs HJ, Kathmann GA, Kramer MF. Human cervical mucus and its mucous glycoprotein during the menstrual cycle. Fertil Steril. 1980;34(3):226-33. PubMed PMID: 7409244.